# COVARIANCE MATRIX ADJUSTMENT TECHNIQUE FOR BEAMFORMING IMPROVEMENT OF ADAPTIVE ARRAY ANTENNA

THANAKORN SUKHONTHAPHONG

A THESIS SUBMITTED IN PARTIAL FULFILLMENT OF
THE REQUIREMENT FOR THE DEGREE OF
MASTER OF ENGINEERING IN
TELECOMMUNICATIONS ENGINEERING
SCHOOL OF GRADUATE STUDIES
KING MONGKUT'S INSTITUTE OF TECHNOLOGY LADKRABANG
2003

ISBN 974-324-743-2

| | |
|---|---|
| **หัวข้อวิทยานิพนธ์** | เทคนิคการปรับเมตริกซ์โคแวเรียนซ์สำหรับการปรับปรุงการจัดรูปแบบลำคลื่นของสายอากาศแถวลำดับปรับตัว |
| **นักศึกษา** | นายธนากร สุคนธพงศ์ |
| **รหัสนักศึกษา** | 44061703 |
| **ปริญญา** | วิศวกรรมศาสตรมหาบัณฑิต |
| **สาขาวิชา** | วิศวกรรมโทรคมนาคม |
| **พ.ศ.** | 2546 |
| **อาจารย์ผู้ควบคุมวิทยานิพนธ์** | รศ.ดร.โมไนย ไกรฤกษ์ |

## บทคัดย่อ

วิทยานิพนธ์ฉบับนี้นำเสนอเทคนิคการปรับเมตริกซ์โคแวเรียนซ์สำหรับการปรับปรุงการจัดรูปแบบลำคลื่นของสายอากาศแถวลำดับปรับตัว เทคนิคที่นำเสนอนี้ถูกนำไปใช้กับระบบการจัดรูปแบบลำคลื่นที่ต้องใช้เมตริกซ์โคแวเรียนซ์ในการคำนวณ จุดประสงค์ของเทคนิคที่นำเสนอนี้เพื่อปรับปรุงและลดปัญหาการลดลงของขนาดของสัญญาณที่รับได้ ซึ่งปัญหานี้จะเกิดขึ้นเมื่ออัตราส่วนระหว่างสัญญาณต่อสัญญาณรบกวน (signal to noise ratio) มีค่าลดน้อยลง และทำให้แบบรูปการตอบสนองของอัตราส่วนสัญญาณต่อผลรวมของสัญญาณแทรกสอดกับสัญญาณรบกวนที่ด้านออกได้รับผลกระทบ โดยส่งผลให้ไม่สามารถจัดการตอบสนองเป็นตำแหน่งศูนย์ (null) ตรงกับทิศทางของสัญญาณแทรกสอด เทคนิคที่นำเสนอนี้คือกระบวนการเพิ่มตัวคูณที่สามารถปรับค่าเฉพาะได้ ทั้งกับเมตริกซ์โคแวเรียนซ์ของสัญญาณที่ต้องการและเมตริกซ์โคแวเรียนซ์ของสัญญาณแทรกสอด ซึ่งได้แสดงผลการจำลองแบบและผลการทดลองระหว่างวิธีการที่นำเสนอกับวิธีแบบฉบับเพื่อเปรียบเทียบและยืนยันความถูกต้องของเทคนิคที่นำเสนอ

| | |
|---|---|
| **Thesis Title** | Covariance Matrix Adjustment Technique for Beamforming Improvement of Adaptive Array Antenna |
| **Student** | Mr. Thanakorn Sukhonthaphong |
| **Student ID.** | 44061703 |
| **Degree** | Master of Engineering |
| **Programme** | Telecommunications Engineering |
| **Year** | 2003 |
| **Thesis Advisor** | Assoc.Prof.Dr.Monai Krairiksh |


## ABSTRACT

This thesis presents the covariance matrix adjustment technique for beamforming improvement of adaptive array antenna. The proposed technique is used with beamforming system which is computed from the covariance matrix. The objective of this proposed technique is for improving the problem of signal reduction, which rises when the signal to noise ratio (SNR) level is diminished. That will affect to the output signal to interference plus noise ratio (SINR) response pattern of adaptive array antenna at the interference direction. The output null response pattern will not exactly be at the interference direction. This proposed technique is the process to add the specific adjustable multipliers with both desired signal covariance matrix and interference signal covariance matrices. The simulation and experimental results of the proposed technique are verified and compared with the conventional technique which demonstrates that the proposed technique can improve and increase the interference cancellation efficiency in adaptive array beamforming better than the conventional technique.

# ACKNOWLEDGEMENTS

I would like to take this opportunity to express my gratitude to many people who concerned in the success of this thesis.

Firstly, my deep and grateful gratitude is dedicated to Associate Professor Monai Krairiksh, my advisor who has been giving me many helpful suggestions and stimulating the progress of this research, since the first time I have presented with it. I also appreciate his kindness and great support for allowing me to have an opportunity to receive the scholarship from the Public Management, Ministry Home Affairs, Posts and Telecommunications (MPHPT) in doing my research at Communications Research Laboratory (CRL), Japan. At the CRL, I am grateful to Dr. Hiroyuki Tsuji, Dr. Ryu Miura and other people involved with this research and also Public Management, Ministry Home Affairs, Posts and Telecommunications (MPHPT) for supporting this research.

In addition, I would like to thank to Associate Professor Jun-ichi Takada of Tokyo Institute of Technology whom I have discussed with. Although there were a few times of discussions, the suggestions are still useful for the research.

Furthermore, I would like to express my gratitude to Assistant Professor Sompol Kosulvit for his kindly discussions. Also I would like to appreciate to Dr. Chuwong Phongcharoenpanich for his helpful suggestion and all kinds of discussion.

Conclusively, I would like to distribute the dedication to all of my teachers along my student life.

Moreover, I would like to thank to Mr. Rangsan Wongsan, Dr. Chanchai Thongsopa, Dr. Komsak Meksamoot, Ms. Wanlika Buasomboon, Ms. Nitikarn Pasri and my colleagues in Wireless Communication Laboratory for their advice and friendship. I also particularly thank to Mr. Phaisan Ngamjanyaporn who helps me in proof reading and preparing my submitted papers.

Lastly, I am so grateful to my parents and younger brother who always stand by my side and encourage for everything and every time in my life.

Thanakorn Sukhonthaphong

# TABLE OF CONTENTS

# TABLE OF CONTENTS (continued)

# TABLE OF CONTENTS (continued)

Page

# LIST OF TABLES

# LIST OF FIGURES

# LIST OF FIGURES (continued)

Fig. Page

# LIST OF FIGURES (continued)

# LIST OF FIGURES (continued)

# LIST OF FIGURES (continued)

Fig. Page

# LIST OF FIGURES (continued)

# LIST OF FIGURES (continued)

Fig. Page

# LIST OF FIGURES (continued)

Fig. Page

# CHAPTER 1
# INTRODUCTION

## 1.1 Statement of the Problem

Adaptive antennas have recently received increasing a role of improving performance of wireless communication systems. These antenna systems compose of various techniques that attempt to enhance the received signal, suppress all interfering signals and increase capacity. Adaptive antenna consists of antenna array, combined with signal processing in both space and time. The concepts of using antenna arrays and innovative signal processing have been used previously with radar and aerospace technology. According to the cost effectiveness, this adaptive array technology has been made in practical system for using in cellular mobile phone or satellite mobile communication systems [1, 2].

The main reliability and capacity of adaptive array antenna are interference reduction and multipath fading mitigation by using adaptive beamforming. Therefore, the beamforming of adaptive array is the key device for increasing the efficiency in wireless communication [2]. For this reason, the main purpose of this thesis is to propose a technique to improve the interference cancellation of beamforming when the weak signal problem occurs in the system. This problem effects to the interfering rejection capability in beamforming system of adaptive array antenna which the beam pattern of the beamforming system can not set the precise null response patterns in the interfering directions [3, 4].

## 1.2 Purpose and Objective of the Thesis

This thesis intends to increase and enhance the adaptive array beamforming efficiency, particularly to improve the interference rejection capability by forming exact deep null response in the interference signal directions and high response in the desired signal direction. Although the weak signal problem happens in the adaptive beamforming system, the proposed technique can still enhance the null beam pattern and peak beam pattern in the interference and desired signal directions, respectively [4]. The simulation and experimentation are obtained to clarify their performances.

## 1.3 Hypothesis and Theory of the Research

The hypothesis of this research is based on the concept of increasing the low power interference signals correlation and decreasing the correlation between the high powers of desired signal and interfering signals. This proposed technique is developed from the automatic gain controller (AGC) Applebaum array [3] that endeavors to solve the slow convergence phenomenon due to an eigenvalue spread in the input covariance matrix by increasing the correlations between the weak signals at the input and output of the array [4]. Thus, the proposed technique applies the AGC Applebaum concept to achieve the enhancement of weak signal problem.

The main theory of this research involves the adaptive array antenna which consists of direction of arrival (DOA) estimation methods, beamforming methods, the concepts of array antenna, wave propagation and covariance matrix. These array processings relate manipulation of signals induced on various antenna elements. Its capabilities of steering nulls to reduce cochannel interferences and pointing the peak beam to the desired user as well as its abilities to achieve DOA estimation play an important role in enhancing the adaptive array system in wireless communications [5]. Thus, this thesis consists of the theory of beamforming method with DOA estimation.

The objective of an adaptive antenna is to choose a suitable set of amplitude and phase weights to combine with the outputs from the elements of an array to provide the optimized far field pattern for the reception of desired signal. According to the substantial improvements in system rejection of the interfering signal performance offered by this kind of array processing, it means that it is the essential requirement for many military radar, communications and navigation systems [2].

## 1.4 Scope of the Thesis

According to the aforementioned of the purpose and objective of this thesis, the scope of the thesis can be illustrated as follows:

Chapter 2 describes adaptive array antenna concept that consists of its operation and mechanism, array signal method, adaptive array model, the expression of adaptive array vector matrix, vector matrix of adaptive array signal calculation and the degrees of freedom.

Chapter 3 presents the adaptive array beamforming that is composed of the derivation of antenna beam pattern, classical beamforming, linearly constrained

minimum-variance (LCMV) method, Applebaum array and automatic gain controller Applebaum array which require the information of the received signal at the array antenna. It can be provided by the estimation of direction of signal arrival. Under these conditions, the DOA estimation methods are presented in the last section of this chapter.

Chapter 4 proposes the covariance matrix adjustment technique. This proposed technique is considered by the covariance matrix computation, covariance matrix analysis, then the simulation results of DOA estimation and beamforming method of all descriptive methods in chapter 3 are shown.

Chapter 5 performs the experimental results. The experimental configuration, calibration process and bit error rate (BER) are obtained. The experimentation is achieved in this chapter to clarify the performance of the proposed covariance matrix adjustment technique and the conventional method by considering their beam pattern and BER.

Chapter 6 is the last part that concludes and summarizes all of the materials that have been obtained in the preceding chapters and includes the discussion for further works.

# CHAPTER 2
# ADAPTIVE ARRAY ANTENNA

## 2.1 Introduction

Adaptive array antennas have recently received increasing a role for using to improve the performance of wireless communication systems. They have a strong interference cancellation capability and are expected to increase the channel capacity of wireless communication. Adaptive arrays cancel or coherently combine multipath components of the desired signal and null interfering signals that have different directions of arrival from the desired signal [1, 6, 7]. Consequently, this chapter presents the principle concept of adaptive array antenna that describes the operation and mechanism of the adaptive array antenna in the first section, followed by array signal model, adaptive array model, adaptive array vector matrix expression, vector matrix of adaptive array signal calculation, degrees of freedom and finally concluding remarks.

## 2.2 Operation and Mechanism of the Adaptive Array Antenna

An adaptive array antenna is an antenna that controls its own pattern, by using the weight control. This controlled weight can be classified by its operation and mechanism. The types of controlled weight are illustrated in Table 2.1 [2, 5, 8, 9].

**Table 2.1** Typical adaptive algorithms

| Type | Method | Weight Determination |
|---|---|---|
| Independent of data | Classic | FIR filter design technique available |
| Dependent of data | Reference Signal LMS (Least Mean Square) | Minimize mean square error |
| | LCMV (Linearly Constrained Minimum-Variance) | Minimize output power with a directional constraint |
| | Howells-Applebaum | Maximize output SINR with a steering vector |
| Blind | CMA (Constant Modulus Algorithm) | Minimize fluctuations of array output amplitude |

In Table 2.1, there are some algorithms of adaptive array which their weight determinations are compared. Each algorithm is suitable for each situation that depends on its system and condition. For example, the LMS (Least Mean Square) uses the comparison between the output and reference signals to pursue the minimization of the mean square error (MSE), whereas the Howells-Applebaum endeavors to seek the maximization of the desired signal-to-interference-plus-thermal noise ratio (SINR). The LMS array requires the desired signal waveform, however, it does not need its incident angle knowledge. On the contrary, Howells-Applebaum can be used when the incident angle of the desired signal is known. Thus adaptive array antenna can be used with various applications such as mobile communication, radar, satellite communication which depend on their conditions and requirements [8].

The beam pattern of adaptive array is changed to track the desired direction. The antenna gain was set to a large value in desired direction and low along the interfering directions. This operation can be shown in Fig. 2.1. The two coherent signals from the 1$^{st}$transmitter impinge the receiving array antenna. The beam pattern of the array antenna was controlled to point the peak and null in the desired and interfering directions, respectively by the weight controller of the adaptive system [7, 10].

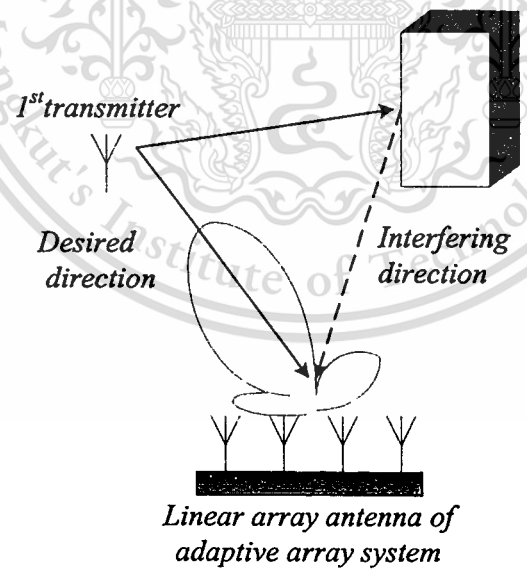


**Fig. 2.1** Operation of adaptive array antenna with two impinging signal directions from the 1$^{st}$transmitter

As the result of this effective property, it is feasible to reduce the effect of fading and cochannel interference. But the most of all, the adaptive array antenna techniques are based on the concepts of array signal model and vector matrix expressions which are described in next section and the details of some adaptive array methods which are used in this thesis will be explained in Chapter 3.

## 2.3 Array Signal Model

The array signal model can be generalized by including $N$ elements of isotropic sources positioned along the x1-axis. Referring to the geometry of Fig. 2.2, let us assume that all the elements are uniform array of identical elements of identical amplitude and with a linear progressive phase [11].

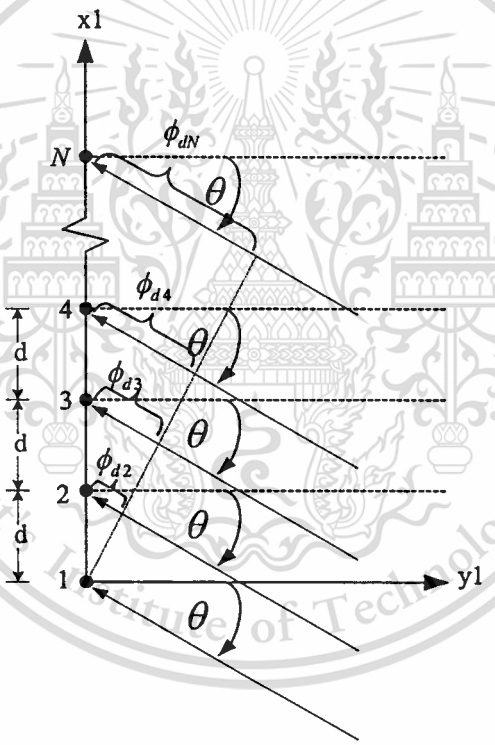


**Fig. 2.2** Far-field geometry of $N$-element array of isotropic sources positioned along the x1-axis

The total received signal at the $N$-element array can be expressed as

$$X = [\bar{x}_1(t), \bar{x}_2(t), \bar{x}_3(t), \bar{x}_4(t), ..., \bar{x}_N(t)]^T . \qquad (2.1)$$

$\bar{x}_1(t), \bar{x}_2(t), \bar{x}_3(t), \bar{x}_4(t), ..., \bar{x}_N(t)$ are the received signals at the $1^{st}$ element, $2^{nd}$ element, $3^{rd}$ element, $4^{th}$ element and $N^{th}$ element, respectively and $^T$ indicates the transposition. The total field [8, 11] can be formed by

$$X = A_o(t)e^{j(\omega_o t+\psi_o+\phi_o(t))}\begin{bmatrix} f_1(\theta) \\ f_2(\theta)e^{-j\phi_{d2}} \\ f_3(\theta)e^{-j\phi_{d3}} \\ f_4(\theta)e^{-j\phi_{d4}} \\ \vdots \\ f_N(\theta)e^{-j\phi_{dN}} \end{bmatrix}, \tag{2.2}$$

where $A_o(t)$ is the amplitude modulation, $\omega_o$ is angular frequency, $t$ is time, $\psi_o$ is progressive phase, $\phi_o(t)$ is the phase modulation, $f_i(\theta)$ is the $i^{th}$ element pattern and $\phi_{di}$ is the inter-element phase shift between element 1 and element $i$ that can be given by

$$\phi_{dn} = \frac{2\pi L_n \sin(\theta)}{\lambda}. \tag{2.3}$$

$L_n$ is the distance between the $n^{th}$ element and the $1^{st}$ element, $\lambda$ is the wavelength and $\theta$ is the angle of received signal. If we define

$$a = A_o(t)e^{j(\omega_o t+\psi_o+\phi_o(t))} \tag{2.4}$$

and

$$U_d = \begin{bmatrix} f_1(\theta) \\ f_2(\theta)e^{-j\phi_{d2}} \\ f_3(\theta)e^{-j\phi_{d3}} \\ f_4(\theta)e^{-j\phi_{d4}} \\ \vdots \\ f_N(\theta)e^{-j\phi_{dN}} \end{bmatrix}, \tag{2.5}$$

then

$$X_d = aU_d . \tag{2.6}$$

## 2.4 Adaptive Array Model

Among the various kinds of adaptive array types, the basic concept of each model can be summarized in this section. In this case, by using the theory of array signal model from last section, it is assumed that the signal received by the array is narrowband. Therefore, the basic adaptive array model can be illustrated in Fig. 2.3 [8].

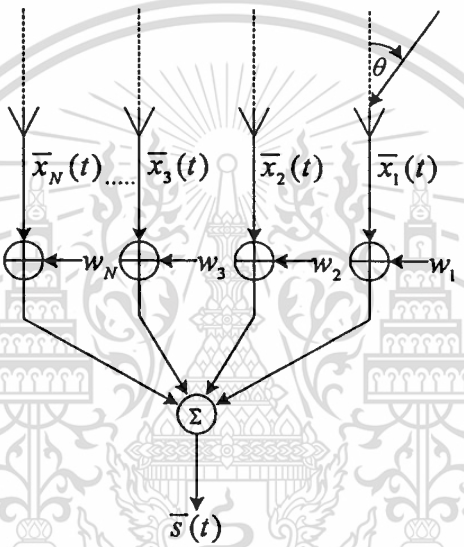


**Fig. 2.3** The *N*-element adaptive array model

The received signals are induced in each branch of the array $\bar{x}(t)$, the signal vector can be shown as

$$X = [\bar{x}_1(t), \bar{x}_2(t), \bar{x}_3(t), ..., \bar{x}_N(t)]^T , \tag{2.7}$$

which consist of the signals from various directions both desired and interference signals and also the noise, as follow:

$$X = X_d + X_i + X_n . \tag{2.8}$$

The received signal in each branch of the array will be multiplied by the complex weight,

$$W = [w_1, w_2, w_3, ...w_N]^T . \tag{2.9}$$

The complex weight $W$ changes the amplitude and phase of received signal and then summed at the final stage to be the result signal

$$\overline{s}(t) = W^T X = \overline{s}_d(t) + \overline{s}_i(t) + \overline{s}_n(t), \tag{2.10}$$

as shown in Fig. 2.4.

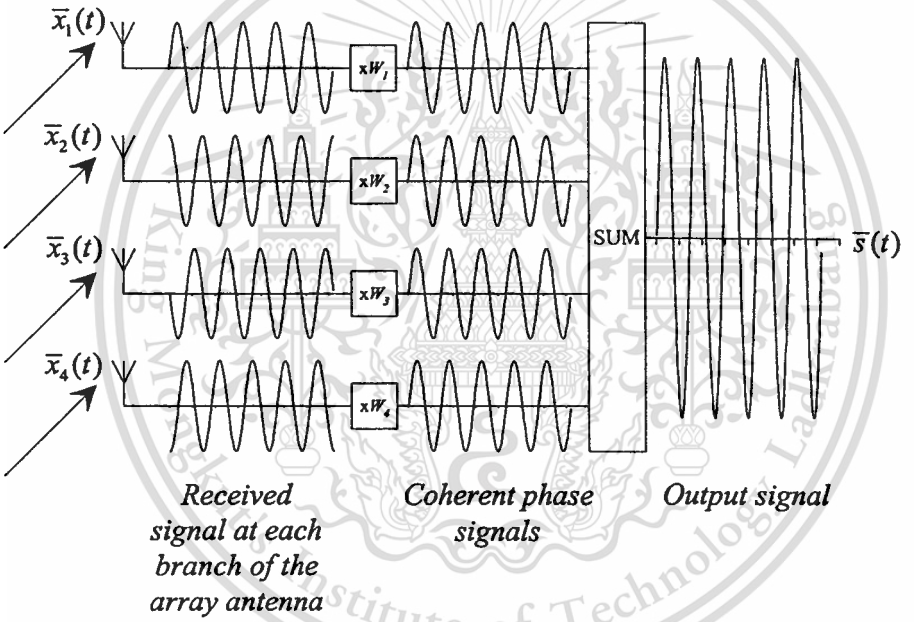


**Fig. 2.4** Example adaptive array model

The specific received signals at the array antenna are treated as waves and synthesized, by phase and amplitude adjusting. Thus, the signal in each branch becomes the coherent signal wave before summing to be the output signal. The complex weight can be computed from various techniques which will be described in chapter 3.

## 2.5 Adaptive Array Vector Matrix Expression

From the previous section, the adaptive array antenna consists of multiple received signals from the array elements. When the signals are handled simultaneously, they can be expressed by using a simplified equation which is easy to process the signal. Therefore, adaptive array uses the vectors and matrices of the signals for the computation. Whereas some vectors and matrices of the handled signals are used in the previous section, thereby for the orderliness, their descriptions are shown in Table 2.2 [8, 9].

**Table 2.2** Descriptions of major parameters

| Parameters | Descriptions | Example |
|---|---|---|
| $x_m(t), \overline{x}_m(t)$ | Received signal scalar and received signal vector in time domain at the $m^{th}$ element | $\overline{x}(t) = [x_1(t), x_2(t), x_3(t), ..., x_N(t)]^T$, |
| $X$ | Matrix consists of received signal vectors | $X = [\overline{x}_1(t), \overline{x}_2(t), \overline{x}_3(t), ..., \overline{x}_N(t)]^T$, |
| $\overline{s}(t)$ | Adaptive array output vector | $\overline{s}(t) = W^T X$ |
| $w_m, W$ | Weight on the $m^{th}$ received signal and weighting vector | $W = [w_1, w_2, w_3, ...w_N]^T$, |
| $y_k(t), \overline{y}(t)$ | $k^{th}$ signal source and signal source vector | $\overline{y}(t) = [y_1(t), y_2(t), y_3(t), ..., y_N(t)]^T$, |
| $Y$ | Matrix consists of signal source vectors | $Y = [\overline{y}_1(t), \overline{y}_2(t), \overline{y}_3(t), ..., \overline{y}_N(t)]^T$, |

**Table 2.2** (continued)

| | | |
|---|---|---|
| $\theta_k$ | Arrival angle of the $k^{th}$ signal source | $\theta_1 = 30°$ |
| $\bar{a}(\theta), A$ | Steering vector and steering matrix | $\bar{a}(\theta) = \left[1, e^{-j2\pi f_c \tau_2(\theta)}, e^{-j2\pi f_c \tau_3(\theta)}, ..., e^{-j2\pi f_c \tau_M(\theta)}\right]^T$ <br> $A = \left[\bar{a}(\theta_1), \bar{a}(\theta_2), ...\bar{a}(\theta_p)\right]$ |
| $u(t), \bar{u}(t)$ | Noise and noise vector | $\bar{u}(t) = [u_1(t), u_2(t), ..u_p(t)]^T$ |
| * | Complex conjugate | $(a+jb)^* = a - jb$ |
| $[\ ]^T$ | Transposition | $\begin{bmatrix} a & b \\ c & d \end{bmatrix}^T = \begin{bmatrix} a & c \\ b & d \end{bmatrix}$ |
| $[\ ]^H$ | Conjugate transposition | $\begin{bmatrix} a & b \\ c & d \end{bmatrix}^H = \begin{bmatrix} a^* & c^* \\ b^* & d^* \end{bmatrix}$ |
| $[\ ]^{-1}$ | Inverse matrix | $\begin{bmatrix} a & b \\ c & d \end{bmatrix}\begin{bmatrix} a & b \\ c & d \end{bmatrix}^{-1} = \begin{bmatrix} 1 & 0 \\ 0 & 1 \end{bmatrix} = I$ |
| $I$ | Unit matrix | $\begin{bmatrix} 1 & 0 \\ 0 & 1 \end{bmatrix}$ |

In each branch of the array elements, the received signal can be expressed by a vector which is referred to the "steering vector". It is defined by

$$\bar{a}(\theta) = \left[1, e^{-j2\pi f_c \tau_2(\theta)}, e^{-j2\pi f_c \tau_3(\theta)}, ..., e^{-j2\pi f_c \tau_M(\theta)}\right]^T, \tag{2.11}$$

where

$$\tau_i = \frac{(i-1)d\sin(\theta)}{c}, \tag{2.12}$$

$d$ is the inter element between the array antenna and $c$ is the wave velocity. In this case $\bar{a}(\theta)$ from (2.11) and $U_d$ from (2.5) are similar, but the difference is, $\bar{a}(\theta)$ is

used with all impinge signal sources at the array. On the contrary, $U_d$ is only used with the desired signal source. Therefore, with the vector expression, the vector $\bar{x}(t)$ received at the $N$ elements array antenna, where the incident angle of certain signal $y(t)$ is $\theta$, can be expressed by $\bar{x}(t) = \bar{a}(\theta)y(t)$. In order to provide a more realistic model, a noise term is added to each element of antenna array to yield equation (2.13).

$$\bar{x}(t) = \bar{a}(\theta)y(t) + \bar{u}(t), \tag{2.13}$$

where $\bar{u}(t)$ is a noise vector composing of elements $\bar{u}_k(t)$.

When the multiple signals $y_1(t), y_2(t), ...y_p(t)$ impinge at the angles $\theta_1, \theta_2, ..\theta_p$ at the received array antenna, the received signal vector can be given by

$$\bar{x}(t) = \sum_{k=1}^{P} \bar{a}(\theta_k)y_k(t) + \bar{u}(t). \tag{2.14}$$

In addition, with $\bar{y}(t) = \left[ y_1(t), y_2(t), ....y_p(t) \right]^T$, thereby the steering matrix is defined as

$$A = \left[ \bar{a}(\theta_1), \bar{a}(\theta_2), ...\bar{a}(\theta_p) \right]. \tag{2.15}$$

Thus the following vector matrix expression is provided:

$$\bar{x}(t) = A\bar{y}(t) + \bar{u}(t). \tag{2.16}$$

## 2.6 Vector Matrix of Adaptive Array Signal Calculation

In adaptive array processing, the array signals must calculate statistics, vectors and matrices, respectively. This section considers the statistics which will be defined and briefly described the vector matrix calculations.

The processing of adaptive array signals often utilizes correlations between signals received at the antenna elements and another correlated signal. In the case of the correlations between signals of the array elements, this refers to the vector and

matrix which arrayed as the "covariance vector" and "covariance matrix". They can be defined as (2.17) and (2.18), respectively [8, 9].

$$\bar{r}_{xd} = E\{\bar{x}(t)d^*(t)\} \tag{2.17}$$

and

$$R_{xx} = E\{\bar{x}(t)\bar{x}^H(t)\}. \tag{2.18}$$

Substituting the array received vector $\bar{x}(t)$ in equation (2.16) into equation (2.18) and expanding the equation, we obtain

$$R_{xx} = E\{\bar{x}(t)\bar{x}^H(t)\}$$

$$= AE\{\bar{y}(t)\bar{y}^H(t)\}A^H + AE\{\bar{y}(t)\bar{u}^H(t)\} + E\{\bar{u}(t)\bar{y}^H(t)\}A^H + E\{\bar{u}(t)\bar{u}^H(t)\}. \tag{2.19}$$

Assuming that the observation noise is Gaussian white noise with a variance of $\sigma^2$ having no correlation with the signal source, the second and third terms become zero. In this case, the covariance matrices of the signal source $\bar{y}(t)$ and the noise $\bar{u}(t)$ can be given by

$$Y \equiv E\{\bar{y}(t)\bar{y}^H(t)\} \tag{2.20}$$

and

$$U \equiv E\{\bar{u}(t)\bar{u}^H(t)\} = \sigma^2 I. \tag{2.21}$$

Then, the following equation is provided :

$$R_{xx} = AYA^H + \sigma^2 I. \tag{2.22}$$

The latter covariance structure is a reflection of the noise having a common variance $\sigma^2$ at all sensors and being uncorrelated among all sensors. Such noise is usually termed spatially white, and is a reasonable model, such as received noise. Whereas, other manmade noise sources need not result in spatial whiteness, in which case the noise must be pre-whitened in many of the methods to be described. In addition, the source covariance matrix, $Y$, is often assumed to be nonsingular or near-singular for highly correlated signals.

In the later development, the spectral factorization of $R_{xx}$ will be of central importance, and its positivity is generally ensured in the covariance matrix for the array antenna received signal which guarantees the following representation [9],

$$R_{xx} = AYA^H + \sigma^2 I = V\Lambda V^H, \tag{2.23}$$

where $V$ is the unitary matrix and $\Lambda$ is the diagonal matrix of real eigenvalues having an order of $\lambda_1 \geq \lambda_2 \geq \lambda_3 \geq ... \geq \lambda_M > 0$. Each is expressed as follows:

$$\Lambda = \begin{bmatrix} \lambda_1 & 0 & 0 \\ 0 & \ddots & 0 \\ 0 & 0 & \lambda_M \end{bmatrix} \tag{2.24}$$

and

$$V = [\overline{v}_1, \overline{v}_2, ..., \overline{v}_M]. \tag{2.25}$$

Here, the eigenvalue $\lambda_i$ and eigenvector $\overline{v}_i$ satisfy the relationship $R_{xx}\overline{v}_i = \lambda_i \overline{v}_i$. The vector orthogonal to matrix $A(M \times P)$ is the eigenvector of $R_{xx}$ having an eigenvalue of $\sigma^2$ indicates that as many as $M - P$ independent eigenvectors exist. As the other eigenvalues become larger than $\sigma^2$ (specifically, $\lambda_1 \geq \lambda_2 \geq ... \geq \lambda_P > \lambda_{P+1} = ... = \lambda_M = \sigma^2$), the pair of an eigenvalue and an eigenvector can be used to separate the signal space from the noise space. Equation (2.23) is rewritten as

$$R_{xx} = V_y \Lambda_y V_y^H + V_u \Lambda_u V_u^H, \tag{2.26}$$

where

$$\Lambda_y = \begin{bmatrix} \lambda_1 & 0 & 0 \\ 0 & \ddots & 0 \\ 0 & 0 & \lambda_P \end{bmatrix} \tag{2.27}$$

and

$$\Lambda_u = \begin{bmatrix} \lambda_{P+1} & 0 & 0 \\ 0 & \ddots & 0 \\ 0 & 0 & \lambda_M \end{bmatrix}. \tag{2.28}$$

Meanwhile

$$V_y \equiv [\overline{v}_1, \overline{v}_2, ..., \overline{v}_P] \tag{2.29}$$

and

$$V_u \equiv [\overline{v}_{P+1}, ..., \overline{v}_M], \tag{2.30}$$

where $\overline{v}_{P+1} = \overline{v}_{P+2} =, ..., \overline{v}_M = \sigma^2$. Since all noises eigenvectors are orthogonal to $A$, the columns of $V_y$ must span the range space of $A$ whereas those of $V_u$ span its orthogonal complement (the nullspace of $A^H$). The projection operators for the signal and noise space are defined as shown below:

$$\Pi = V_y V_y^H = A(A^H A)A^H \tag{2.31}$$

and

$$\Pi^{\perp} = V_u V_u^H = I - A(A^H A)A^H , \tag{2.32}$$

provided that the inverse in the expressions exists. It then follows

$$I = \Pi + \Pi^{\perp}. \tag{2.33}$$

According to the aforementioned of covariance matrix calculation, all formulations are assumed the existence of exact quantities, i.e. infinite observation time. It is clear that in practice only sample estimates, thus a natural estimate of covariance matrix ($R_{xx}$) is the sample covariance matrix

$$R_{xx} = \frac{1}{N}\sum_{t=1}^{N} \overline{x}(t)\overline{x}^{H}(t). \tag{2.34}$$

This representation will be extensively used in the description and implementation of the subspace-based estimation algorithms.

## 2.7 Degrees of Freedom

The degrees of freedom [8] is the one factor that affects the performance obtainable with an adaptive array. This is the basic limitation that affects any adaptive array and does not depend on the particular weight control technique used.

Degrees of freedom is the first limitation that must be aware of an $N$-element array has only $N$-1 degrees of freedom in its pattern. Therefore, there is a limit to the number of events an array pattern can provide at one time.

Starting with considering an N-element array as shown in Fig. 2.3, assume a unit amplitude signal at frequency $\omega$ impinges in the angle $\theta$ with respect to broadside. This signal produces the signal vector [8] in the array as

$$X = e^{j\omega t}\left[1 \;\; e^{-j\phi_2} \cdots \; e^{-j\phi_N}\right]^{T}, \tag{2.35}$$

where

$$\phi_j = \frac{2\pi L_j \sin(\theta)}{\lambda}. \tag{2.36}$$

In this relation, the signal on the element 1 is arbitrarily assumed to have zero phase and the variable $\phi_j$ is the phase shift between the element 1 and the element $j$. $L_j$ is the distance between the $1^{st}$ element and the $j^{th}$ element and $\lambda$ is the wavelength at frequency $\omega$. The signal from each element is multiplied by a complex weight $w_j$ and summed to give the output signal $\overline{s}(t)$ of an array as

$$\overline{s}(t) = \left[ w_1 + w_2 e^{-j\phi_2} + ... + w_N e^{-j\phi_N} \right] e^{j\omega t} . \tag{2.37}$$

The quantity in brackets is defined as $f(\theta)$,

$$f(\theta) = w_1 + w_2 e^{-j\phi_2} + ... + w_N e^{-j\phi_N} . \tag{2.38}$$

The function $f(\theta)$ is the voltage pattern for any given set of $w_j$ of the array. When the factor one of weights is out of the expression for $f(\theta)$. If $w_1$ is factored out, $f(\theta)$ is

$$f(\theta) = w_1 [1 + \frac{w_2}{w_1} e^{-j\phi_2} + ... + \frac{w_N}{w_1} e^{-j\phi_N}] . \tag{2.39}$$

In this form, the dependence of $f(\theta)$ on $\theta$ is contained in the bracketed term. The factor $w_1$ has no effect on the shape of the pattern (i.e., its relative strength at different angles). It merely controls the overall amplitude and phase of the entire pattern. Under these circumstances, there are $N-1$ coefficients $(w_2/w_1, w_3/w_1, ..., w_N/w_1)$ in the bracketed term. It can be seen that there are $N-1$ degrees of freedom in $f(\theta)$.

## 2.8 Concluding Remarks

The basic concepts and the mathematical models of adaptive array antenna are described and considered. The operation and mechanism of adaptive array antenna are obtained and illustrated. The adaptive array antenna schemes and their characteristics are briefly explained since the weight determination of each type is different from each other. The descriptive main types of adaptive algorithm are

shown. The first one is the independent of data scheme that its weight determination is FIR filter design technique. The second is the dependent of data algorithm which composes of reference signal method LMS, LCMV method and Howells–Applebaum method which their weight determinations consider the mean square error minimizing, output power minimizing with a directional constraint and output SINR maximizing with a steering vector, respectively. The description of the last type is blind algorithm that is CMA method by using the fluctuations minimizing of array output amplitude for the weight determination. Besides the various typical adaptive array algorithms above, the array signal model is also important and needs to be considered because it is the basic of adaptive algorithms. In this section, the array signal model expresses the principle concepts of array signal model which are used in adaptive array model.

Furthermore, the adaptive array model is described and explained for using with adaptive array process. The adaptive array model can be obtained from array signal model and also uses the vector matrix model which is achieved in the adaptive array vector matrix expression. In case of adaptive array vector matrix expression section, the array vector matrices need to be used in adaptive array process which is shown in Table 2.2. The major parameters and their examples are summarized and exemplified.

In addition, the vector matrices of adaptive array are calculated and proceed. The array covariance vectors and matrices are computed and calculated for determining the complex weight of array beamforming and direction finding of adaptive array antenna in the next chapter.

Moreover, the degrees of freedom, the factor that affects to the limitation of adaptive array antenna performance, is explained and proved. This limitation is also unavoidable and needs to be considered before achieving adaptive array processing.

# CHAPTER 3
# ADAPTIVE ARRAY BEAMFORMING

## 3.1 Introduction

Adaptive array processing techniques play an important role in enhancing the performance of array antenna used to receive signal in the presence of interference. These antenna systems are composed of many components which the one important component is beamforming system that attempts to enhance the desired signal and suppress the interference signals [4, 5]. The objective of an adaptive antenna is to select a set of amplitude and phase weights with which to combine the outputs from the elements of an array to provide the far field pattern for optimizing the reception of desired signal [2]. According to, the beamforming techniques briefly explained in chapter 2, it was found that they have their limitations. Some techniques require the desired signal waveform, while the others need the incident angle knowledge or the direction of arrival (DOA) of the received signal [3, 12]. Thus this chapter presents the concepts of beamforming methods which will be used in the research of this thesis and also the DOA estimation techniques. The detail of this chapter begins with the antenna beam pattern derivation followed by classical beamforming method [5]. The next is linearly constrained minimum-variance (LCMV) method [5, 9, 13], then the Applebaum array that was proposed by Sidney P. Applebaum [8, 14] will be explained. The improved technique of Applebaum array algorithm that was called an automatic gain controller (AGC) Applebaum array by Kyu-Man Lee and Dong-Seog Han [3] will be addressed. The final section is the estimation of direction of signal arrival that consists of conventional method [5], Capon's minimum-variance method [5, 9, 15, 16], multiple signal classification (MUSIC) method [5, 17] and spatial smoothing technique [9, 18].

## 3.2 Antenna Beam Pattern Derivation

According to (2.10) the received signals at the elements of the array antenna are given respective weights, then are synthesize for the output power of the system as

$$s(t) = w^T \bar{x}(t) = w^H \bar{a}(\theta) y(t) . \tag{3.1}$$

Thus

$$E\{s(t)s^*(t)\} = E\left\{(w^H\bar{a}(\theta)y(t))(y^*(t)\bar{a}^H(\theta)w)\right\}$$

$$= w^H\bar{a}(\theta)E\left\{y(t)y^*(t)\right\}\bar{a}^H(\theta)w$$

$$= \left|w^H\bar{a}(\theta)\right|^2$$

$$\triangleq P(\theta). \tag{3.2}$$

$P(\theta)$ in equation (3.2) is referred to the antenna beam pattern which provides the array antenna output in the direction $\theta$ when weights $w$ are given.

### 3.3 Classical Beamforming

The classical beamforming scheme [19] is a simple beamforming that sets an angular direction ($\theta$) by only adjusting the weights on the phase of the antenna. The weight vector is adjusted to provide the desired beamforming response independent of the received signal. Their weights in the data independent beamformer do not depend on the array data and suitable beamforming response, are chosen. In this case, the scheme is similar to the classical filter design. For instance, the undesired signals from other directions should be rejected. On the contrary, the desired signal from a certain direction should be received which are the requirements. This requirement is in the same way to that in the design of a band-pass or band stop filter. When the geometry of the array antenna is linear and antenna directivity is set at one angular, the weights are provided as [5, 19]

$$w_c = \left[w_1, w_2, ..., w_M\right]^T, \tag{3.3}$$

where

$$w_m = \frac{1}{\sqrt{M}} e^{-j2\pi \frac{d \sin\theta}{\lambda_c}(m-1)} . \quad (3.4)$$

That is similar to the steering vector in equation (2.11). The output power can be given by

$$P_c(\theta) = w_c^H R_{xx} w_c . \quad (3.5)$$

As the directivity of antenna matches one of the signals, output of the signal incident from this direction can be precisely estimated. In this beamforming scheme, the beam pattern can set its main beam in only one direction from all arrival signal directions.

## 3.4 Linearly Constrained Minimum-Variance (LCMV) Method

Using linear constraint is a very general approach that permits extensive control over adapted response of the beamforming system. The linearly constrained minimum-variance (LCMV) method [13, 19] suppresses arriving interference signals from the directions other than that of the desired signal [9, 13]. This method is based on the principle that the weights are adjusted to minimize the output power of adaptive array under the conditions which are set in consideration of the adaptive array space and its frequency response characteristic [19]. Thus the objective of this approach is to minimize the mean-squared output,

$$\min_w E[|s(t)|^2] = \min_w w^H R_{xx} w \quad (3.6)$$

subject to the following linear constraint:

$$C^H w = h , \quad (3.7)$$

where $C$ is the *constraint matrix*, consisting of constraint vector $c_i$ and $h$ is *constraint response vector*. The minimization condition of output power from (3.6) and (3.7) can provide the weight formulation by using Lagrange's undetermined coefficients method [20, 21], as illustrated below:.

From the Lagrange multiplier, $\lambda$ and the minimizing unconstrained objective function:

$$Q_R(w,\lambda) = w^H R_{xx} w + \lambda(h - w^H C) \tag{3.8}$$

is set the gradient of $Q_R(w,\lambda)$ with respect to $w^H$ equal to zero. Since

$$\nabla_{(w^H)} Q_R(w,\lambda) = R_{xx} w - \lambda C = 0, \tag{3.9}$$

then

$$w = \lambda R_{xx}^{-1} C. \tag{3.10}$$

The value of Lagrange multiplier is then found by setting the derivative of $Q_R(w,\lambda)$ with respect to $\lambda$ equal to zero can be illustrated as

$$\frac{\partial Q_R(w,\lambda)}{\partial \lambda} = h - w^H C = 0, \tag{3.11}$$

thus

$$w^H = C^{-1} h. \tag{3.12}$$

Substituting (3.12) into (3.10) gives

$$(hC^{-1})^H = \lambda R_{xx}^{-1} C \tag{3.13}$$

and solving for $\lambda$ as

$$\lambda = (R_{xx}^{-1} C)^{-1} (hC^{-1})^H$$

$$= (C^H R_{xx}^{-1} C)^{-1} h. \tag{3.14}$$

Lastly, substituting (3.14) into (3.10) yields

$$w_{opt} = R_{xx}^{-1}C(C^H R_{xx}^{-1}C)^{-1}h\,. \tag{3.15}$$

The constraint matrix $C$ can be set as the desired signal, while this expression $h$ is set as a complex constant.

The single linear constraint in (3.7) is easily generalized to multiple linear constraints for added control over the beampattern. For instance, if there is the interference source fixing at a known direction $\phi$, then it maybe desirable to force to equal zero gain in that direction in addition to maintaining the response $h$ to the desired signal direction $\theta$ [19, 22]. Its constraint matrix and constraint response vector can be expressed as

$$\begin{bmatrix} a^H(\theta, f) \\ a^H(\phi, f) \end{bmatrix} w = \begin{bmatrix} h^* \\ 0 \end{bmatrix}. \tag{3.16}$$

From above, the weights are optimized to maintain the antenna gain by $h$ in a desired direction, and 0 in the other directions. Therefore the weights can be determined to make the arrived signal from the desired angular direction $\theta$ pass to the output, and shut the arrived signal from interfering angular direction $\phi$ off.

## 3.5 Applebaum Array

The Applebaum array or Howells-Applebaum adaptive antenna proposed by S. P. Applebaum [14] was widely known since 1976. The Applebaum array is based on the concept of maximizing the desired-to-undesired (interference and noise) signal ratio at the array output [8, 14, 19]. This beamforming method also suppressed interfering signals arriving from directions other than that of the desired signal direction [3, 8]. In addition, this method needs its incident angle knowledge for determining weight that can be provided by the DOA estimation. The DOA of the desired signal is input to the adaptive antenna via a steering vector that is the complex conjugate of the array response vector of the desired signal [8].

As the aforementioned that Applebaum array is based on the maximization of the desired signal to undesired signal ratio, thus the optimum weight of the

Applebaum array method can be derived by using the desired signal-to-interference-plus-thermal noise ratio (SINR) [8] as

$$SINR = \frac{P_d}{P_u} = \frac{P_d}{P_i + P_n}, \tag{3.17}$$

where $P_d$, $P_u$, $P_i$ and $P_n$ are desired signal power, undesired signal power, interference signal power and noise power, respectively. They can be given as

$$P_d = \frac{1}{2}\mathrm{E}\left\{\left|\overline{s}_d(t)\right|^2\right\}, \tag{3.18}$$

$$P_i = \frac{1}{2}\mathrm{E}\left\{\left|\overline{s}_i(t)\right|^2\right\} \tag{3.19}$$

and

$$P_n = \frac{1}{2}\mathrm{E}\left\{\left|\overline{s}_n(t)\right|^2\right\}. \tag{3.20}$$

The total undesired power at the array output is defined by $P_u$ to be

$$P_u = P_i + P_n. \tag{3.21}$$

Meanwhile, the received desired signal $X_d$ as illustrated in (2.6) of the previous chapter, can provide the output desired signal from the array as

$$\overline{s}_d(t) = W^T X_d = aW^T U_d. \tag{3.22}$$

Therefore, the output desired signal power can be written

$$P_d = \frac{1}{2}\mathrm{E}\left\{\left|\overline{s}_d\right|^2\right\} = \frac{1}{2}\mathrm{E}\left\{\left|a\right|^2\right\}\left|W^T U_d\right|^2. \tag{3.23}$$

In case of received undesired signal power $P_u$, it can be expressed by using covariance matrix $R_{xx}$ and the complex weight matrix $W$ as

$$R_{xx} = \mathrm{E}(X^* X^T) = \mathrm{E}(X_d^* X_d^T) + \mathrm{E}(X_i^* X_i^T) + \mathrm{E}(X_n^* X_n^T)$$

$$= R_d + R_i + R_n . \tag{3.24}$$

Note that

$$R_{xx} = R_d + R_u , \tag{3.25}$$

where

$$R_u = R_i + R_n . \tag{3.26}$$

In order to provide the weight vector $W$, the undesired signal at the output $\overline{s}_u(t)$ of an array is

$$\overline{s}_u(t) = \overline{s}_i(t) + \overline{s}_n(t) = W^T (X_i + X_n) = (X_i + X_n)^T W . \tag{3.27}$$

Therefore, the undesired output power is

$$P_u = \frac{1}{2}\mathrm{E}\left\{|\overline{s}_u|^2\right\} = \frac{1}{2}\mathrm{E}\left\{\left|W^T (X_i + X_n)\right|^2\right\} = \frac{1}{2}\mathrm{E}\left\{W^H (X_i^* + X_n^*)(X_i^T + X_n^T) W\right\}$$

$$= \frac{1}{2} W^H \left[\mathrm{E}(X_i^* X_i^T) + \mathrm{E}(X_n^* X_n^T)\right] W$$

$$= \frac{1}{2} W^H \left[R_i + R_n\right] W = \frac{1}{2} W^H R_u W . \tag{3.28}$$

Thus, the quantity to be the maximized in the Applebaum array is

$$SINR = \frac{P_d}{P_u} = \frac{\frac{1}{2}E\left\{|a|^2\right\}\left|W^T U_d\right|^2}{\frac{1}{2}W^H R_u W} = \mathrm{E}\left\{|a|^2\right\}\frac{\left|W^T U_d\right|^2}{W^H R_u W}. \tag{3.29}$$

To determine the optimum complex weight, the coordinates of the weight vector will be made the rotation. Let

$$W = AV, \tag{3.30}$$

where $A$ is an $N \times N$ matrix and $V$ is an $N \times 1$ column vector with elements $v_i$. Substituting (3.30) into (3.28) yields

$$P_u = \frac{1}{2}V^H A^H R_u A V. \tag{3.31}$$

The matrix $A$ may be chosen so that

$$A^H R_u A = I, \tag{3.32}$$

$$R_u = (AA^H)^{-1}, \tag{3.33}$$

a relation (3.33) will be useful later.

From this stage, the transformation matrix $A^T$ will transform $X_d$, $X_i$, $X_n$ to $K_d$, $K_i$, $K_n$ that can be shown in Fig. 3.1, which can represent as

$$K_i = A^T X_i, \tag{3.34}$$

$$K_n = A^T X_n, \tag{3.35}$$

$$K_d = A^T X_d = aA^T U_d = aZ_d, \tag{3.36}$$

where

$$Z_d = A^T U_d . \tag{3.37}$$

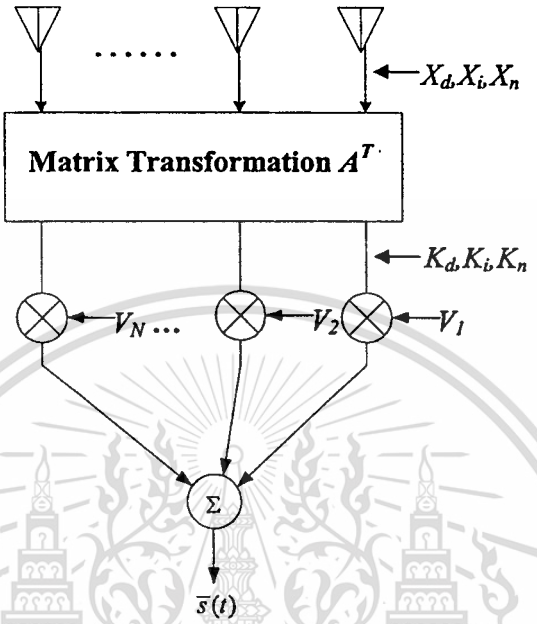


**Fig. 3.1** The transformation $A^T$

Therefore, the desired signal at the output of an array can be obtained as

$$\bar{s}_d(t) = V^T K_d = aV^T Z_d , \tag{3.38}$$

then the output power of the desired signal is

$$P_d = \frac{1}{2}\mathrm{E}\left\{\left|\bar{s}_d(t)\right|^2\right\} = \frac{1}{2}\mathrm{E}\left[|a|^2\right]\left|V^T Z_d\right|^2 . \tag{3.39}$$

Thus inserting (3.31), (3.32) and (3.39) in (3.29), one obtains

$$SINR = \frac{P_d}{P_u} = \mathrm{E}\left[|a|^2\right]\frac{\left|V^T Z_d\right|^2}{V^H V} . \tag{3.40}$$

The ratio in (3.40) is maximized by choosing

$$V = V_{opt} = \mu Z_d^*, \tag{3.41}$$

where $\mu$ is an arbitrary constant. In this case, we use the Schwarz inequality:

$$\left|V^T Z_d\right|^2 = \left|\sum_{i=1}^{N} v_i z_{di}\right|^2 \le \sum_{i=1}^{N}|v_i|^2 \sum_{i=1}^{N}|z_{di}|^2 = V^H V Z_d^H Z_d, \tag{3.42}$$

where $v_i$ and $z_{di}$ are the components of $V$ and $Z_d$, respectively. Substituting this inequality into (3.40) yields

$$SINR = \frac{P_d}{P_u} \le \mathrm{E}\left[|a|^2\right] \frac{V^H V Z_d^H Z_d}{V^H V} = \mathrm{E}\left[|a|^2\right] Z_d^H Z_d. \tag{3.43}$$

In contrast, if $V = \mu Z_d^*$ one finds from (3.40) that

$$SINR = \frac{P_d}{P_u} = \mathrm{E}\left[|a|^2\right] \frac{\mu^2 (Z_d^H Z_d)^2}{\mu^2 (Z_d^T Z_d^*)} = \mathrm{E}\left[|a|^2\right] Z_d^H Z_d. \tag{3.44}$$

Consequently, the SINR achieves its maximum possible value for the $V$ in (3.41). However, the weight vector $V_{opt}$ applied after the transformation $A^T$ is equivalent to a weight vector $W$ given by

$$W = W_{opt} = A V_{opt} = \mu A Z_d^*. \tag{3.45}$$

Inserting in (3.37) for $Z_d$ and then using (3.33) yields

$$W_{opt} = \mu A A^H U_d^* = \mu R_u^{-1} U_d^*. \tag{3.46}$$

The Applebaum feedback loop structure [8] can be shown as Fig. 3.2.

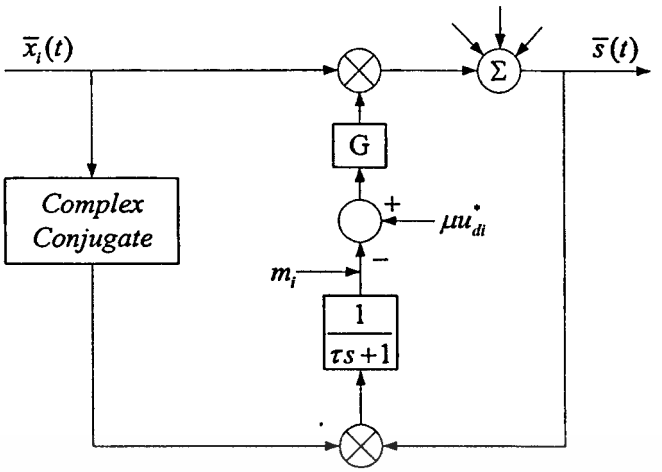


**Fig. 3.2** The Applebaum feedback loop

From the $W_{opt}$ illustrated in (3.46), it is achieved by using the diagram in Fig. 3.2. In this figure, $G$ is a gain constant, $\tau$ is the time constant of the lowpass filter, $s$ denotes the complex frequency and the variable $u_{di}^*$ is the $i$th element of $U_d^*$. To show that the loop in Fig. 3.2 provides the correct steady-state weights $W_{opt}$ in the array, let us determine the differential equation for $w_i$ with this loop. Let the output of the lowpass filter be denoted by $m_i$ as indicated in Fig. 3.2. Then $m_i$ satisfies the equation

$$\tau \frac{dm_i}{dt} + m_i = \bar{x}_i^*(t)\bar{s}(t). \tag{3.47}$$

However, $w_i$ is related to $m_i$ by

$$w_i = G[\mu u_{di}^* - m_i], \tag{3.48}$$

thus,

$$m_i = \mu u_{di}^* - \frac{1}{G} w_i, \tag{3.49}$$

and

$$\frac{dm_i}{dt} = -\frac{1}{G}\frac{dw_i}{dt}. \tag{3.50}$$

Substituting (3.49) and (3.50) into (3.47) provides the differential equation for $w_i$,

$$\frac{\tau}{G}\frac{dw_i}{dt} + \frac{w_i}{G} = \mu u_{di}^{*} - \overline{x}_i^{*}(t)\overline{s}(t). \tag{3.51}$$

In vector notation, this becomes

$$\frac{\tau}{G}\frac{dW}{dt} + \frac{W}{G} = \mu U_d^{*} - X^{*}\overline{s}(t). \tag{3.52}$$

Finally, inserting $\overline{s}(t) = X^T W$ and rearranging gives

$$\frac{\tau}{G}\frac{dW}{dt} + [\frac{1}{G}I + X^{*}X^{T}]W = \mu U_d^{*}. \tag{3.53}$$

As mentioned in chapter 2, we approximate $X^{*}X^{T}$ in (3.53) by

$$X^{*}X^{T} \to E(X^{*}X^{T}) = R_{xx}, \tag{3.54}$$

therefore, the weight differential equation becomes

$$\frac{\tau}{G}\frac{dW}{dt} + [\frac{1}{G}I + R_{xx}]W = \mu U_d^{*}. \tag{3.55}$$

Thus, with this loop, the steady-state weight vector will be

$$W = [\frac{1}{G}I + R_{xx}]^{-1}\mu U_d^{*}. \tag{3.56}$$

In this case, if the value of loop gain $G$ is large, equation (3.56) is approximated in the same way

$$W \cong \mu R^{-1} U_d^*, \tag{3.57}$$

as a result

$$R_u \cong R_{xx}. \tag{3.58}$$

## 3.6 Automatic Gain Controller (AGC) Applebaum Array

According to the Applebaum array method described in the previous section, this section presents the technique to overcome the eigenvalue spread of the input covariance matrix of an array system by orders of magnitude, that the conventional Applebaum array is unable to remove all interference signals quickly. This particular technique is an automatic gain controller (AGC) Applebaum array [3] which is described in this section.

From the $i^{th}$ feedback loop of the Applebaum array in Fig. 3.2, we first point out that by making a minor change in the feedback loop configuration, the $1/G$ term in (3.56) can be eliminated. It can be shown in Fig. 3.3 instead.

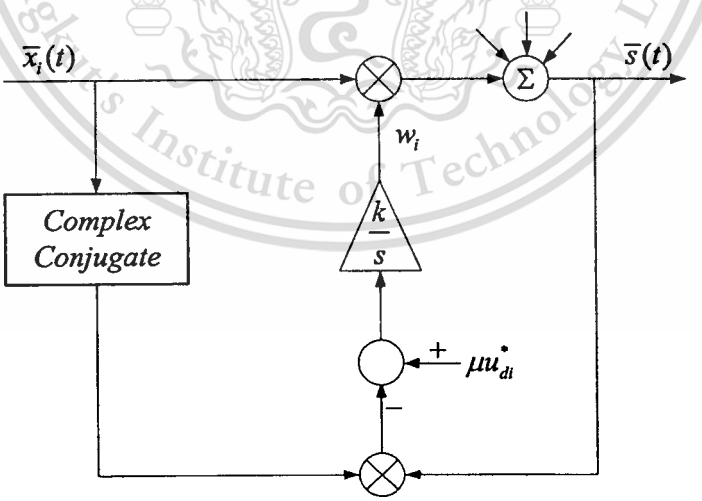


**Fig. 3.3** The Alternative form of Applebaum feedback loop

From Fig. 3.3, it can be considered

$$\frac{dw_i}{dt} = k[\mu u_{di}^* - \bar{x}_i^*(t)\bar{s}(t)], \tag{3.59}$$

where k represents the scalar constant, that (3.59) can be expressed again in the vector form as

$$\frac{dW}{dt} = k[\mu U_d^* - X^*(t)\bar{s}(t)]. \tag{3.60}$$

Substituting $\bar{s}(t) = X^T W$ and rearranging then yields

$$\frac{dW}{dt} + kX^* X^T W = k\mu U_d^* \tag{3.61}$$

and making the substitution by (3.54) then

$$\frac{dW}{dt} + kR_{xx}W = k\mu U_d^*. \tag{3.62}$$

This feedback loop produces the steady-state weight vector

$$W = \mu R_{xx}^{-1} U_d^*. \tag{3.63}$$

In this case, there is no requirement that $G$ be large. Moreover, this Applebaum array can be expressed in discrete form by using the derivation from equation (3.60) that steering vector will be used by considering time variation. Thus the time varying steering vector can be written as

$$T = [t_1, t_2, \ldots]^T. \tag{3.64}$$

The steering vector can be inserted instead of $U_d$ in (3.62), as follow the reference [8, 14]. In this paper, Applebaum also mentioned that it is not necessary to use the vector

$U_d^*$ in the feedback loop. One may use a vector slightly differing from $U_d^*$ that the relation in (3.60) can be given as

$$\frac{dW}{dt} = k[\mu T^* - X^*(t)\overline{s}(t)]. \tag{3.65}$$

Replacing $dW/dt$ by

$$\frac{dW}{dt} \cong \frac{W(n+1) - W(n)}{\Delta t}, \tag{3.66}$$

thus, equation (3.66) can be expressed as

$$W(n+1) - W(n) = k\Delta t[\mu T^* - X^*(t)\overline{s}(t)]. \tag{3.67}$$

For convenience of absorbing $\Delta t$ into the gain constant, let us define

$$\gamma = k\Delta t, \tag{3.68}$$

that yields

$$W(n+1) - W(n) = \gamma[\mu T^* - X^*(t)\overline{s}(t)], \tag{3.69}$$

then

$$W(n+1) = W(n) + \gamma\mu T^* - \gamma X^*(t)\overline{s}(t). \tag{3.70}$$

Inserting $\overline{s}(t) = X^T W$ and rearranging gives

$$W(n+1) + [\gamma X^* X^T - I]W(n) = \gamma\mu T^*, \tag{3.71}$$

then, replacing $X^* X^T$ with $R_{xx}$,

$$W(n+1)+[\gamma R_{xx}-I]W(n)=\gamma\mu T^{*}. \tag{3.72}$$

By rotating coordinates to diagonalize $\gamma R_{xx}-I$ which is described in [8]. The solution of (3.72) is obtained as

$$W(n)=\sum_{i=1}^{N}p_i(1-\gamma\lambda_i)^n+\mu R_{xx}^{-1}T, \tag{3.73}$$

where $\lambda_i$ and $p_i$ are the $i^{th}$ eigenvalue of $R_{xx}$ and the complex scalar constant, respectively. The time constant $\tau_i$ which is the time required for $(1-\gamma\lambda_i)^n$ to decay to $1/e$ can be expressed as

$$\tau_i=\frac{1}{\gamma\lambda_i}. \tag{3.74}$$

According to the derivation above, it is acceptable that Applebaum array completely depends on the eigenvalues of the input covariance matrix. Equation (3.73) converges to a steady-state if the gain constant $\gamma$ is

$$-1<(1-\gamma\lambda_i)<1. \tag{3.75}$$

Hence, the maximum value of $\gamma$ depends on the maximum eigenvalue $\lambda_{max}$, which is similar to the total power of the input interference signal since

$$\lambda_{max}\le\sum_{i=1}^{N}\lambda_i$$

$$=trace\,R_{xx}=\sum_{i=1}^{N}E\left\{\left|x_i(n)\right|^2\right\}=P_T. \tag{3.76}$$

Consequently, if the eigenvalue spread of the input covariance matrix is very high, $\tau$ corresponding to the smallest eigenvalue may be very long. As mentioned, since the

convergence rate depends highly on the minimum eigenvalue, the convergence rate of the system will be very low. Although changing the gain constant of the conventional Applebaum in order to automatically shorten the convergence time is existed, it is just effective when a single interference signal is incident. However, it can not shorten the convergence time while multiple interference signals causing the eigenvalue spread are incident on the array. The modified automatic gain controller (AGC) is used to solve the disadvantages described. The AGC Applebaum array is shown in Fig. 3.4. It is not much different from a conventional Applebaum array except for the additional AGC block, which is the key to improve the eigenvalue spread problem and increasing the array convergence rate. In this case, it is assumed that the desired signal is only present for the short period of time while the interference and thermal noise signals are present during the adaptation period. Suppose that the received signal, $x_i$, at the $i^{th}$ antenna element consists of two interference signals causing a large eigenvalue spread and both signals are uncorrelated which can be separated into

$$x_i = x_{iSI} + x_{iWI} + x_{iN}, \tag{3.77}$$

where $x_{iSI}$, $x_{iWI}$ and $x_{iN}$ are a strong interference signal, weak interference signal, and thermal noise, respectively.

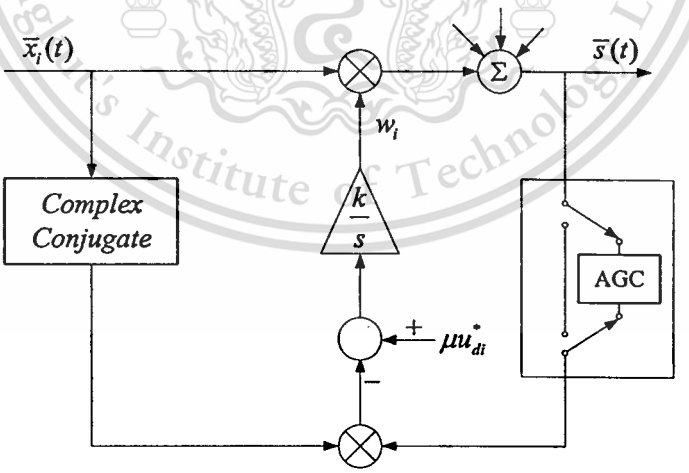


**Fig. 3.4** The AGC Applebaum feedback loop

To calculate the weight vector by using the Applebaum feedback loop, as Fig. 3.3, the cross-correlation, $\phi_i$, between the $i^{th}$ array input and output signals is obtained as

$$\phi_i = x_i^* s = x_i^* \sum_{l=1}^{N} w_l x_l$$

$$= (x_{iSI}^* + x_{iWI}^* + x_{iN}^*)(s_{SI} + s_{WI} + s_N), \tag{3.78}$$

where $s$ and $w_l$ are the output and weights of the array, respectively. When the correlation of the strong interference signal is very high, the interference signal related to the largest eigenvalue is quickly removed even though multiple interference signals are impinged on the array. After a few iterations, only a weak interference signal with a small eigenvalue and thermal noise will remain in the array output. Finally, the cross-correlation between the input and output signals is given by

$$\phi_i = (x_{iSI}^* + x_{iWI}^* + x_{iN}^*)(s_{WI} + s_N). \tag{3.79}$$

Since, the operation of the adaptive feedback loop removes the strong interference signal, the cross-correlation among the weak interference signals will still be low. As a result, making a null pattern in the direction of the low power interfering signal is very hard. When $x_{iSI}$ and $x_{iWI}$ are uncorrelated, the correlation between $x_{iSI}$ and $x_{iWI}$ seems like the noise and does not contribute to change the weights.

To improve the eigenvalue spread, the magnitude of all the eigenvalues is equalized by increasing the correlations between the weak signals at the input and output of the array. The magnitude of each eigenvalue will tend to be directly proportional to the power of the corresponding incident signal. Thus, the problem can be solved by controlling the amplitude of the incident interfering signals.

The characteristic of the AGC block in the feedback loop is to amplify the power level of the remaining signal in the array output up to that of the input signal. Thereafter, the correlation between the low power interference signals becomes as large as that of the high power interference signals. Consequently, the weights of the AGC adaptive array adapt to the remaining interference signal and result in the formation of a null pattern for both interference signals [3].

## 3.7 Estimation of Direction of Signal Arrival

According to some techniques of beamforming require the information of the direction of arrival (DOA), the direction estimation of the arriving signal is important for adaptive array antenna. Therefore, this section illustrates the direction of signal arrival estimation techniques which consist of conventional method, Capon's minimum-variance method, multiple signal classification (MUSIC) method and spatial smoothing technique. The most DOA estimation techniques based on the eigendecomposition of the covariance matrix of the signals received by an array antenna. Generally, most DOA estimation methods are capable to estimate and predict the direction of arrival signal exactly if the arrival signals are noncoherent. In contrast, the arrival signals are so coherent that the DOA methods can not give the effective results. It is due to the coherent signals are correlated with each other, conversely with noncoherent signals which are not correlated. Thus, the spatial smoothing technique that is capable to separate the coherent arrival signals is presented in this section [18].

### 3.7.1 Conventional method

This DOA estimation method uses the beamforming to predict the arrival directions of signals. The characteristic resolution of this method is determined based on aperture length of the array antenna such as the number of elements, thus a large number of antenna elements is possible to give the high resolution. Additionally, this method can precisely estimate the intensity of the arriving signal [5]. As mentioned in the previous section, the array output power in angular direction $\theta$ is given by:

$$P_c(\theta) = w_c^H(\theta) R_{xx} w_c(\theta), \tag{3.80}$$

then

$$w_c(\theta) = [w_1, w_2, ..., w_M]^T, \tag{3.81}$$

where

$$w_m = \frac{1}{\sqrt{M}} e^{-j2\pi \frac{d \sin\theta}{\lambda_c}(m-1)} . \quad (3.82)$$

The direction of arrival signals are estimated by changing $\theta$ and measuring the intensity of this output.

### 3.7.2 Capon's minimum-variance method

Capon method has been introduced by Jack Capon since 1969. This method estimates the direction of received signal or DOA [9, 15, 23, 24] which includes the desired signal arriving from the expected direction and other signals or interference waves arriving from other directions. In order to estimate the arriving signal direction, this method considers the means of minimizing the level of interference caused by signals other than the desired one, by maintaining sensitivity in the target direction. Under these circumstances, the minimization problem is solved under constraint conditions.

$$\min_w w^H R_{xx} w \quad (3.83)$$

subject to

$$\left| w^H a(\theta) \right| = 1 , \quad (3.84)$$

where $a(\theta)$ is the steering vector. In this case, weight vector is obtained by

$$w_c = \frac{R_{xx}^{-1} a(\theta)}{a^H(\theta) R_{xx}^{-1} a(\theta)} . \quad (3.85)$$

It is optimized from the solution of LCMV beamforming method which is already described that $w_{opt} = R_{xx}^{-1} C (C^H R_{xx}^{-1} C)^{-1} h$ from (3.15).

From the array output power derivation in (3.80), thus the intensity of array output at the specific time is given by

$$P_c(\theta) = \frac{1}{a^H(\theta) R_{xx}^{-1} a(\theta)}. \tag{3.86}$$

The DOA of signal sources are found by taking $\theta$ which minimizes $a^H(\theta) R_{xx}^{-1} a(\theta)$ or maximizes $P_c(\theta)$ in (3.86).

### 3.7.3 Multiple signal classification (MUSIC) method

Multiple signal classification or MUSIC method is proposed by Ralph O. Schmidt since 1979. The term of MUSIC is used to explain theoretical and experimental techniques involved in determining the parameters of multiple wavefronts arriving at an antenna array from measurements made on the signals received at the array elements [5, 9, 17, 21, 25]. This technique enables DOA estimation with the exact accuracy since it satisfies these following requirements:

- Data has been collected over the adequate long period.
- SNR is adequate high.
- The signal model is adequate accurate.

The MUSIC method is a relatively simple and efficient eigenstructure method of DOA estimation. In its standard form, also known as spectral MUSIC, the method estimates the noise subspace from the available samples which can be obtained by either eigenvalue decomposition of the estimated array correlation matrix or singular value decomposition of the data matrix.

To derive the MUSIC space spectrum, the first step is considering the eigenvalue decomposition of the covariance matrix which is described in (2.22) of chapter 2:

$$R_{xx} = AYA^H + \sigma^2 I \tag{3.87}$$

and (2.23)

$$R_{xx} = AYA^H + \sigma^2 I = V \Lambda V^H, \tag{3.88}$$

where $V$ is the unitary matrix and $\Lambda$ is the diagonal matrix of real eigenvalues which already illustrated and described in chapter 2.

Among the independent eigenvalues of $R_{xx}$, as many as *M-P* eigenvectors are orthogonal to the matrix, $A(M \times P)$, and have an eigenvalue ($\sigma^2$).

In addition, all eigenvalues of $R_{xx}$ are greater than $\sigma^2$ and $\lambda_1 \geq \lambda_2 \geq \lambda_3 \geq ...$ $... \geq \lambda_P > \lambda_{P+1} = ... = \lambda_M = \sigma^2$. Since $AYA^H$ contains a full rank, $\Lambda_y$ contains as many as $P$ eigenvalues. Then, the noise space can be separated from the signal space by equation (2.26) that is

$$R_{xx} = V_y \Lambda_y V_y^H + V_u \Lambda_u V_u^H$$

$$= V_y \Lambda_y V_y^H + \sigma^2 V_u V_u^H, \tag{3.89}$$

where $\Lambda_y$, $\Lambda_u$, $V_y$ and $V_u$ are illustrated as equation (2.27), (2.28), (2.29) and (2.30), respectively. When the eigenvector of $V_u$ is orthogonal to $A$, the following equation is provided:

$$V_u^H a(\theta_i) = 0, \tag{3.90}$$

where $i$=1, ...,$P$. In the mean time, the relation in equation (3.90) illustrates that the noise vector is orthogonal to the DOA vector, because their scalar product is zero. That means the direction of arriving signal can be determined from the angle which makes the noise vector produces in scalar with $a(\theta_i)$ to be zero since $a(\theta_i)$ is obtained from properly selected angles. Thus, if the incoming signals are coherent signals which are the correlated signals, this method can not classify those signals.

The covariance matrix of the reception vector is practically estimated, and its eigenvector is then separated into signal and noise vectors, as shown by (3.88) and (3.89). In the final stage, the steering vector found is orthogonal to noise vector.

To find the direction of the signal source, the variable $\theta$ in the following equation is scanned to seek the peak response in the MUSIC space spectrum given below:

$$P(\theta) = \frac{a^H(\theta)a(\theta)}{a^H(\theta)V_u V_u^H a(\theta)}. \tag{3.91}$$

### 3.7.4 Spatial smoothing technique

The Capon's minimum-variance method and MUSIC direction finding techniques which are based on the constraint conditions and the eigendecomposition of the covariance matrix of the received signal vector, respectively, are described in the previous section. Both Capon and MUSIC methods have an inability for handling perfectly correlated or highly correlated signals which arise quite often in practice due to the multipath propagation. The multipath phenomenon occurs due to the obstruction posed such as buildings, trees, etc. For this reason, this section presents the spatial smoothing technique which can reduce the influence of signal correlation. This technique makes it possible to use MUSIC method in the presence of arbitrary signal correlation under certain conditions which require a linear uniformly spaced array. This approach is based on estimating the outputs of a virtual array from the outputs of the real array.

This spatial smoothing technique uses the forward and backward of subarrays and uniformly combines the obtained signals in the linear array antenna [18, 21]. Suppose the total number of antenna elements is $M$ and the number of subarray elements is $M_0$, the number of subarrays ($L$) becomes

$$L = M - M_0 + 1. \tag{3.92}$$

The forward subarrays can be expressed by:

$$x_l^f(t) = [\overline{x}_l(t), \overline{x}_{l+1}(t), \overline{x}_{l+2}(t), \ldots, \overline{x}_{l+M_0-1}(t)]^T, \tag{3.93}$$

where

$$l=1,2,\ldots,L \tag{3.94}$$

and the covariance matrix of the forward subarray can be given as

$$R_l^f = E\{\bar{x}_l^f(t)(\bar{x}_l^f(t))^H\}. \tag{3.95}$$

The space averaged covariance matrix ($R^f$), for the forward subarrays is provided by averaging the respective subarrays as

$$R^f = \frac{1}{L}\sum_{l=1}^{L} R_l^f \ . \tag{3.96}$$

In the same way, the backward subarray and covariance matrix are obtained by

$$x_l^b(t) = [\bar{x}_{M-l+1}(t), \bar{x}_{M-l}(t), \bar{x}_{M-l-1}(t), ..., \bar{x}_{L-l+1}(t)]^T \tag{3.97}$$

$$l=1,2,...,L \tag{3.98}$$

$$R_l^b = E\{\bar{x}_l^b(t)(\bar{x}_l^b(t))^H\}, \tag{3.99}$$

$$R^b = \frac{1}{L}\sum_{l=1}^{L} R_l^b \ . \tag{3.100}$$

Thus, finally covariance matrix of Forward/Backward spatial smoothing is completed by:

$$\tilde{R} = \frac{R^f + R^b}{2}. \tag{3.101}$$

This covariance matrix can be used with MUSIC method that is based on the subspace method and uses eigenvalue decomposition.

## 3.8 Concluding Remarks

The concepts of beamforming methods and the DOA estimation methods which are needed for some adaptive beamforming schemes are described in this chapter that composed of:

The first section presents the antenna beam pattern derivation of adaptive array antenna.

In second section, the classical beamforming method is explained. This method uses only the phase adjusting for adapting the main beam pattern of an array antenna to the desired direction but neglecting the other directions of the received signal source.

The third section describes linearly constrained minimum-variance (LCMV) method. This scheme is based on the principle of output power minimization under the linear constraint condition which requires the knowledge of arrival signal directions. The adjusting weight of this beamforming algorithm can be used to set the peak and null patterns in the direction of desired and interfering directions, respectively.

The fourth section illustrates Applebaum array method which is based on the concept of maximizing the desired-to-undesired (interference and noise) signal ratio at the array output. The weight computation of this method needs the incident angle knowledge both desired and undesired or interfering angles. Therefore, this method is capable to form peak and null beam pattern in both desired and interference directions.

The fifth section obtains the automatic gain controller (AGC) Applebaum array that endeavors to overcome the eigenvalue spread problem and increase the array convergence rate in the conventional Applebaum array by using the automatic gain controller in the feedback loop of the Applebaum array.

The last section is the estimation of direction of signal arrival that discusses the direction of arrival estimation methods which consist of the conventional method, Capon's minimum-variance method, multiple signal classification or MUSIC method and the last subsection is spatial smoothing technique that can be used to reduce the influence of signal correlation in DOA estimation. Thus spatial smoothing technique can solve the disadvantage of the coherent signal separation of the DOA estimation.

All concepts in this chapter will be illustrated by the computer simulation results in the next chapter in order to compare and discuss the efficiency and performance later.

# CHAPTER 4
# COVARIANCE MATRIX ADJUSTMENT TECHNIQUE

## 4.1 Introduction

The adaptive array beamforming and the direction of arrival estimation are described and illustrated in the previous chapter. Generally, the beamforming can be effectively used in adaptive array system, but since the level of the incident signal at the array especially the interference to noise ratio (INR) level decreases and fluctuates, the null response pattern in its direction will be disturb and can not set null pattern [3, 4, 26]. Therefore, this chapter presents the proposed technique [4] to overcome the aforementioned problem in the beamforming system of adaptive antenna. This technique includes the specific adjustable multipliers in both desired signal and interference signal covariance matrices of complex weight in order to overcome some disadvantages and improve the interference cancellation efficiency in the beamforming of adaptive array. The proposed beamforming technique is based on the complex weight which uses the covariance matrix for the computation. Thus, the Applebaum array and LCMV are used in this proposed technique. In addition, the computer simulation of those beamforming methods both the conventional techniques and the proposed technique, and their direction of arrival estimation are shown in this chapter.

## 4.2 Covariance Matrix Computation

The covariance matrix is briefly explained in section 2.6 of chapter 2, however this section will describe the covariance matrix computation for using with the proposed covariance matrix adjustment technique. The covariance matrix is the one signal parameter that is important in the weight computation of this technique that it can be represented in the same way of (2.18) as

$$R_{xx} = E\{\overline{x}(t)\overline{x}^{H}(t)\},$$

that can be separated as

$$R_{xx} = E\{\overline{x}(t)\overline{x}^H(t)\}$$

$$= E(\overline{x}_d(t)\overline{x}_d^H(t)) + E(\overline{x}_i(t)\overline{x}_i^H(t)) + E(\overline{x}_n(t)\overline{x}_n^H(t)). \quad (4.1)$$

In vector notation, this becomes

$$R_{xx} = E(XX^H) = E(X_d X_d^H) + E(X_i X_i^H) + E(X_n X_n^H)$$

$$= R_d + R_i + R_n. \quad (4.2)$$

This formulation will be used for the weight computation in this proposed technique.

## 4.3 Covariance Matrix Analysis

From equation (4.2), the covariance matrix is separated into three terms, desired signal, interference signal and noise. In practice, only sample can be estimated, therefore, the natural covariance matrix estimation can be calculated following equation (2.34). Therefore $R_d$, $R_i$ and $R_n$ in (4.2) can be represented as

$$R_d = \frac{1}{N}\sum_{t=1}^{N} \overline{x}_d(t)\overline{x}_d^H(t), \quad (4.3)$$

$$R_i = \frac{1}{N}\sum_{t=1}^{N} \overline{x}_i(t)\overline{x}_i^H(t) \quad (4.4)$$

and

$$R_n = \frac{1}{N}\sum_{t=1}^{N} \overline{x}_n(t)\overline{x}_n^H(t). \quad (4.5)$$

In order to compute the covariance matrices as shown above, the desired received signal and interfering received signal can be provided by using DOA estimations which are described in the previous chapter. In this case, the noise is already included in the desired signal and the interfering signal in the DOA estimation. For this reason,

the covariance matrix of noise is included in the covariance matrix of the desired signal and interference. Thus in the weight computation, the covariance matrix consists of the desired signal covariance matrix and interfering signal covariance matrix. To estimate the number of true DOAs and the power level of each received signal direction, the Capon method is used by applying its output power, to the decision criterion [23, 27]. The Capon's minimum-variance method can be used when the received signals are not correlated (noncoherent signal) with each other, nevertheless Capon method can not be used to estimate the direction of the impinge signals (correlate signal or coherent signal). In that case, the spatial smoothing technique can be applied with the MUSIC to estimate the direction of the received signals.

## 4.4 Covariance Matrix Adjustment Technique

Since the descriptive disadvantage of the conventional techniques occurs when the SNR level of the received signal decreases or the noise increases, we propose the covariance matrix adjustment technique to improve that mentioned disadvantage.

This proposed technique is developed from the AGC Applebaum array that is described in the last chapter. The AGC Applebaum array uses the AGC block in the feedback loop to amplify the power level of the remaining signal at the output of an array, thereby the correlation between the low power interference signals becomes as large as that of the high power interference signals. From this concept, the covariance matrix adjustment technique is proposed by adding the adjustable multipliers to the covariance matrix both interference signal covariance matrix $R_i$ and desired signal covariance matrix $R_d$, in the complex weight analysis, instead of the AGC block in the feedback loop. To increase the low power interference signals correlation, the adjustable multiplier with $R_i$ should be high, meanwhile to decrease the correlation between the high powers of desired signal and interfering signals, the adjustable multiplier with $R_d$ should be low. In contrast, the AGC Applebaum does not consider the correlation of the high desired signal power from the feedback loop at the output, thus it will be an effect for controlling output null beam pattern in the interfering signal directions and output peak response in the desired signal direction. The proposed adjusted covariance matrix ($R_{adj}$) is defined as

$$R_{adj} = BR_d + CR_i . \tag{4.6}$$

Since $B$ multiplies with the desired signal matrix, therefore $B$ has to be low value in complex weight computation. In the mean time $C$ will multiply with the interference covariance matrix, when there is the interference, thus $C$ has to be high value. The value of $B$ and $C$ depend on the value of input signal to noise ratio (SNR) and input interference to noise ratio (INR), respectively. If there are the interference signals from many directions, the interference covariance matrix will consist of many interference covariance matrices. For example, if there are the interference from three directions, $R_i$ will consist of $R_{i1}$, $R_{i2}$ and $R_{i3}$. Hence, $C$ will consist of $C_1$, $C_2$ and $C_3$ that can be expressed as

$$R_{adj} = BR_d + C_1R_{i1} + C_2R_{i2} + C_3R_{i3} . \tag{4.7}$$

In this regard, if each input INR of interference signals is different, each $C_i$ of interference covariance matrices will not be identical.

The values of $B$ and $C$ are considered from the relative input signal of the system. Thus, it is necessary to have the control operation for comparing the input signal level and its threshold which are illustrated as the flow chart in Fig. 4.1. The operation of covariance matrix adjustment technique begins with DOA receives the input signal to estimate the signal directions and their powers. The next process is the decision part for considering the number of interference signals. If there is no interference, the adjusted covariance matrix will be set as desired signal covariance matrix, then its determinant is checked. The covariance matrix will be inverted ($R^{-1}$) in the complex weight computation [9], thus the covariance matrix should be the nonsingular matrix ($\det(R) \neq 0$). The important cause of singular matrix problem is the signal reduction or the weakness of the signal [4] that can be improved by readjusting covariance matrix to increase the values of $B$ and $C$. In addition, this technique has to include the degree of freedom [8, 19] decision to divide and choose the interference in the suitable direction, because the number of null response pattern directions that can be set for interference cancellation of the linear array system is equal to the degree of freedom (N-1), where N is the number of the array elements. If

the number of interference signals is more than the degree of freedom, it is necessary to choose the suitable interference from the consecutive high INR level.

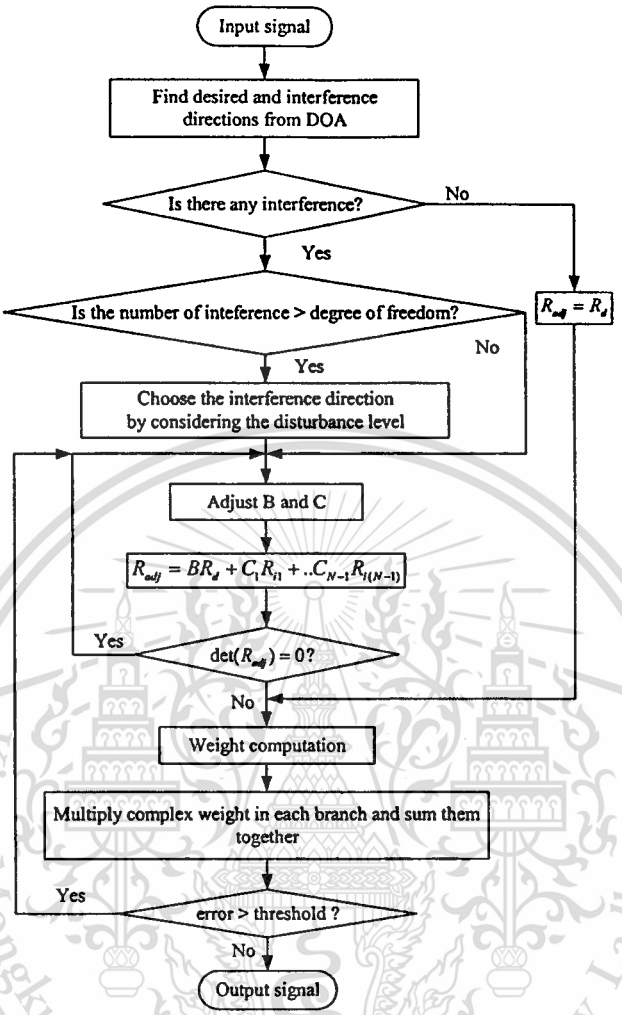


**Fig. 4.1** Flow chart of the proposed technique

After the adjusted covariance matrix is obtained, the complex weight can be computed. We can then see that the weight solution of the improved covariance matrix adjustment technique both Applebaum array and LCMV method will multiply with the input signal of each array element and summed to be an output signal that calculates its error by considering the bit error rate to compare with the threshold for adjusting $B$ and $C$ to be the suitable values.

For example the values of $B$ and $C$ can be considered from Fig. 4.2 and Fig. 4.3 which are the examples of relation between the level of output SINR Applebaum array and $B$ at various $C$ values in the $30^0$, 40 dB SNR desired signal and $60^0$, 30 dB INR interference signal case while the array antenna is 4 elements of half

wavelength dipole. Fig. 4.2 and Fig. 4.3 illustrate that the output SINR in the desired signal direction and the output SINR in the interfering direction are proportional and inversely proportional to the value of $B$ and $C$, respectively. To minimize the output SINR in interfering direction, and maximize the output SINR in the desired direction simultaneously, $B$ and $C$ can be set to 0.002 and 30, respectively, while SNR value of desired signal and INR value of interference signal are between 5 dB and 50 dB.

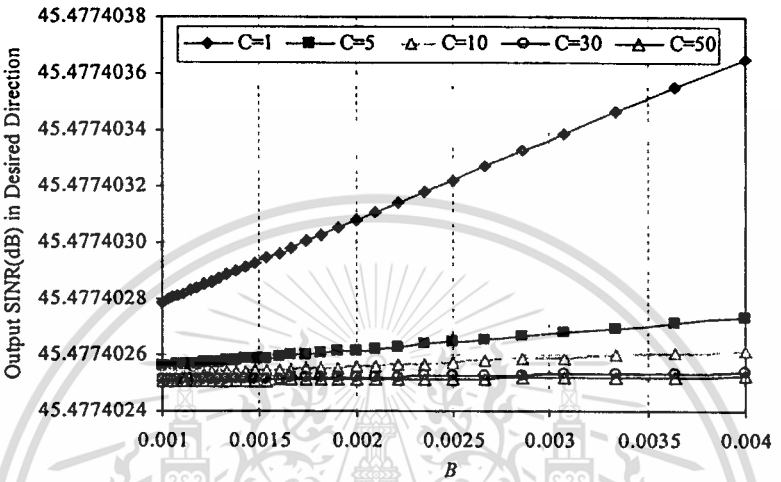


**Fig. 4.2** The comparison of output SINR in the desired direction versus $B$ for various $C$ values of 30° 40 dB SNR desired signal and 60° 30 dB INR interference signal

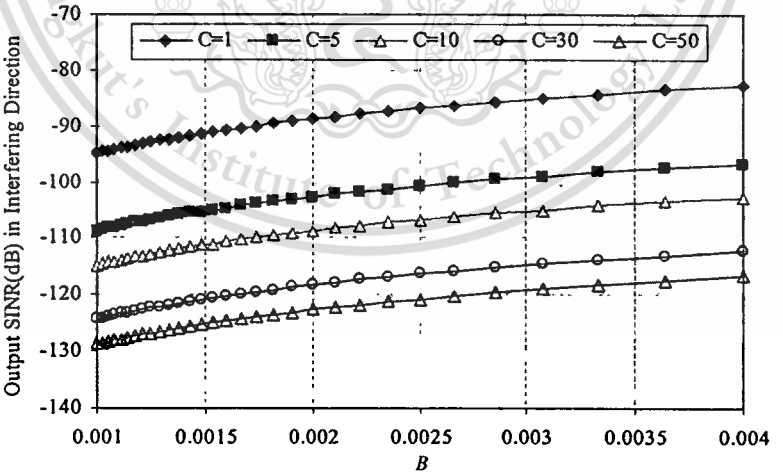


**Fig. 4.3** The comparison of output SINR in the interfering direction versus $B$ for various $C$ values of 30° 40 dB SNR desired signal and 60° 30 dB INR interference signal

When each of the SNR and INRs of the desired signal and interference signals, consecutively changes, $B$ and $C$ will change in the opposite manner. If each of the SNR and INRs increases to be larger than the upper threshold, the values of $B$ and $C$ will be decreased or inversely proportional to their SNR and INR values which relate to the previous revolutionary sample, respectively. On the contrary, if each of the SNR and INRs decrease lowered than the lower threshold, the value of $B$ and $C$ will be increased or inversely proportional to their SNR and INR, respectively. Otherwise, if each of the SNR and INRs are between the upper and the lower thresholds, $B$ and $C$ will change directly proportional to their SNR and INR values which relate to the previous revolutionary sample.

In practice, the $B$ and $C$ values are set by considering the comparative threshold values of both $B$ and $C$ which depend on each system. Thus the B and C threshold values of each system should be provided after the implementation process exists and adjusted when the power level of the received signal changes. The $B$ and $C$ values used in the real experiment will be described in chapter 5. The adjusting operation of the multiplier can be shown as Fig. 4.4.

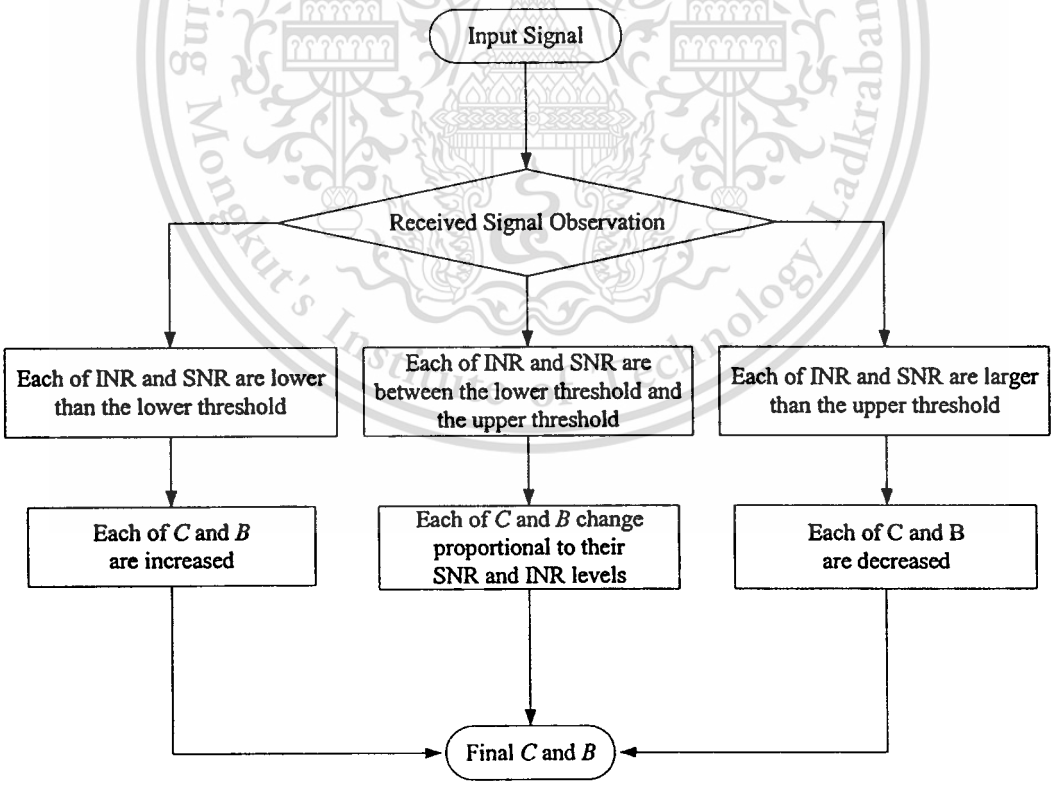


**Fig. 4.4** The flow chart of the adjusting operation of the multiplier $B$ and $C$

In the case of each SNR and INR increases to be larger than the upper threshold or decreases to be lower than the lower threshold:

$$B = B_{ref} \times \frac{Ad_{ref}}{Ad}, \tag{4.8}$$

$$C = C_{ref} \times \frac{Ai_{ref}}{Ai_n}, \tag{4.9}$$

In contrast with the case of each SNR and INR is between the upper and the lower thresholds:

$$B = B_{ref} \times \frac{Ad}{Ad_{ref}}, \tag{4.10}$$

$$C = C_{ref} \times \frac{Ai_n}{Ai_{ref}}, \tag{4.11}$$

where $B_{ref}$ and $C_{ref}$ are the reference values of $B$ and $C$, respectively which are set to be the constant values. $Ad_{ref}$ and $Ai_{ref}$ are the reference values of the desired signal and interfering signal amplitudes which can be provided by the DOA estimation at the reference situation. $Ad$ and $Ai_n$ are the amplitudes of the received desired signal and $n^{th}$ interfering signal, respectively which can be achieved by DOA estimation instantaneously in the adaptive process.

## 4.5 Simulation Results

According to the aforementioned of the direction of arrival estimation and the beamforming methods explained in the previous chapter, this section illustrates the simulation results of their method and the comparison results between the conventional method and the proposed technique.

In this computer simulation, the received array antenna is assumed to be isotropic array antenna with half wavelength apart between elements while the source is the point source with carrier frequency of 2.335 GHz.

### 4.5.1 Simulation results of the direction of signal arrival estimation

For the DOA estimation simulation, the number of array element is 8 as shown in Fig. 4.5.

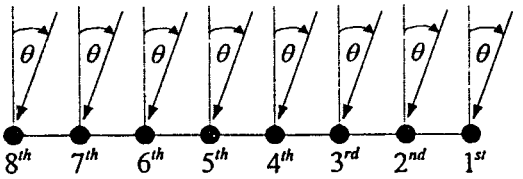


**Fig. 4.5** The geometry of eight-element isotropic of the receiving array antenna

In the mean time, the signal source is assumed to be located at the far field distant from the receiving array antenna.

The first case: there are three noncorrelated signal sources impinging at the array antenna with identical power 5 dB SNR in the direction $\theta$ from $-40^{\circ}$, $-10^{\circ}$ and $70^{\circ}$, simultaneously.

- Conventional method:

This method needs the calculation of the covariance matrix of the received signal at the array antenna and scanning the incident angle of signal arrival ($\theta$) based on the array output power as illustrated in equation (3.80) by using the complex weight formula as shown in (3.82) that is

$$w_m = \frac{1}{\sqrt{M}} e^{-j2\pi \frac{d \sin\theta}{\lambda_c}(m-1)},$$

while the array output power:

$$P_c(\theta) = w_c^H(\theta) R_{xx} w_c(\theta).$$

Therefore, the direction of the arrival signal can be estimated from Fig. 4.6.

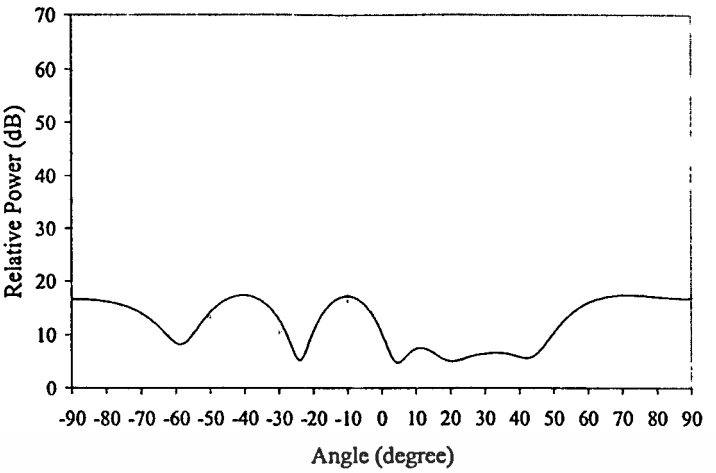


**Fig. 4.6** The DOA estimation by using the conventional method

- Capon's minimum-variance method:

The DOA estimation of this method is in like manner of the conventional method which considers the intensity of array output as shown in (3.86) that is

$$P_c(\theta) = \frac{1}{a^H(\theta) R_{xx}^{-1} a(\theta)}.$$

Thus, the direction of the arrival signal can be estimated from Fig. 4.7.

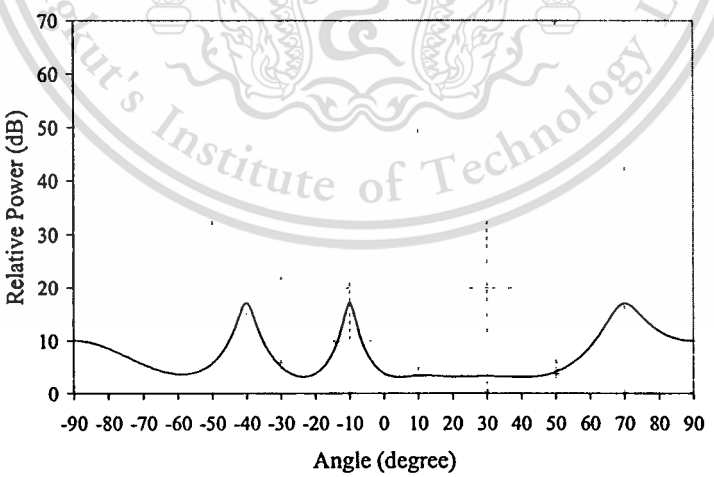


**Fig. 4.7** The DOA estimation by using the Capon's minimum-variance method

- Multiple signal classification (MUSIC) method:

In the case of MUSIC method, the covariance matrix is subject to eigenvalue decomposition. To estimate the direction of the signal arrival, the variable $\theta$ is scanned to find the peak response of the MUSIC space spectrum that is illustrated in equation (3.91). It is given as

$$P(\theta) = \frac{a^H(\theta)a(\theta)}{a^H(\theta)V_u V_u^H a(\theta)}.$$

The direction of the arrival signal can be obtained from Fig. 4.8.

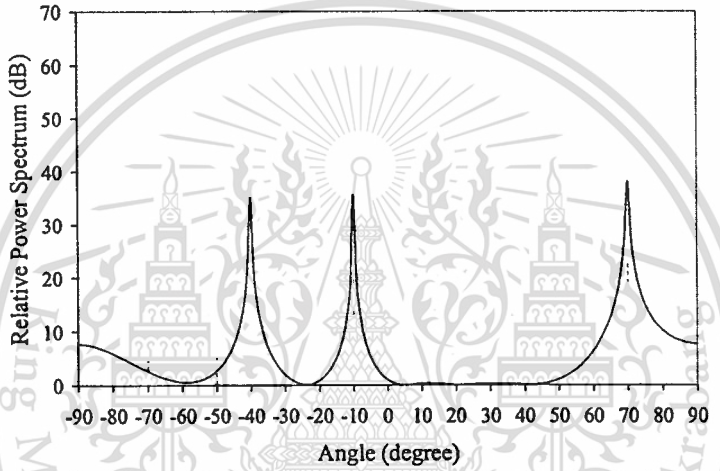


**Fig. 4.8** The DOA estimation by using the MUSIC method

- Spatial smoothing technique:

This technique is used with the subspace-based method by using the forward and backward of the subarrays and uniformly combines the obtained signals in the linear array antenna. In this case, the spatial smoothing technique is used with the MUSIC method to estimate the direction of the signal arrival by setting the number of subarrays equal four. The simulation results can be shown as Fig. 4.9.

From the simulation results of the DOA estimation Fig. 4.6 to Fig. 4.9, they can be compared as illustrated in Fig. 4.10 and Fig. 4.11.

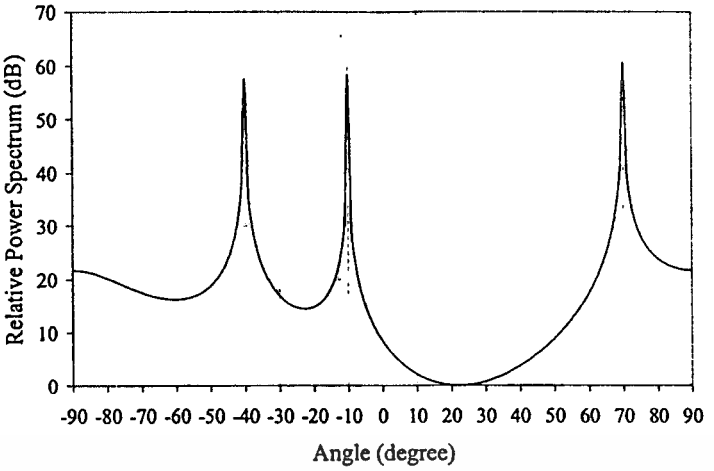


**Fig. 4.9** The DOA estimation by using the MUSIC method with spatial smoothing

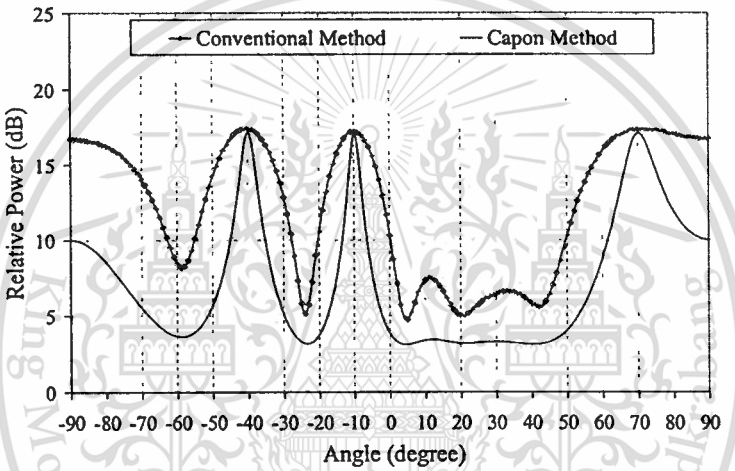


**Fig. 4.10** The comparison of the simulation results of the DOA estimation between the conventional method and the Capon method

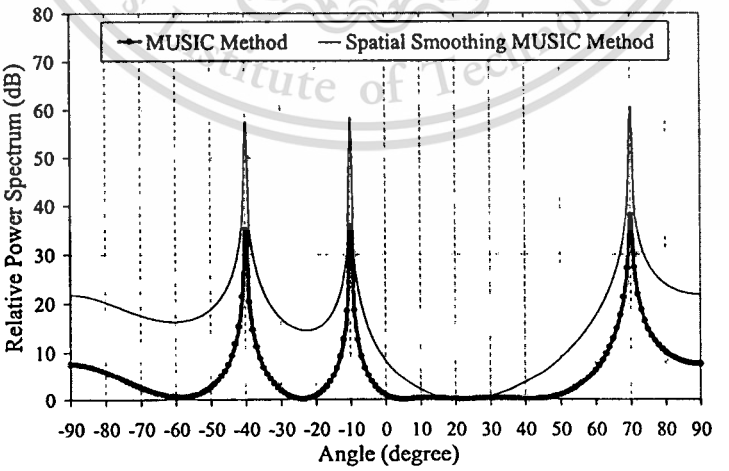


**Fig. 4.11** The comparison of the simulation results of the DOA estimation between the MUSIC method and the spatial smoothing MUSIC method

In Fig. 4.10, the Capon method can provide the power response in the direction of the arrival signals sharper than the conventional method which in some angle of the arrival signal ($70^\circ$) can not be estimated. In case of Fig. 4.11, both MUSIC and spatial smoothing MUSIC give the sharp peak response exact in all DOAs.

From all above simulation results of the DOA estimation, it is evident that the subspace-based method (MUSIC and spatial smoothing MUSIC) can give more accurate results than the output power based method (conventional method and Capon method).

The second case: there are three correlated signal sources impinging at the array antenna with identical power 5 dB SNR in the direction $\theta$ from $-40^\circ$, $-10^\circ$ and $70^\circ$, simultaneously.

In case of the conventional method versus Capon's minimum-variance method, the simulations of DOA estimation can be shown as Fig. 4.12. Meanwhile, the simulations of DOA estimation of the MUSIC method versus spatial smoothing method can be shown as Fig. 4.13.

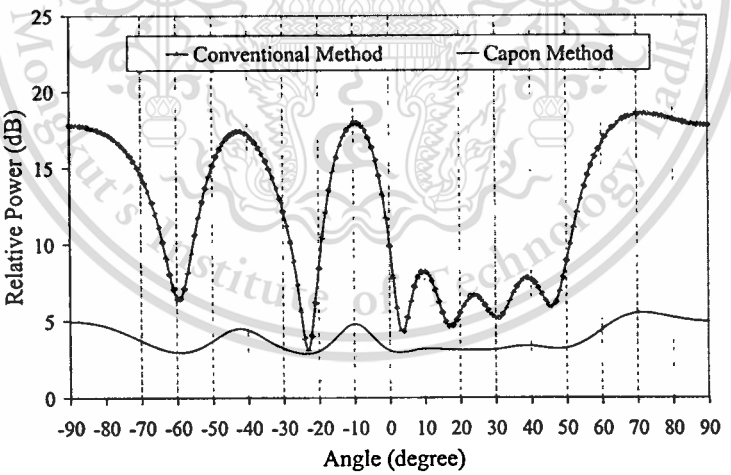


**Fig. 4.12** The comparison of the simulation results of the DOA estimation between the conventional method and the Capon method

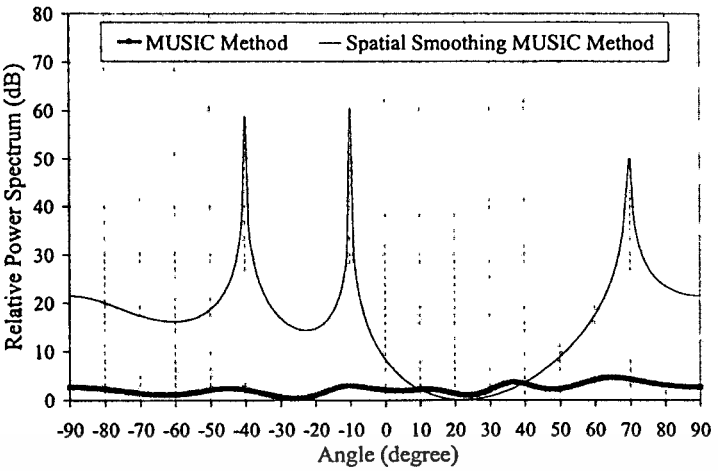


**Fig. 4.13** The comparison of the simulation results of the DOA estimation between the MUSIC method and the spatial smoothing MUSIC method

From Fig. 4.12, it was found that the response pattern of the conventional method can still provide the response power in the same way as the first case which the signal sources are noncorrelated, on the contrary, the Capon method can not estimate DOA. In the mean time, the simulation result in Fig. 4.13 illustrates that the DOA of the three correlated signal sources can be precisely estimated by the spatial smoothing MUSIC, on the other hand, the normal MUSIC method can not estimate DOA.

Therefore, the technique used to achieve the DOA estimation should perform with considering the effect of the correlated signals or coherent signals which usually exist in the practical situation. Although the spatial smoothing MUSIC can achieve the DOA estimation when the signal sources are correlated signal sources, but there are some limitations and the disadvantages of this method. For example, firstly, the MUSIC required the number of the signals before performing the DOA estimation. Secondly, the DOA spectrum value in each direction of the arrival signals of MUSIC method can not be used in the weight computation of the beamforming system, because it is not the realistic power at the array output. Thus the spatial smoothing MUSIC can be effectively used to estimate only the DOA when the number of the impinging signal is limited by the number of subarrays.

Under these conditions, the Capon method has a role to overcome the disadvantages of the spatial smoothing MUSIC method and normal MUSIC method. As mentioned before, the Capon's minimum-variance method based on the output

power, its intensity of array output power can provide the power of each impinging signal in their DOAs. Moreover, this method can be achieved to find the number of the impinging signal at the array because there is no requirement for the number of the received signal to obtain the DOA.

Therefore, to obtain the number DOA, the Capon's minimum-variance method has been performed then spatial smoothing MUSIC has been used to estimate the DOAs which will be used again with the Capon's minimum-variance method to provide the power of each impinging signal at the array antenna, afterwards.

### 4.5.2 Simulation results of the beamforming method

In this section the simulations results of the beamforming, both the conventional method and the proposed method, in various situations are compared. The effect of the degree of freedom that depends on the number of the array, the different angle between the directions of desired signal and interfering signal and the number of the incoming signals are taken into account.

The beam pattern of the four-element, five-element and eight-element array antennas can be obtained as Fig. 4.14 which their half-power beamwidth (HPBW) can be summarized as Table 4.1.

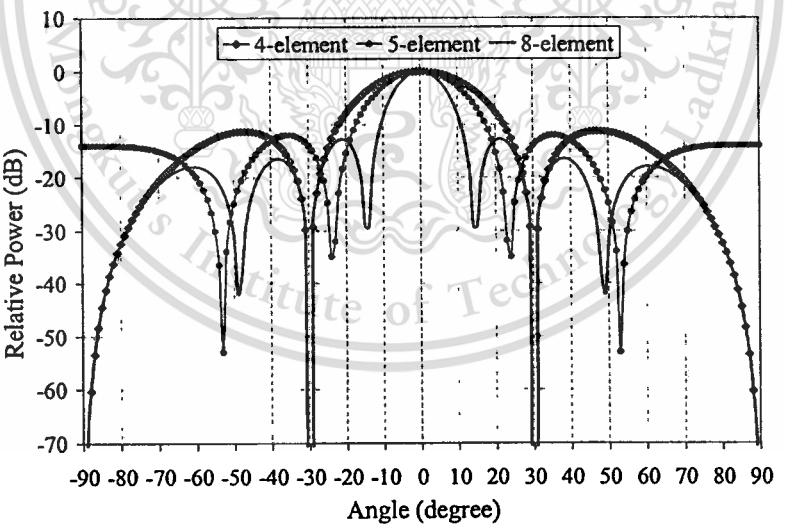


**Fig. 4.14** The antenna beam patterns at various number of array element

**Table 4.1** The half-power beamwidth of array antenna beam patterns from Fig. 4.14

| Number of Array Element | 4-Element | 5-Element | 8-Element |
|---|---|---|---|
| HPBW | 26.27 | 20.71 | 12.73 |

From Fig. 4.14 and Table 4.1, it can be concluded that the HPBW and the number of null response of the beam pattern are inversely proportional and proportional to the number of array element which are related to the degrees of freedom of the system. Thus these will effect to the performance of beamforming in adaptive array antenna.

The first case: the four signal sources impinging at the array antenna with identical power 5 dB SNR. The desired signal comes from 30° and three interference signals come from –40°, –10° and 70°, simultaneously while the number of array elements are four, five and eight. The inter element is half wavelength.

- Classical beamforming

The beam pattern of this method can be achieved by using the complex weight of equation (3.4)

$$w_m = \frac{1}{\sqrt{M}} e^{-j2\pi \frac{d \sin\theta}{\lambda_c}(m-1)},$$

that can be shown as Fig. 4.15.

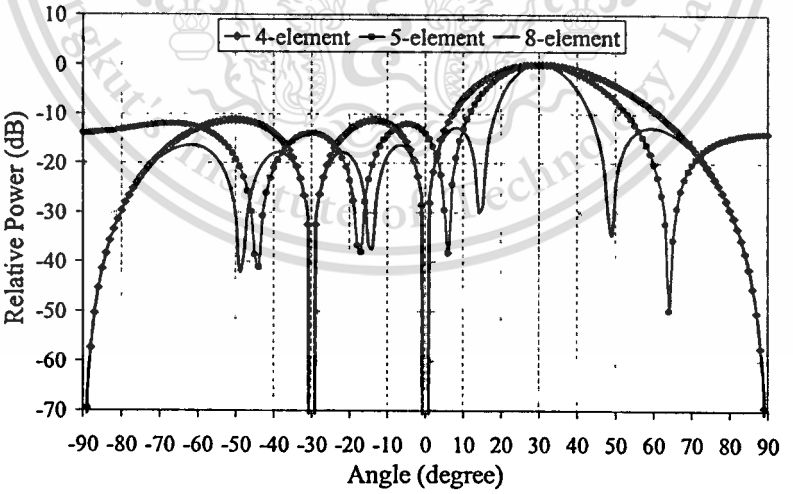


**Fig. 4.15** The antenna beam patterns at various numbers of array by using the classical beamforming

The beamforming can not be achieved by the proposed covariance matrix adjustment technique because the weight computation of the classical method does not consider the covariance matrix.

- Linearly constrained minimum-variance (LCMV) method

This method requires the constrained matrix and constrained vector which are illustrated as equation (3.16) that is

$$\begin{bmatrix} a^H(\theta, f) \\ a^H(\phi, f) \end{bmatrix} w = \begin{bmatrix} h^* \\ 0 \end{bmatrix}.$$

The value of $h$ has been performed as the gain in the desired signal direction of the beamforming operation, in this case $h$ is set to 5 that is obtained in the weight computation formula in (3.15):

$$w_{opt} = R_{xx}^{-1} C (C^H R_{xx}^{-1} C)^{-1} h .$$

The antenna beam patterns of the first case by using this method can be provided by Fig. 4.16(a). In contrast, the simulation results of the LCMV method with the proposed technique can be shown as Fig. 4.16(b).

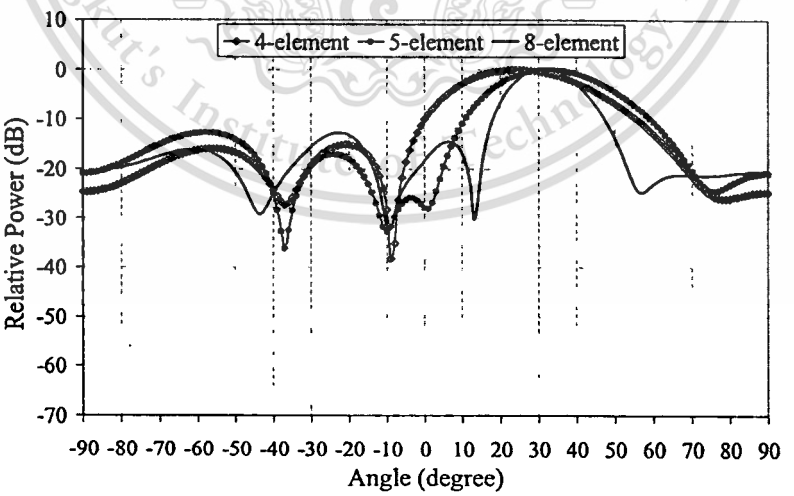


**Fig. 4.16(a)** The antenna beam patterns at various numbers of array by using the conventional LCMV method

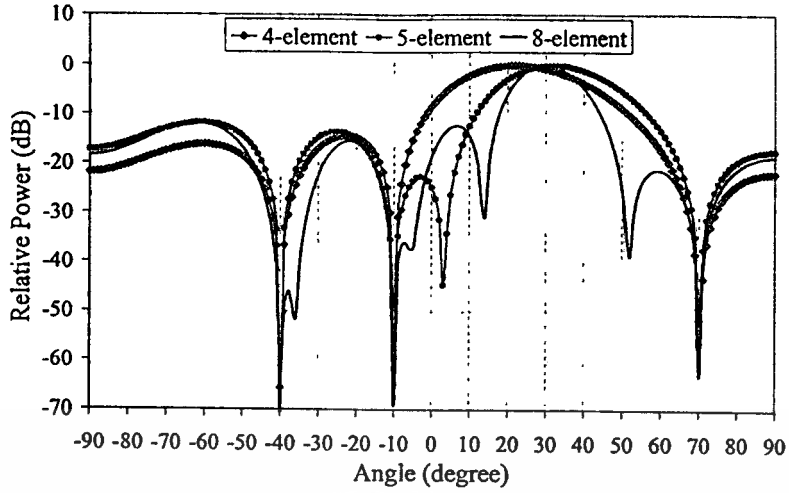


**Fig. 4.16(b)** The antenna beam patterns at various numbers of array by using the LCMV method with the proposed technique

The adjustable multipliers $B$ and $C$ of the proposed technique with LCMV and Applebaum array in this case, are set to 0.002 and 30, respectively.

- Applebaum array

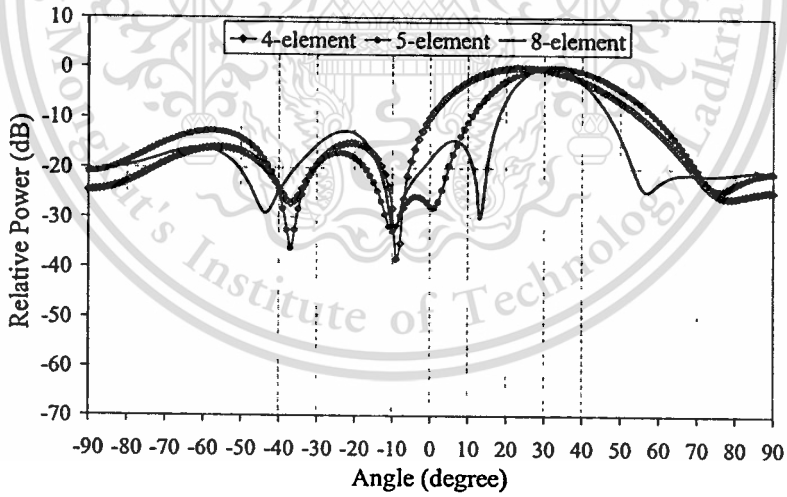


**Fig. 4.17(a)** The antenna beam patterns at various numbers of array by using the conventional Applebaum array

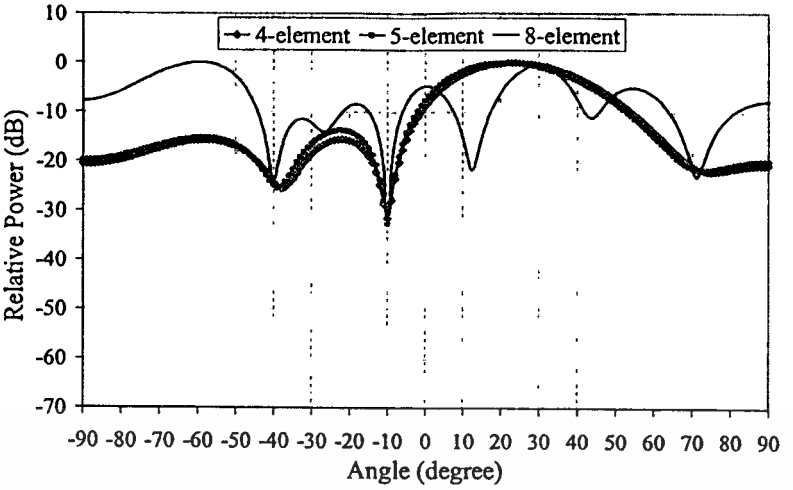


**Fig. 4.17(b)** The antenna beam patterns at various numbers of array by using the AGC Applebaum array

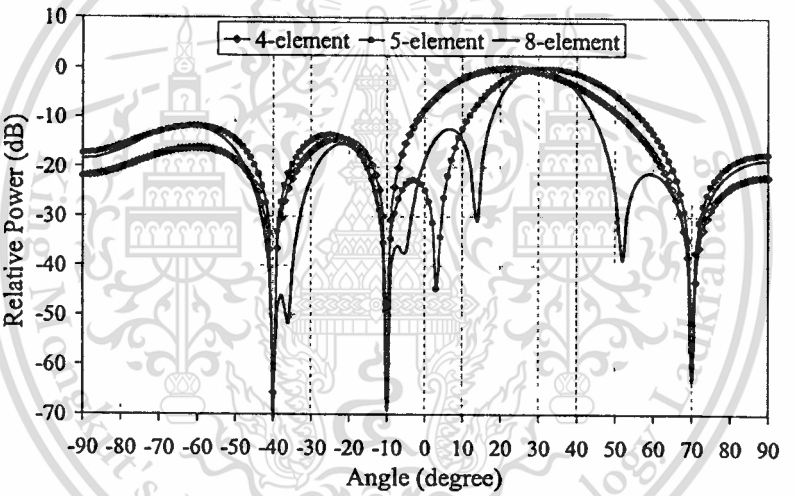


**Fig. 4.17(c)** The antenna beam patterns at various numbers of array by using the Applebaum array with the proposed technique

The antenna beam pattern of the Applebaum array can be obtained by using the weight formula in equation (3.57),

$$W \cong \mu R^{-1} U_d^*,$$

where the arbitrary constant $\mu$ is set to 5 that equals the gain $h$ of the LCMV method. The conventional Applebaum array method can perform the simulation

results of the antenna beam pattern in Fig. 4.17(a), while the AGC Applebaum Array and the Applebaum array with proposed technique can be achieved as Fig. 4.17(b) and Fig. 4.17(c), respectively. The gain of the AGC Applebaum Array is set to 30 in all various number of the array elements while the adjustable multipliers $B$ and $C$ of the proposed technique are set to 0.002 and 30, respectively.

The second case: the four signal sources impinging at the array antenna with identical power 5 dB SNR. The desired signal comes from $-10^{\circ}$ and three interference signals come from $-60^{\circ}$, $-30^{\circ}$ and $30^{\circ}$, simultaneously while the numbers of array element are four, five and eight and the inter element is half wavelength.

- Classical beamforming

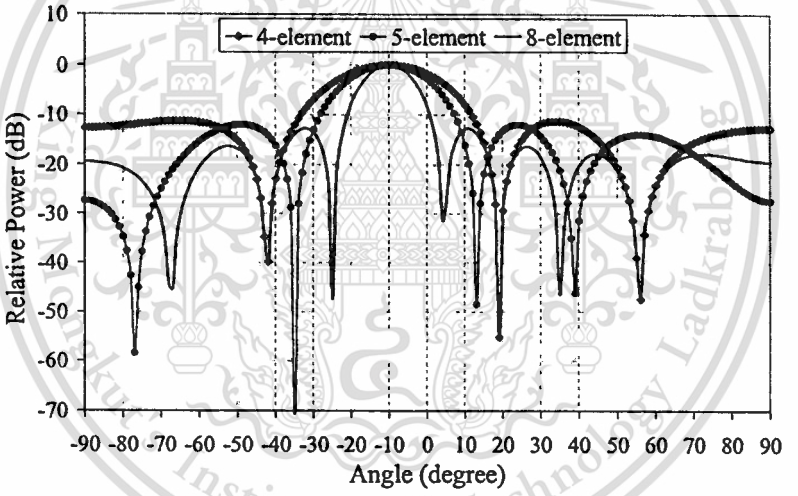


**Fig. 4.18** The antenna beam patterns at various numbers of array by using the classical beamforming

From Fig. 4.18, the main beam of the array antenna is at $-10^{\circ}$ or the desired signal direction but the null pattern does not change to the interfering directions. In addition, the null pattern value of the 4-element array is lower than 5-element and 8-element consecutively.

- Linearly constrained minimum-variance (LCMV) method

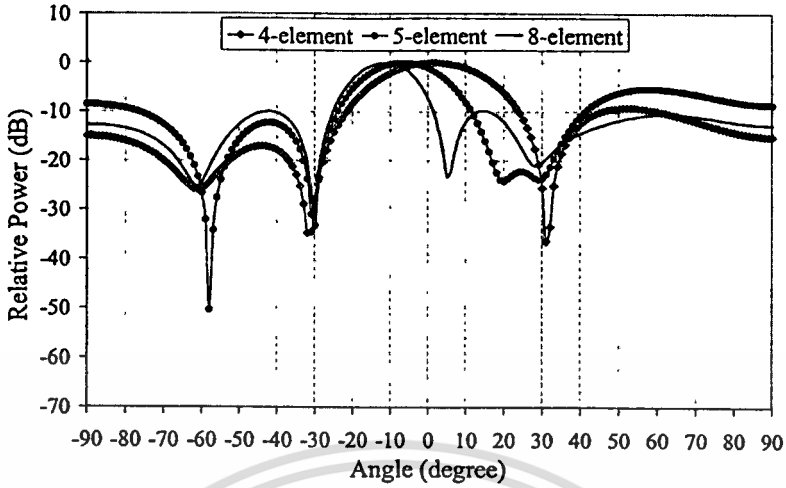


**Fig. 4.19(a)** The antenna beam patterns at various numbers of array by using the conventional LCMV method

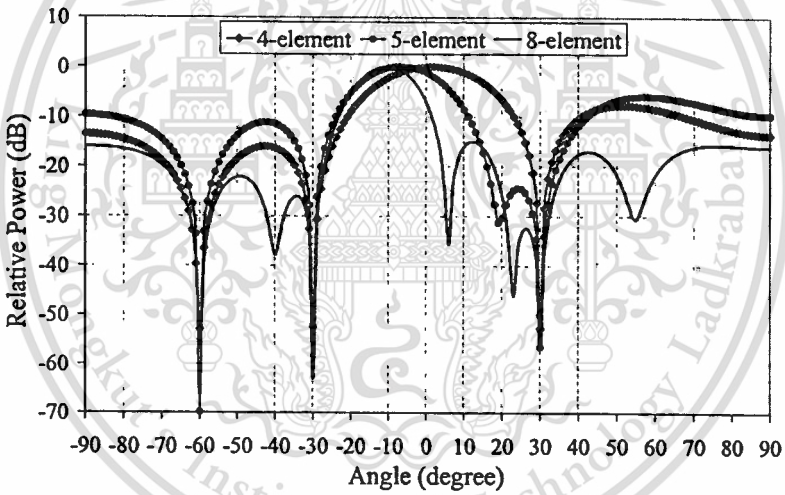


**Fig. 4.19(b)** The antenna beam patterns at various numbers of array by using the LCMV method with the proposed technique

In Fig. 4.19(a) and Fig. 4.19(b), the direction of the main beam both conventional method and proposed technique is closed to the desired direction or $-10^{\circ}$ while the null patterns of the proposed technique are more precise and deep in the interfering directions than the conventional methods. Moreover, since the number of the array element increases as eight-element, the peak beam pattern of the array antenna is closer to the desired direction than five and four elements, consecutively.

- Applebaum array

In case of Applebaum array, it was found that the beam pattern is similar to the LCMV method because the gain and the derivation of both methods are bases on the same concept of desired signal power and undesired signal power ratio. From Fig. 20(a) to Fig. 20(c), the beam patterns of the received array antenna are consecutively high enhanced. The beam pattern of an AGC Applebaum array can be controlled by its controlling gain in the feed back loop of adaptive array system. In this case, the AGC gain is set as 5.

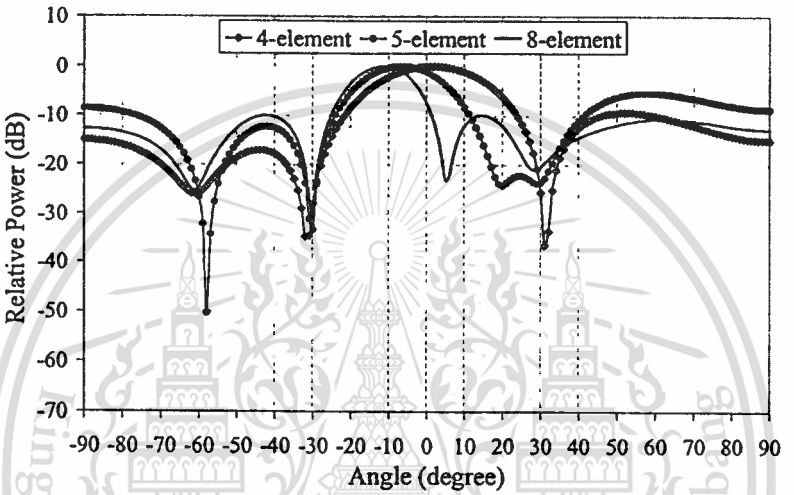


**Fig. 4.20(a)** The antenna beam patterns at various numbers of array by using the conventional Applebaum array

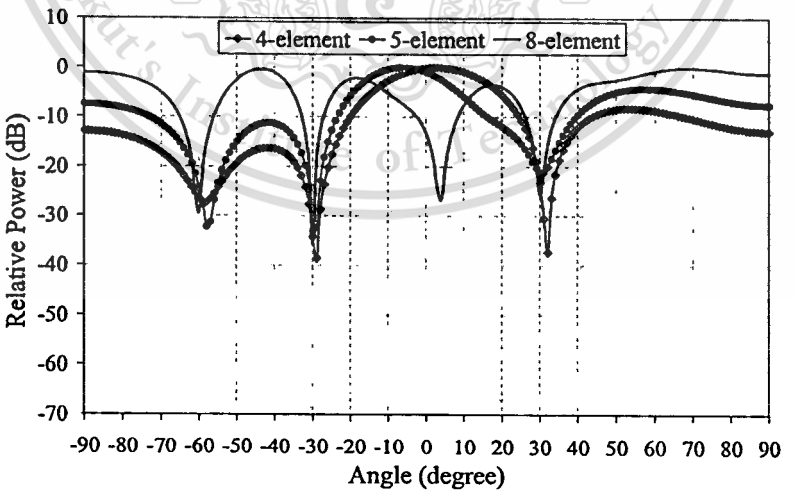


**Fig. 4.20(b)** The antenna beam patterns at various numbers of array by using the AGC Applebaum array

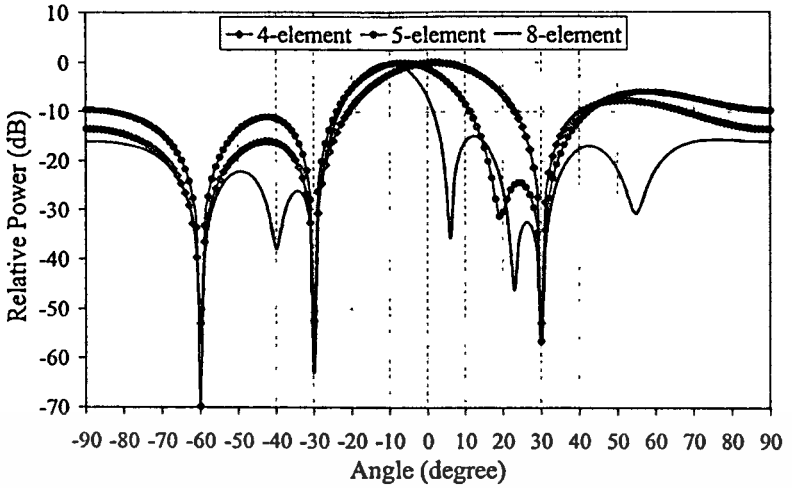


**Fig. 4.20(c)** The antenna beam patterns at various numbers of array by using the Applebaum array with the proposed technique

The third case: the five signal sources impinging at the array antenna with identical power 5 dB SNR. The desired signal comes from $-10^{\circ}$ and four interference signals come from $-60^{\circ}$, $-30^{\circ}$, $0^{\circ}$ and $30^{\circ}$, simultaneously while the numbers of array element are four, five and eight and the inter element is half wavelength.

- Classical beamforming

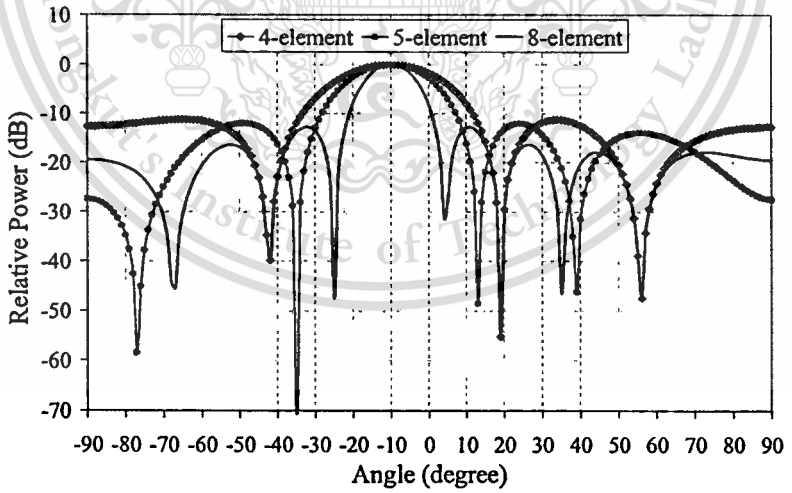


**Fig. 4.21** The antenna beam patterns at various numbers of array by using the classical beamforming

From Fig. 4.21, it was found that the beam pattern of the classical beamforming does not change, although the number of the interfering signal is increased. It is because the weight computation of this method does not consist of the component of interfering angle, thus there is no affection to the beam pattern from the interference variation in this kind of beamforming.

- Linearly constrained minimum-variance (LCMV) method

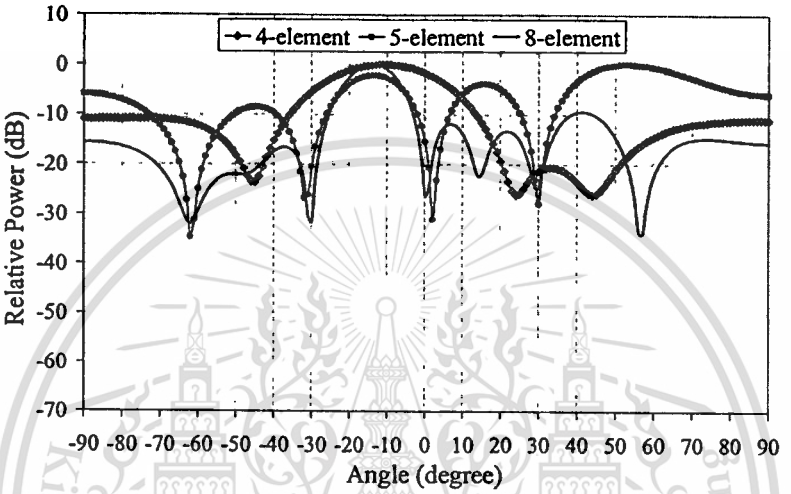


**Fig. 4.22(a)** The antenna beam patterns at various numbers of array by using the conventional LCMV method

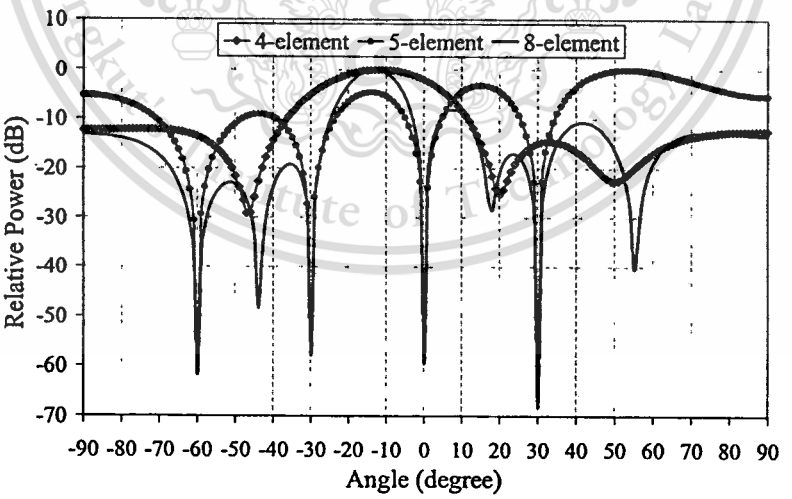


**Fig. 4.22(b)** The antenna beam patterns at various numbers of array by using the LCMV method with the proposed technique

In Fig. 4.22(a) and Fig. 4.22(b), it is evident that the beam pattern of all four-element array beamforming can not provide the precise null patterns in their interfering directions because the number of interference is more than its degrees of freedom which equals *N*-1 or 3. On the contrary, the five and eight-element array beamforming can still provide the effective beam pattern in both desired signal direction and interfering directions, in particularly in the proposed technique.

- Applebaum array

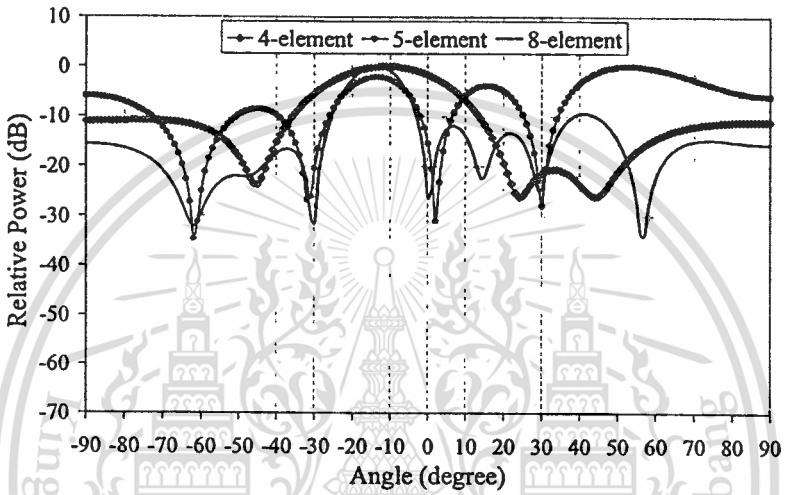


**Fig. 4.23(a)** The antenna beam patterns at various numbers of array by using the conventional Applebaum array

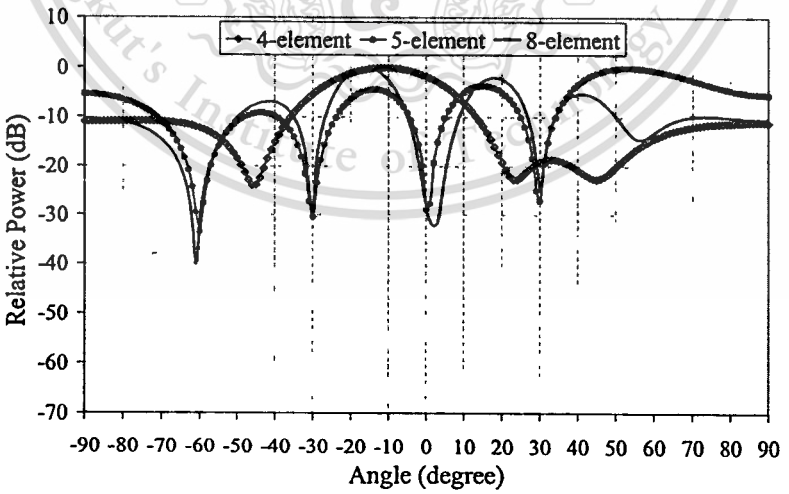


**Fig. 4.23(b)** The antenna beam patterns at various numbers of array by using the AGC Applebaum array

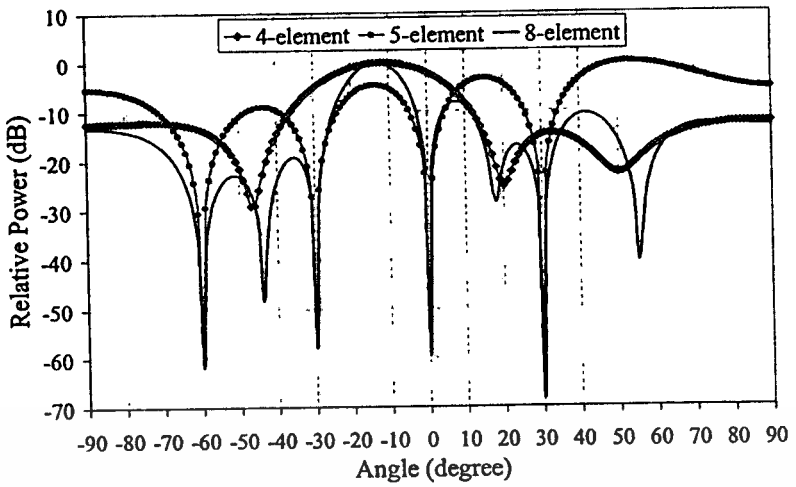


**Fig. 4.23(c)** The antenna beam patterns at various numbers of array by using the Applebaum array with the proposed technique

From Fig. 4.23(a) to Fig. 4.23(c), the beam pattern of the four-element array in all beamforming method can not provide the exact null pattern in their interfering directions similar to the previous case in LCMV method because it is under the same condition of degrees of freedom. In contrast, the other number of array element can still achieve the efficient beamforming especially the proposed technique

To clarify the efficiency of each beamforming method, the signal to interference ratio (SIR) of the simulation results of all beamforming methods which can be calculated by equation (4.12), are demonstrated as Table 4.2.

$$SIR = \frac{Pd}{\sum_{k=1}^{n} Pi_k}, \tag{4.12}$$

where $Pd$ is the desired signal power, $n$ is the number of interference signals and $Pi_k$ is the power of the $k^{th}$ interfering signal.

From all simulation results above, it is evident that the classical beamforming can set only its main beam to the desired DOA in particular while ignore the interfering signal direction. Thus, the efficiency of the classical beamforming depends on the radiation pattern of the used array antenna which the larger array element number, the higher directivity and the higher efficiency. This can be clarified

by Table 4.2, the SIR of the eight-element is consecutively higher than the SIRs of the five-element and the four-element. On the contrary, the LCMV method and Applebaum array can control their beam patterns both the directions of the peak and null beam patterns to the direction of desired signal and interfering signal, respectively. As a result, the SIRs of LCMV method and Applebaum array are higher than the classical method since the number of array elements are the same.

**Table 4.2** The SIR of the beamforming simulations

| Type | Element | SIR (dB) 1st Case | SIR (dB) 2nd Case | SIR (dB) 3rd Case |
|---|---|---|---|---|
| Normal Beam Pattern | 4-element | -310.06 | 12.71 | -1.84 |
| | 5-element | -11.83 | 7.67 | -3.15 |
| | 8-element | -304.04 | 9.52 | -8.47 |
| Classical Beamforming | 4-element | 9.00 | 4.70 | -0.07 |
| | 5-element | 12.66 | 9.39 | 1.92 |
| | 8-element | 13.22 | 11.80 | 6.77 |
| LCMV Method | 4-element | 18.69 | 19.45 | -0.14 |
| | 5-element | 18.90 | 21.31 | 11.10 |
| | 8-element | 19.42 | 18.59 | 20.10 |
| LCMV Method With Proposed Technique | 4-element | 46.39 | 45.71 | -0.06 |
| | 5-element | 48.93 | 49.33 | 38.17 |
| | 8-element | 58.55 | 53.42 | 53.84 |
| Applebaum Array | 4-element | 18.69 | 19.45 | -0.14 |
| | 5-element | 18.90 | 21.31 | 11.10 |
| | 8-element | 19.42 | 18.59 | 20.10 |
| AGC Applebaum Array | 4-element | 18.59 | 18.68 | -0.14 |
| | 5-element | 18.72 | 18.82 | 18.29 |
| | 8-element | 18.83 | 18.57 | 18.93 |
| Applebaum Array With Proposed Technique | 4-element | 46.39 | 45.71 | -0.06 |
| | 5-element | 48.93 | 49.33 | 38.17 |
| | 8-element | 58.55 | 53.42 | 53.84 |

The simulation results of both the LCMV method and the Applebaum array seem to be similar because they are also based on maximization of the desired signal power and minimization of the undesired signal power. Besides, the values of their gains are the same. In the first and second cases of the beamforming simulations, the number of interfering signals is three that is equal to the degrees of freedom of the four-element array antenna. Thus their beamforming can control the null response pattern exactly in all interfering directions. However in the third case, the number of undesired signal direction is increased to four that is more than the degrees of freedom of the four-element array antenna. In this case, all beamforming methods of the four-element array can not control their null response patterns to be precise in their interfering directions since all four interfering signals are used in the weight computation. Consequently, the SIRs of the four-element of the third case in all beamforming method are lower than the other cases. For this reason, in adaptive array process as shown in Fig. 4.1 has the operation for choosing the suitable direction of the interfering signal that has the consecutive high power level. The number of the selecting interfering direction is equal to the degrees of freedom. Therefore, the number of array antenna elements has a role to increase the efficiency of the beamforming in adaptive array.

Consider the comparison of the simulating antenna beam patterns of the conventional methods, both the LCMV method and the Applebaum array, the AGC Applebaum array and the proposed technique, the antenna beam pattern of the proposed technique can provide the exact deep null beam patterns in the interfering directions and the peak beam pattern in the desired direction better than the AGC Applebaum array and the conventional methods. Therefore, the SIRs of the proposed technique are higher than the AGC Applebaum array and the conventional method.

For the different desired signal and interference signal directions in the other cases, the results of the proposed technique are still more effective than the conventional methods, which can be clarified by the illustrative figures and the SIR values of all three cases in Table 4.2 above. In addition, although the number of array elements is increased, the proposed covariance matrix adjustment technique can still set null response pattern exact in the interference directions better than the conventional beamforming methods and the AGC Applebaum array which is consistent with the SIR values in Table 4.2.

Furthermore, when the power of received signals are decreased and the incoming signal directions are closed to each other, the simulation results can be performed as follow the fourth and fifth cases.

The fourth case: the four signal sources impinging at the array antenna with identical power 5 dB SNR. The desired signal comes from –20° and three interference signals come from –45°, 0° and 20°, simultaneously while the number of array elements are four, five and eight and the inter element is half wavelength.

- Classical beamforming

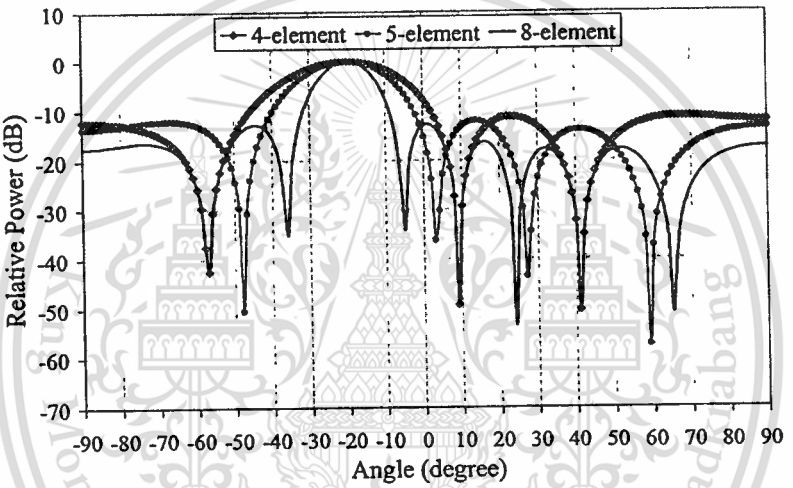


**Fig. 4.24** The antenna beam patterns at various numbers of array by using the classical beamforming

From Fig. 4.24, the main beam of the received array antenna points in the desired signal direction, in contrast, the null patterns do not controlled to be in the interfering directions.

- Linearly constrained minimum-variance (LCMV) method

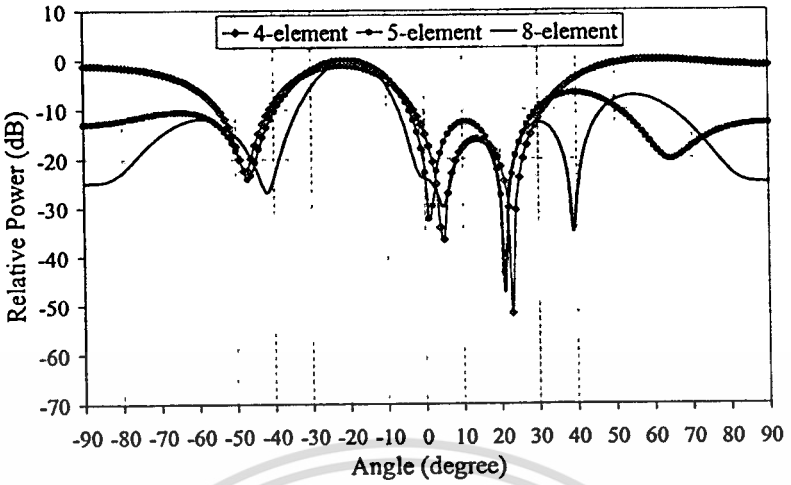


**Fig. 4.25(a)** The antenna beam patterns at various numbers of array by using the conventional LCMV method

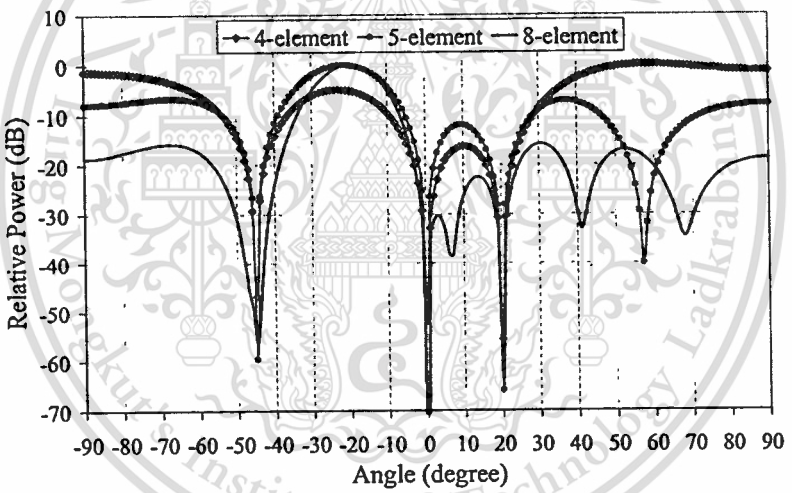


**Fig. 4.25(b)** The antenna beam patterns at various numbers of array by using the LCMV method with the proposed technique

In Fig. 4.25(a) and Fig. 4.25(b), the main beam of the received array antenna is point to the desired signal direction ($-20^{\circ}$), meanwhile the directions of null pattern are exact in the interfering directions, particularly deep null in the proposed technique.

- Applebaum array

From Fig. 4.26(a) to Fig. 4.26(c), it is obvious that the proposed technique provides more efficient in beamforming than the conventional method and the AGC technique. The null patterns of the proposed technique are deeper and more precise than the conventional method and the AGC technique, in the mean time the peak beam is still exact in the desired signal direction.

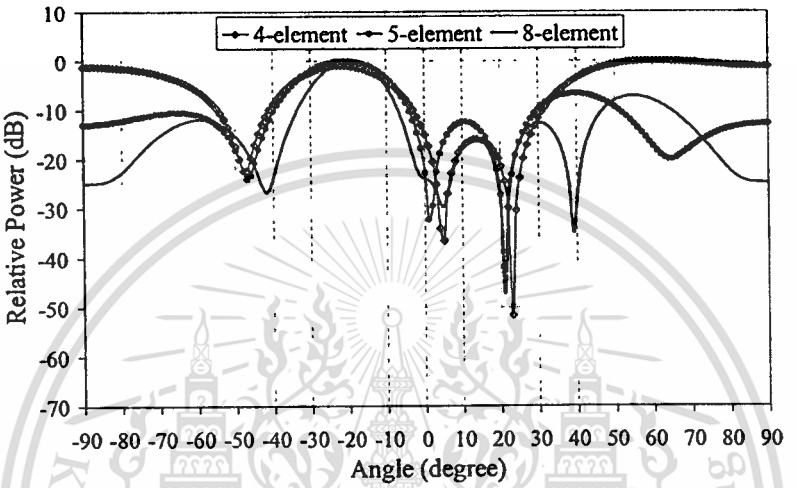


**Fig. 4.26(a)** The antenna beam patterns at various numbers of array by using the conventional Applebaum array

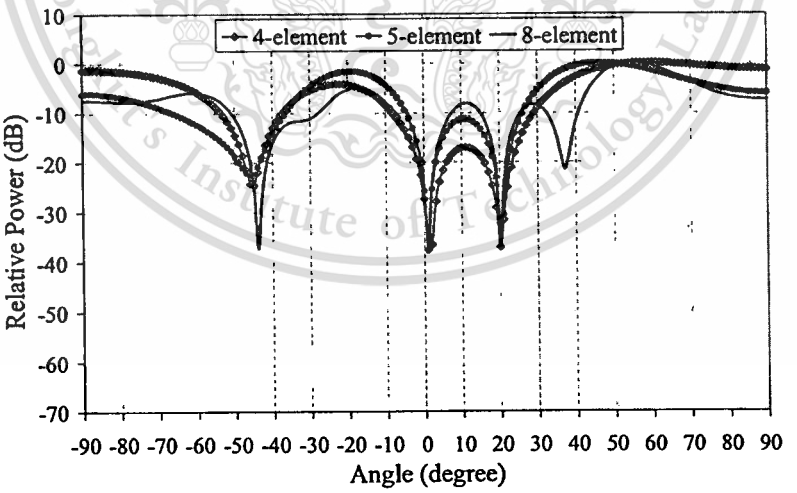


**Fig. 4.26(b)** The antenna beam patterns at various numbers of array by using the AGC Applebaum array

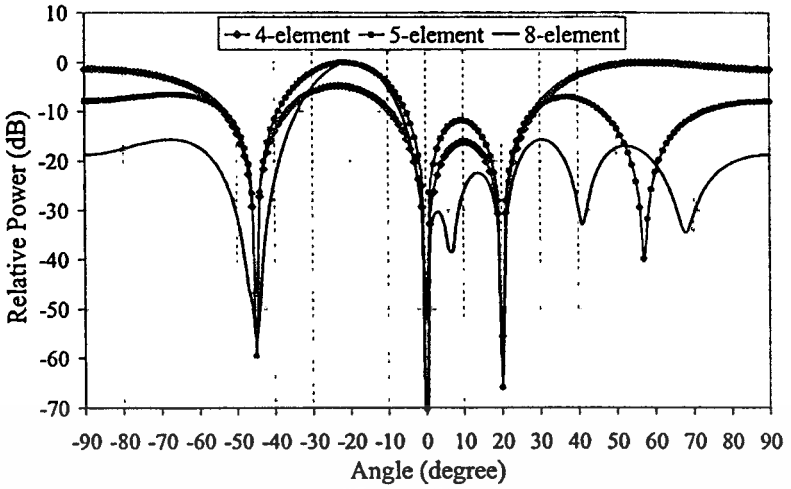


**Fig. 4.26(c)** The antenna beam patterns at various numbers of array by using the Applebaum array with the proposed technique

The fifth case: the four signal sources impinging at the array antenna with identical power 1 dB SNR. The desired signal comes from $-20^{\circ}$ and three interference signals come from $-45^{\circ}$, $0^{\circ}$ and $20^{\circ}$, simultaneously while the number of array elements are four, five and eight and the inter element is half wavelength.

For the proposed technique of this case, the $B$ and $C$ values are adjusted as equation (4.8) and (4.9), respectively. It is because the SNR of received signal is lower than the lower threshold that is set when the SNR of received signal equals 5 dB SNR (in this adaptive array operation).

- Classical beamforming

In this case, the beam pattern of the array antenna can be shown in Fig. 4.27. This beam pattern is similar to Fig. 4.24 because the classical beamforming can control only its main beam to the desired signal direction and the power level of desired signal equals the interfering signal.

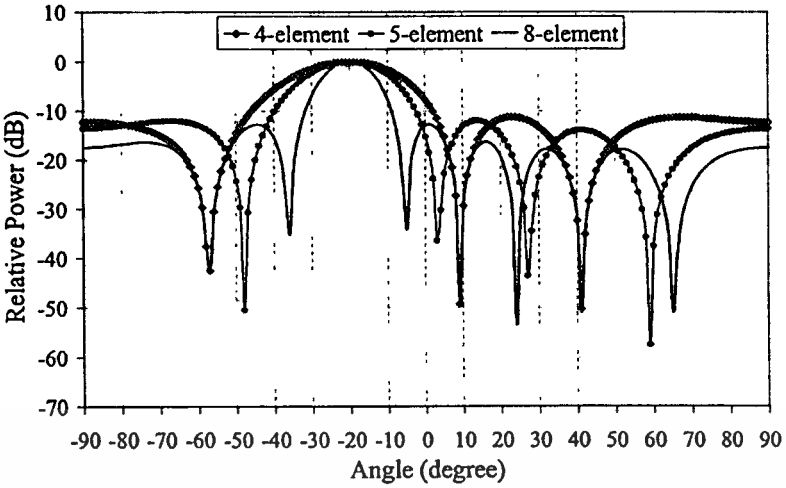


**Fig. 4.27** The antenna beam patterns at various numbers of array by using the classical beamforming

- Linearly constrained minimum-variance (LCMV) method

In Fig. 4.28(a), it was found that the null patterns of the received array antenna can not be exactly provided in the interfering directions of all element number. On the contrary, the beam pattern of the proposed technique in Fig. 4.28(b) can provide the precise null pattern in the interfering direction.

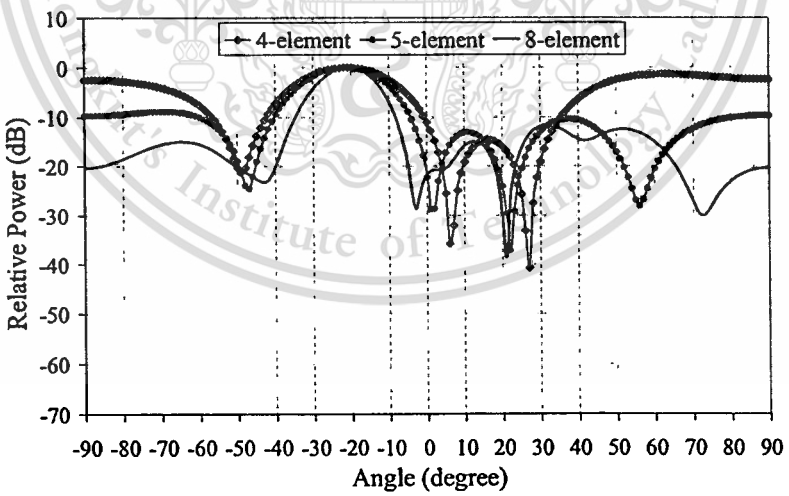


**Fig. 4.28(a)** The antenna beam patterns at various numbers of array by using the conventional LCMV method

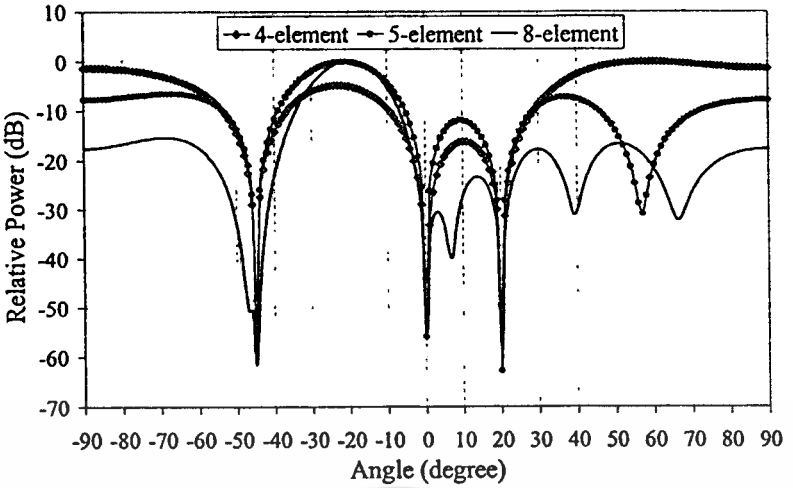


**Fig. 4.28(b)** The antenna beam patterns at various numbers of array by using the LCMV method with the proposed technique

- Applebaum array

From the simulation results in Fig. 4.29(a), the null patterns are not exact in the interfering directions. In the mean time, the beam pattern of the AGC Applebaum array in Fig. 4.29(b) can provide the null patterns closer to their interfering directions than the conventional method. However its null pattern can be developed by using the proposed technique that is shown in Fig. 4.29(c). In this figure, the null patterns

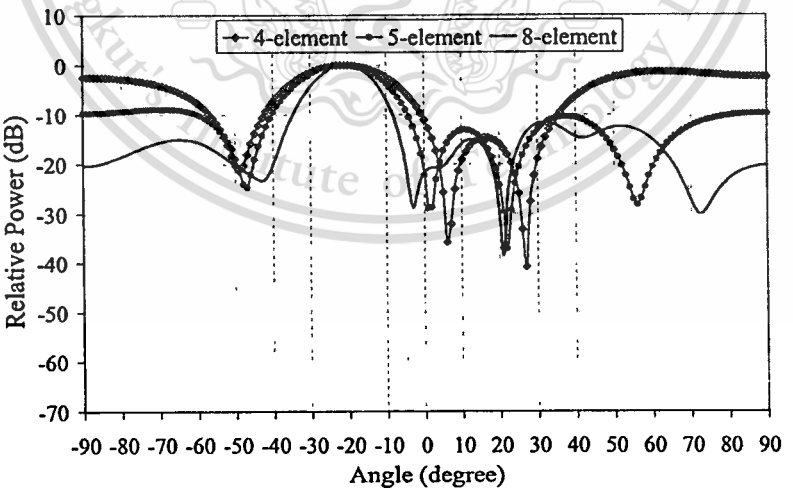


**Fig. 4.29(a)** The antenna beam patterns at various numbers of array by using the conventional Applebaum array

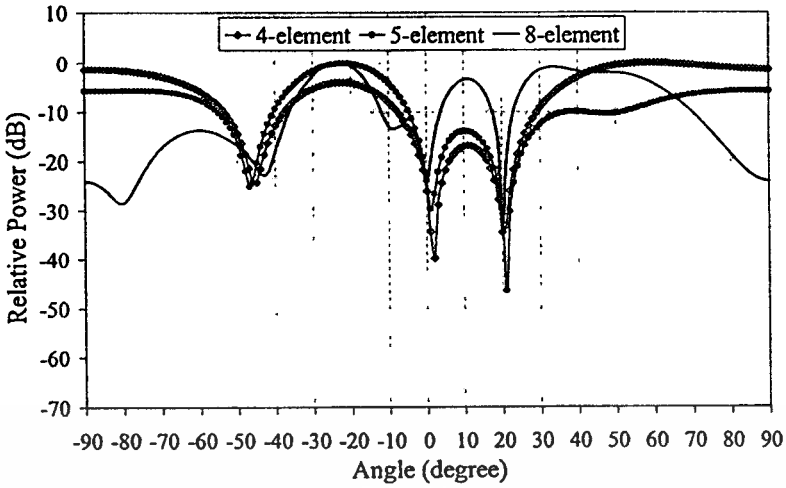


**Fig. 4.29(b)** The antenna beam patterns at various numbers of array by using the AGC Applebaum array

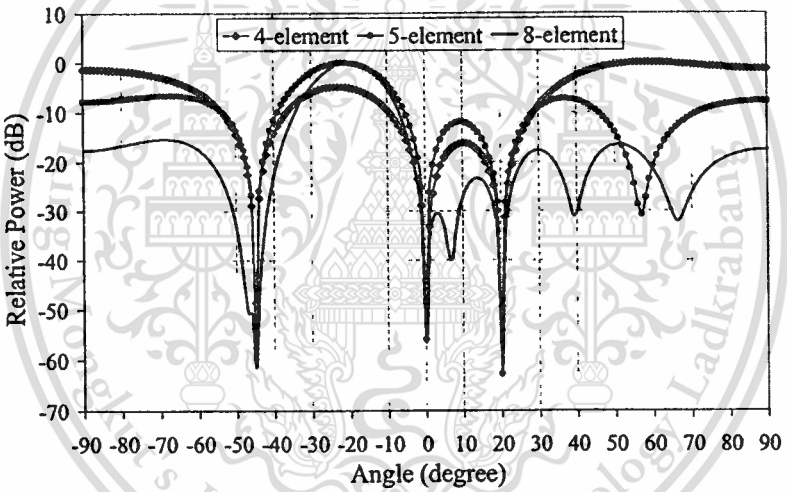


**Fig. 4.29(c)** The antenna beam patterns at various numbers of array by using the Applebaum array with the proposed technique

are more exact and deep in their interfering direction than the AGC Applebaum array. Therefore, it is obvious that the accuracy of the proposed technique is consecutively higher than the AGC Applebaum array and the conventional methods.

**Table 4.3(a)** The null position of the beam pattern

| Case | Method | Element | $\theta_{i1}$ (–45°) | $\theta_{i2}$ (0°) | $\theta_{i3}$ (20°) |
|---|---|---|---|---|---|
| 4th | LCMV | 4-element | –48° | 5° | 23° |
| | | 5-element | –47° | 1° | 21° |
| | | 8-element | –42° | 5° | 21° |
| 5th | LCMV | 4-element | –49° | 6° | 27° |
| | | 5-element | –47° | 1° | 22° |
| | | 8-element | –43° | –3° | 21° |
| 4th | LCMV Proposed Technique | 4-element | –45° | 0° | 20° |
| | | 5-element | –45° | 0° | 20° |
| | | 8-element | –45° | 0° | 20° |
| 5th | LCMV Proposed Technique | 4-element | –45° | 0° | 20° |
| | | 5-element | –45° | 0° | 20° |
| | | 8-element | –45° | 0° | 20° |

**Table 4.3(b)** The error (%) of the null beam pattern

| Case | Method | Element | $\theta_{i1}$ (–45°) % | $\theta_{i2}$ (0°) % | $\theta_{i3}$ (20°) % | Average Error (%) |
|---|---|---|---|---|---|---|
| 4th | LCMV | 4-element | 1.66 | 2.76 | 1.66 | 2.03 |
| | | 5-element | 1.10 | 0.55 | 0.55 | 0.74 |
| | | 8-element | 1.66 | 2.76 | 0.55 | 1.66 |
| 5th | LCMV | 4-element | 2.21 | 3.31 | 3.87 | 3.13 |
| | | 5-element | 1.10 | 0.55 | 1.10 | 0.92 |
| | | 8-element | 1.10 | 1.66 | 0.55 | 1.10 |
| 4th | LCMV Proposed Technique | 4-element | 0 | 0 | 0 | 0 |
| | | 5-element | 0 | 0 | 0 | 0 |
| | | 8-element | 0 | 0 | 0 | 0 |
| 5th | LCMV Proposed Technique | 4-element | 0 | 0 | 0 | 0 |
| | | 5-element | 0 | 0 | 0 | 0 |
| | | 8-element | 0 | 0 | 0 | 0 |

**Table 4.4** The SIR of the beamforming simulations

| Type | Element | SIR (dB) 4th Case | SIR (dB) 5th Case |
|---|---|---|---|
| Normal Beam Pattern | 4-element | -8.70 | -8.70 |
| | 5-element | -15.51 | -15.51 |
| | 8-element | -13.24 | -13.24 |
| Classical Beamforming | 4-element | 4.50 | 4.50 |
| | 5-element | 11.44 | 11.44 |
| | 8-element | 9.46 | 9.46 |
| LCMV Method | 4-element | 11.25 | 8.41 |
| | 5-element | 18.04 | 16.51 |
| | 8-element | 19.30 | 18.89 |
| LCMV Method With Proposed Technique | 4-element | 38.06 | 36.84 |
| | 5-element | 51.03 | 53.02 |
| | 8-element | 55.48 | 53.90 |
| Applebaum Array | 4-element | 11.25 | 8.41 |
| | 5-element | 18.04 | 16.51 |
| | 8-element | 19.30 | 18.89 |
| AGC Applebaum Array | 4-element | 18.30 | 17.74 |
| | 5-element | 18.73 | 18.41 |
| | 8-element | 18.68 | 18.55 |
| Applebaum Array With Proposed Technique | 4-element | 38.06 | 36.84 |
| | 5-element | 51.03 | 53.02 |
| | 8-element | 55.48 | 53.90 |

From the simulation results of the beamforming all above, it is evident that when the SNRs of the received signal, both desired signal and interfering signals decrease, the beam pattern of the conventional technique can not set the null beam patterns exactly in the direction of interfering signal. Meanwhile, the proposed technique gives the more effective in controlling the null pattern exactly in the direction of the interfering signal which can be clarified by the null positions of both conventional beamforming method and the proposed technique in Table 4.3. The signal to interference ratio (SIR) of the simulation results of the fourth and fifth cases

can be demonstrated in Table 4.4.

From Table 4.3, the error of the null beam pattern of the four-element is larger than the others and the error in the fifth case is more than the fourth case. This is because the power of the received signal of the fifth case (1 dB) is lower than the fourth case (5 dB). Moreover, when consider the SIRs of the conventional technique and the proposed technique in Table 4.4, it is evident that the SIRs of the proposed technique are higher than the conventional technique, even though the received signal power is decreased. Furthermore, the SIRs of conventional method in the fifth case are less than the fourth case, the four-element in particular.

Therefore, the proposed technique can be used to increase the efficiency in the beamforming system of adaptive antenna which their methods are enforced by the covariance matrix.

## 4.6 Concluding Remarks

The covariance matrix adjustment technique is proposed and described. The most important of this technique is the adjustable multipliers which multiply with the covariance matrices of desired signal and interfering signals. The proposed technique enforces the beam pattern of the array antenna peak and null in the DOAs of desired signal and interfering signals, respectively, more efficient than the conventional method.

The simulation results of DOA estimation and the beamforming methods are demonstrated and discussed. The suitable DOA methods are chosen for the proposed technique by considering the behavior of each DOA method. The Capon's minimum-variance method is used to estimate the number and the relative power of the received signal. In the mean time, the spatial smoothing technique with MUSIC method is used to estimate the DOA of the correlated signals or coherent signals. Additionally, the beamforming simulation results are illustrated and considered in various situations which their efficiency of the SIR and null response controlling are summarized in Table 4.3 and 4.4, respectively. These results clarify that the proposed covariance matrix adjustment technique is more efficient than the conventional methods and capable to improve the null beampattern setting of adaptive array, although the power of received signal decreases. Thus the proposed technique can be used to overcome the weak signal problem when the signal to noise ratio of the received signal is low.

The feature of this proposed method is that the efficiency of setting the beam peak in the desired signal and null in the interference directions. The computer simulation results illustrate that the proposed covariance matrix adjustment technique can improve interference cancellation in the adaptive array beamforming method which uses covariance matrix for the complex weight computation: Applebaum array and LCMV method. Although, there are many incident interference signals as much as the degree of freedom of the system, the proposed covariance matrix adjustment technique can solve the weak signal problem for the interference rejection. Moreover, this technique can be effectively used with many number of received array antenna element and also used with both noncoherent and coherent received signals.

# CHAPTER 5
# EXPERIMENTAL RESULTS

## 5.1 Introduction

According to the aforementioned simulation results of adaptive array in the previous chapter, this chapter performs experiment to clarify the advantages [28] of the proposed covariance matrix adjustment technique in adaptive array beamforming. The weight computation in various experimental situations were computed and used to adjust the beam pattern of the received array antenna. By multiplying the complex weight with the beam pattern of the receiving antenna, the interference rejection capability can be realized. In addition, the DOA has been estimated and demonstrated in this chapter to utilize its information in the weight computation.

Furthermore, the calibration process for the experiment is described and used to decrease the effects from the non identical of each channel of the array. The phase and magnitude of the received signal in each channel of the array is calibrated before using in adaptive array process.

## 5.2 Experimental Configuration

The experiments were conducted in the anechoic chamber that was provided by Communications Research Laboratory (CRL) Japan at Yokosuka Radio Communications Research Center.

The equipments of the experiment consist of

1. eight-element patch array antenna and two dummy elements with down converter in the back side
2. horn antenna
3. single patch antenna
4. 1st signal generator: $\pi/4$-shiftQPSK, 42kbps
5. 2nd signal generator: $\pi/4$-shiftQPSK, 42kbps
6. 2 attenuators
7. computer
8. power supply
9. AD converter
10. anechoic chamber and control room

The pictures of equipment can be shown in Fig. 5.1.

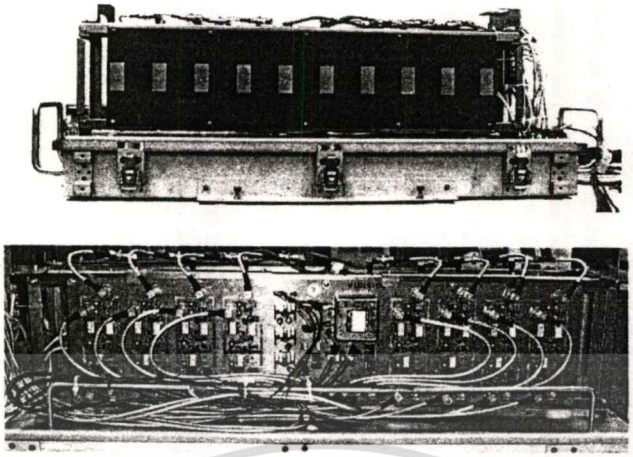

(a)

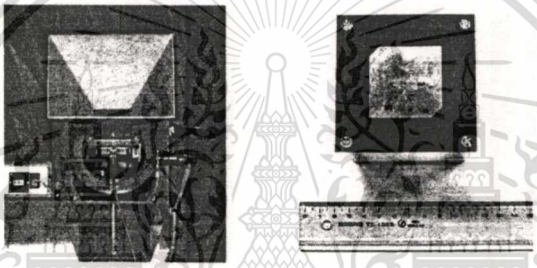

(b) (c)

(d)

**Fig. 5.1** Photographs of the equipment: **(a)** eight-element patch array antenna and two dummy elements with down converters in the back side, **(b)** horn antenna, **(c)** single patch antenna, **(d)** anechoic chamber

The configuration of transmitters and receiver are illustrated in Fig.5.2. The desired transmitting antenna is a horn antenna. The interfering transmitting antenna is a single patch while the receiving antenna is an eight-element patch antenna array with half wavelength inter-element and two dummy elements are placed at both ends of the antenna elements to equalize the characteristics. The transmitter transmits $\pi/4$ QPSK modulation signal, with the carrier frequency of 2.335 GHz. The sampling rate of the receiver is 1.8 MHz with the IF of 450 kHz. All 8 elements of the array antenna were connected to down converters for converting the received signal in each branch of array antennas down to IF of 450 kHz. The 450 kHz IF in each channel passed the A/D converter for converting analog signal to digital signal before adaptively processed by the computer. The block diagram of the receiver can be shown in Fig. 5.3.

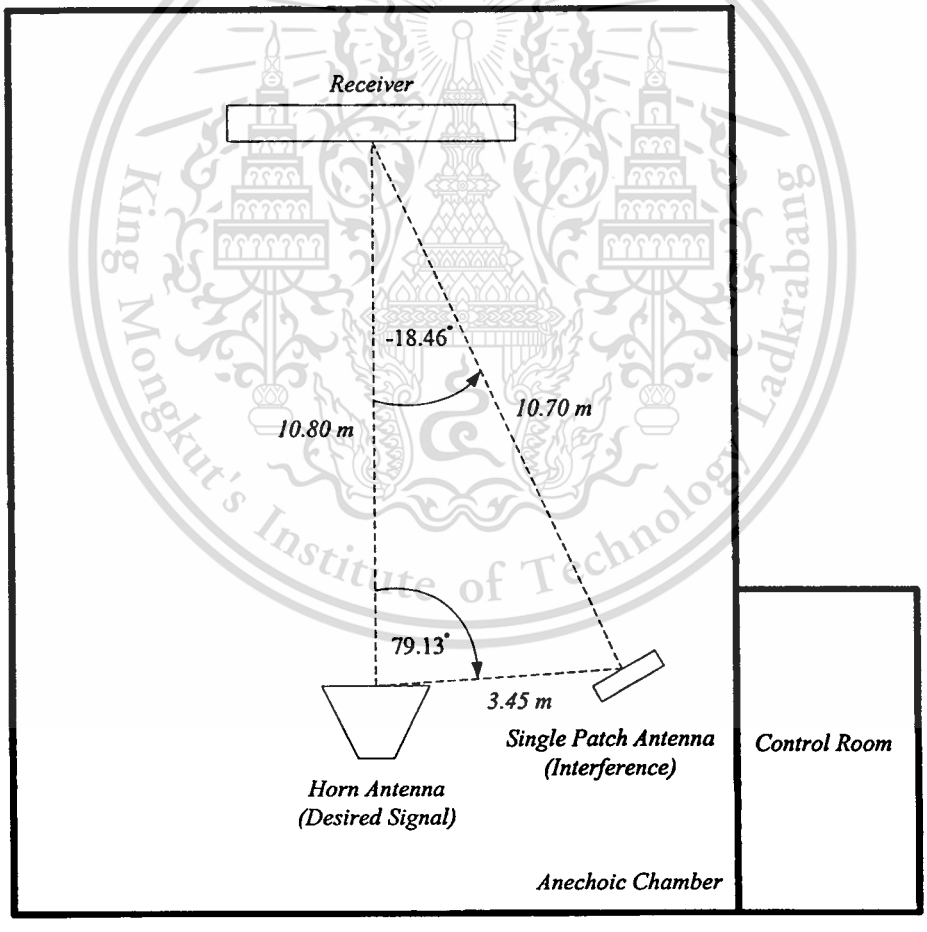


**Fig. 5.2** Configuration of the experiment (not to scale)

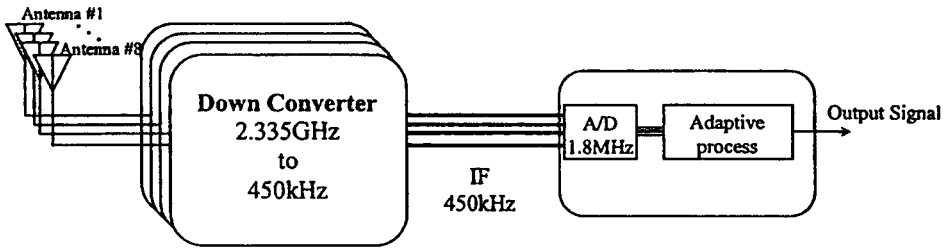


**Fig. 5.3** Block diagram of the receiver

In the adaptive process, the signal from each branch was collected separately among the other branches. The collected data were used to estimate the direction of incident signal and the relative power intensity by DOA methods [13] before the complex weight computation. In this case, the relative power intensities in the incident directions of the received signals were used to provide covariance matrix for the complex weight computation.

## 5.3 Calibration Process

In order to realize the precise beamforming and DOA estimation, the calibration process is indispensable since there are several unavoidable factors that degrade the adaptive array process. In particular the imbalance of the amplitude and phase in the received array signal between RF circuits needs to be calibrated frequently and quickly when the array system exists in the changeable environment since the imbalance easily occurs due to thermal characteristics of each RF circuit [29, 30].

The calibration process of the experiment has been done since the transmitter and the receiver are arranged in their line of sight that the DOA of impinging signal is $0^{\circ}$. The calibration process begins with the amplitude calibration. The received signals in each branch of the array antennas have been shown in equation (2.7):

$$X = [\bar{x}_1(t), \bar{x}_2(t), \bar{x}_3(t), ..., \bar{x}_N(t)]^T,$$

which their amplitude calibration can be achieved by using equation (5.1).

$$X_{AmpCall} = X \times \frac{\tilde{x}_m}{\tilde{X}}, \tag{5.1}$$

where $\tilde{x}_m$ and $\tilde{X}$ are the time average of the received signal in element $m$ and time average of the received array signals which can be obtained as

$$\tilde{x}_m = \frac{1}{NN}\sum_{t=1}^{NN} x_m(t) \tag{5.2}$$

and

$$\tilde{X} = \frac{1}{NN}\sum_{t=1}^{NN} X(t). \tag{5.3}$$

The subscript $m$ represents the reference element of the array that is usually set as the element number at the both end of the array because the angle of the arrival signal generally refers to the DOA at the edged element of the adaptive array beamforming. Meanwhile, $NN$ is the number of the collecting sample. After the received signals amplitude calibration, their phases have been calibrated by equation (5.4)

$$X_{output} = X_{AmpCal} \times e^{j\bar{\phi}}, \tag{5.4}$$

where

$$\bar{\phi} = \text{angle of} \left\{ \frac{X^*_{AmpCal} \times X_{AmpCal_m}}{X^*_{AmpCal} \times X_{AmpCal}} \right\}. \tag{5.5}$$

$\bar{\phi}$ is the calibration phase matrix that can be calculated from the average different phase between the $X_{AmpCal}$ and the $X_{AmpCal}$ at the reference element $m$ ($X_{AmpCal_m}$).

As mentioned, the calibration process has to be done while the DOA of the received signal is $0^\circ$. This can provide the amplitude and phase calibration factors for calibrating through all situations [29, 30, 31]. The amplitude and phase calibration factors can be demonstrated as

$$\text{Amplitude Calibration Factor} = \frac{\bar{X}_{m \text{ at } 0^\circ}}{\bar{X}_{\text{at } 0^\circ}} \tag{5.6}$$

and

$$\text{Phase Calibration Factor} = e^{j\bar{\phi}_{\text{at } 0^\circ}}. \tag{5.7}$$

Thus, from this process the received signal calibration both amplitude and phase can be achieved. The experimental results of the calibration can be shown in Fig. 5.4. In Fig. 5.4, the non-modulated signal is transmitted by the 1st generator face to face with the receiver that the DOA of the received signal is $0^\circ$. It is seen that the received signal from each channel after calibration seems to be the same both amplitude and phase. In contrast the non-calibration process gives the different phase and amplitude in each channel due to the non-identical of each channel in the array which results are shown in Fig. 5.5.

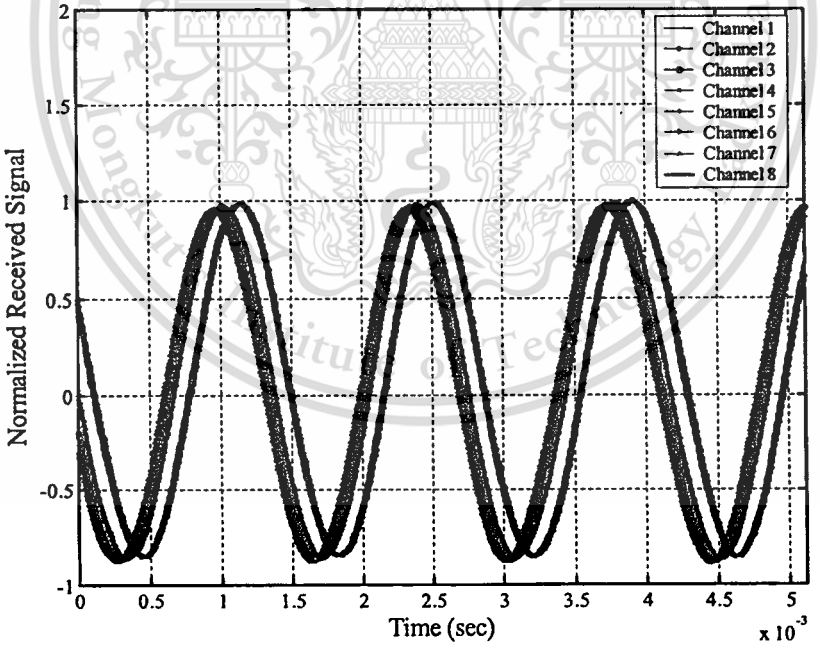


**Fig. 5.4(a)** The non-modulated received signal after amplitude calibration when the DOA of received signal is $0^\circ$

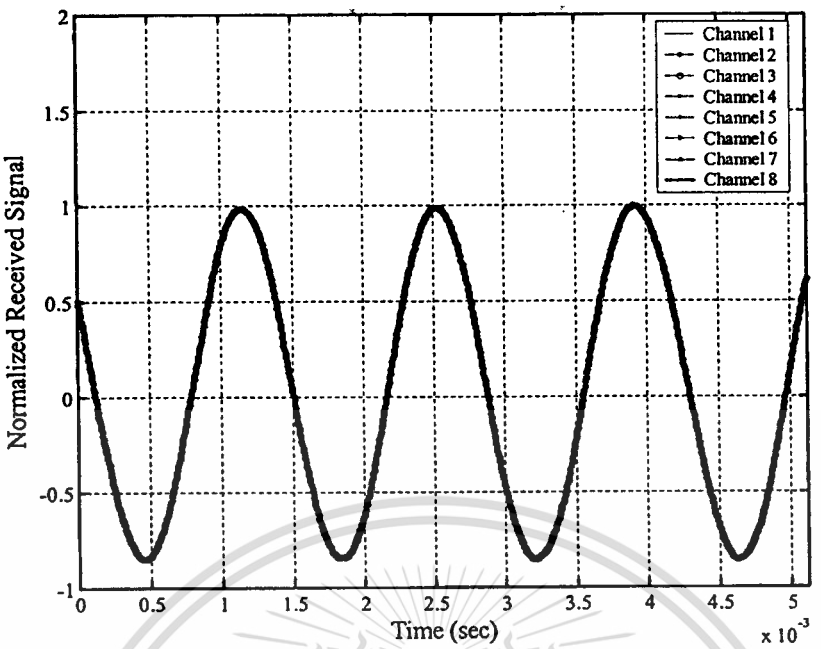


**Fig. 5.4(b)** The non-modulated received signal after amplitude and phased calibration when the DOA of received signal is $0^{\circ}$

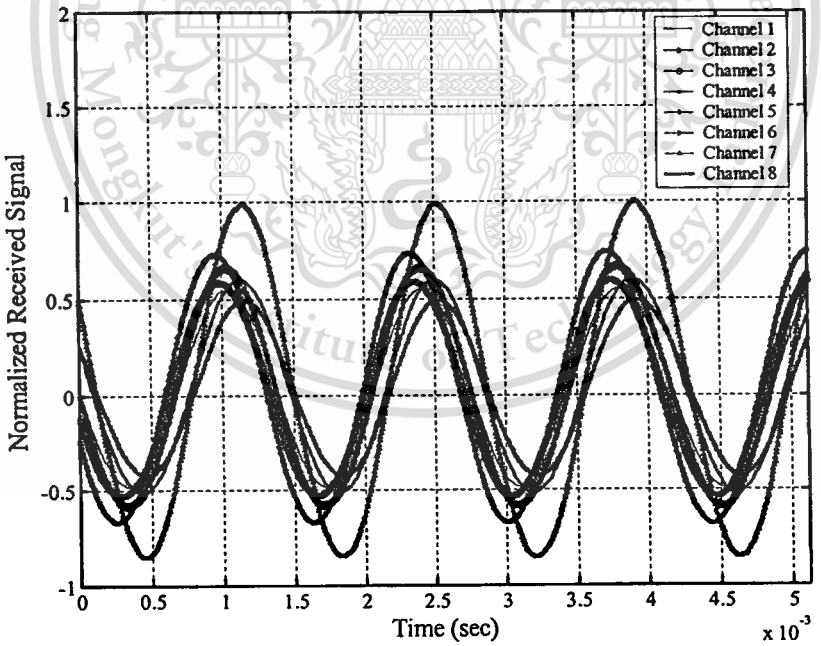


**Fig. 5.5** The non-calibration results of the non-modulated received signal when the DOA of received signal is $0^{\circ}$

Again, by changing the DOA of the received signal to 30° and –30°, the non-modulated received signal after calibration can be obtained by using the calibration factors that is calculated when the DOA is 0°. Their comparative results between the non-calibration and calibration of the DOA estimation when the single DOA of the impinging signal are 30° and then –30°, can be shown in Fig. 5.6 and Fig. 5.7, respectively. It is evident that the effect of non-calibration degrades the DOA estimation of the adaptive array antenna. The DOA estimations of the non-calibration can not provide the precise DOA of the incoming signal, both two cases 30° and –30°, on the contrary the DOA estimations with calibration give the exact direction of the incoming signal. As the calibration of the non-modulated received signal has been done, the calibration of the modulated signal can be obtained in the same manner that will be used in next section.

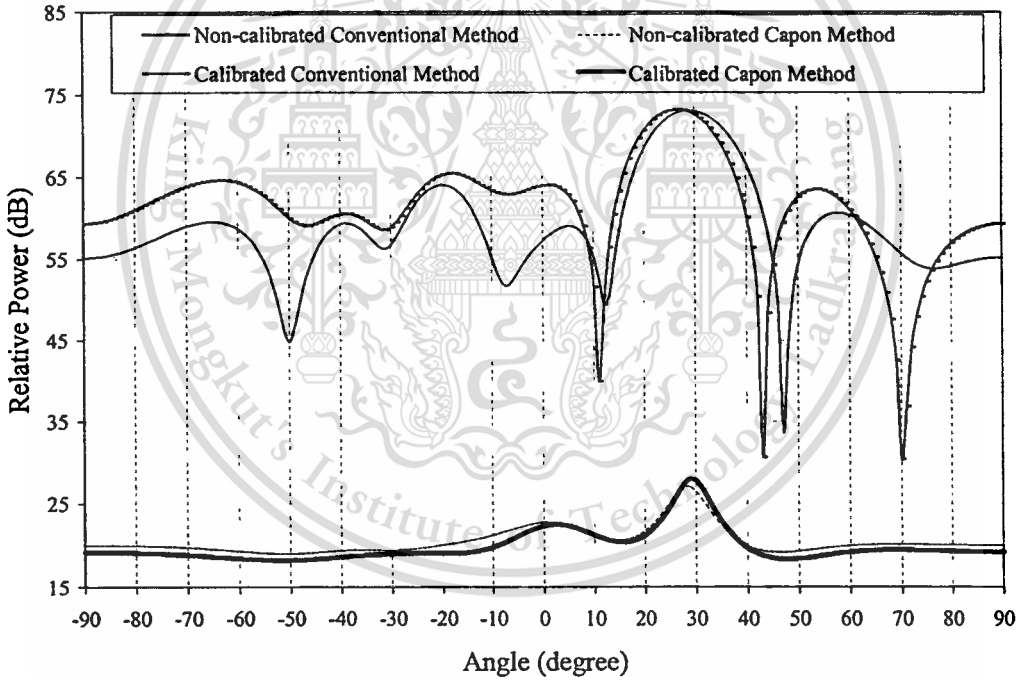


**Fig. 5.6(a)** The comparative results of conventional and Capon methods between non-calibration and calibration when the DOA is 30°

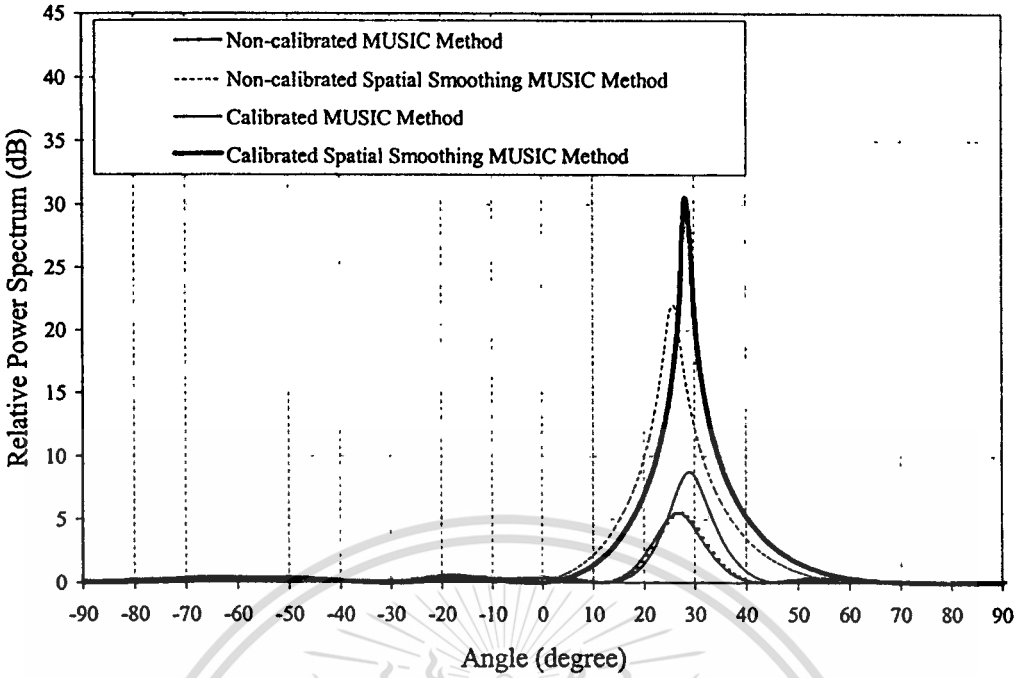


**Fig. 5.6(b)** The comparative results of MUSIC and spatial smoothing MUSIC methods between non-calibration and calibration when the DOA is 30°

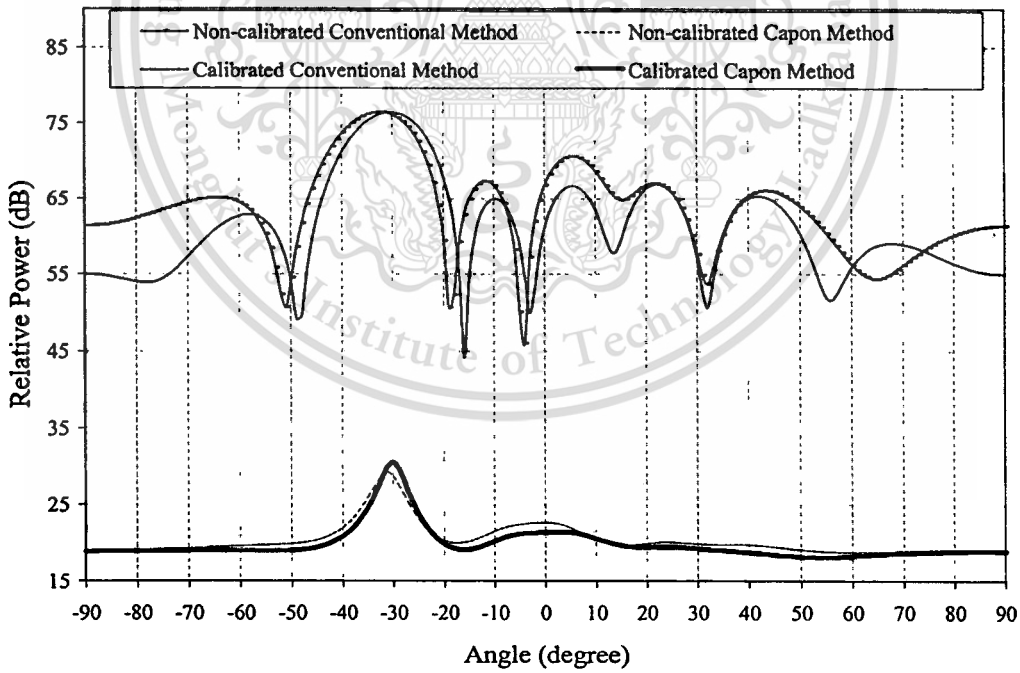


**Fig. 5.7(a)** The comparative results of conventional and Capon methods between non-calibration and calibration when the DOA is −30°

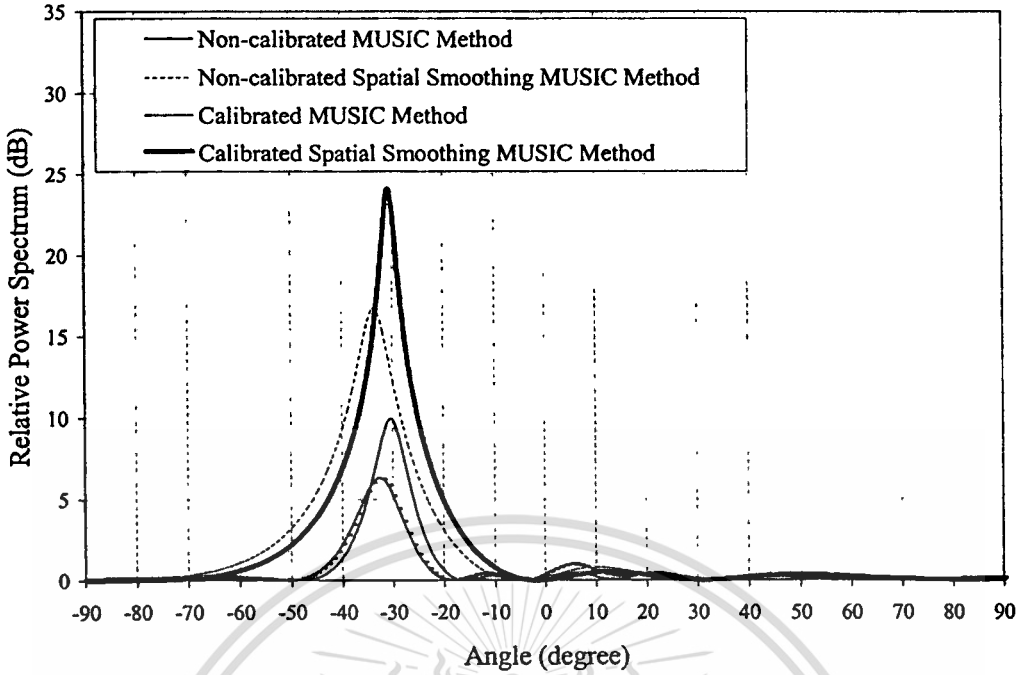


**Fig. 5.7(b)** The comparative results of MUSIC and spatial smoothing MUSIC methods between non-calibration and calibration when the DOA is $-30^{\circ}$

As the degradation in DOA estimation of the non-calibration occurs, this will affect the beamforming of adaptive array antenna. Thus, the calibration is the one important process that is indispensable in the array system.

## 5.4 Bit Error Rate (BER)

In digital communication, the bit error rate or BER is the parameter that is used to evaluate the efficiency of the digital communication system. Thus, to clarify the efficiency of the proposed covariance matrix adjustment technique in adaptive array beamforming, the BER will be obtained by using [21],

$$\text{BER}=\frac{\text{Bits in Error}}{\text{Total bits received}}. \tag{5.8}$$

## 5.5 Experimentation

In this section, the DOA of the received signals are estimated and their information are used for the weight computation in various kinds of the experimental situations. The complex weights were computed and used to adjust the beam pattern of the received array antenna by multiplying the complex weight with the beam pattern of the receiving array antenna for realizing the interference rejection capability. In addition the BER of the adaptive array output signal in each situation has been calculated and discussed.

In this experiment, the DOA estimations and weight computation use 1024 samples from each element per one cycle of the calculation [32, 33].

### 5.5.1 Radiation pattern of the receiving array antenna experiment

The receiving antenna is eight-element patch array antenna with half wavelength inter-element which its radiation pattern is measured and illustrated in Fig. 5.8. The separation of data measurement is ten degrees.

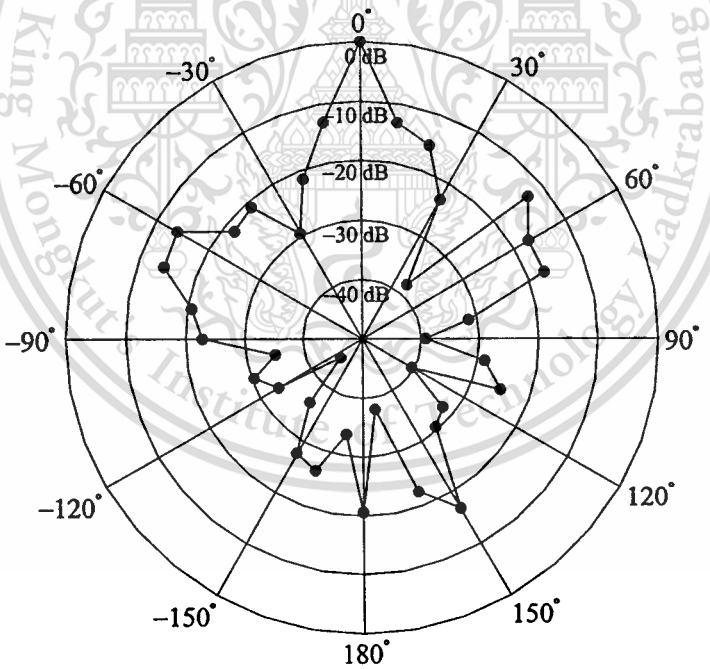


**Fig. 5.8(a)** The radiation pattern of eight-element patch array antenna in polar form

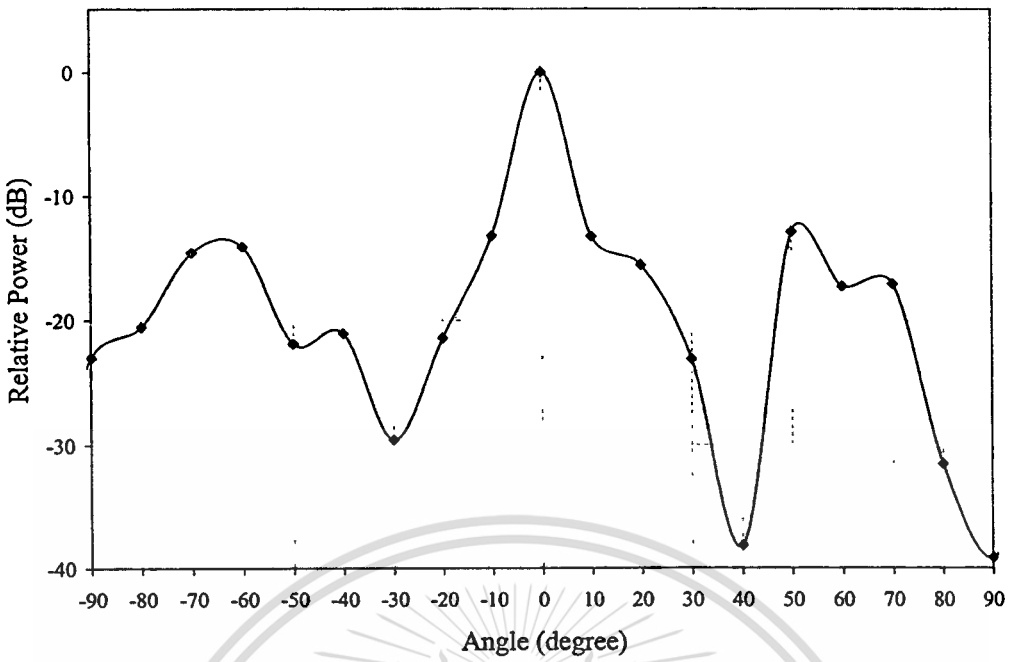


**Fig. 5.8(b)** The radiation pattern of eight-element patch array antenna in rectangular form

### 5.5.2 Single modulated signal experiment

The one signal is transmitted from the 1st signal generator to the receiving array antenna by using horn antenna in various DOA situations. Their positions are placed in Fig. 5.1. The output power 1 watt or 0 dB of the signal generator is passed through the 49 dB attenuator to the horn antenna. For this experiment the number of the DOA of the incoming signal is only one, thus the proposed technique obtains the same complex weight of the conventional technique. For this reason, there are only the results of conventional method in this experiment.

To perform this experiment, the receiving array antenna should be rotated to the opposite direction of the DOA. For example, when the DOA is $-50^{\circ}$, the receiving array antenna will be rotated to the direction $50^{\circ}$. In contrast, when the DOA is $50^{\circ}$, the rotating direction of the receiving array antenna is $-50^{\circ}$.

In all cases of this section, the DOA estimation and weight computation use one cycle for the operation which their results can be illustrated as follows while the BER is obtained by using 15 time cycles of 1024 samples.

5.5.2.1 The DOA is $-50^{\circ}$

- DOA estimation

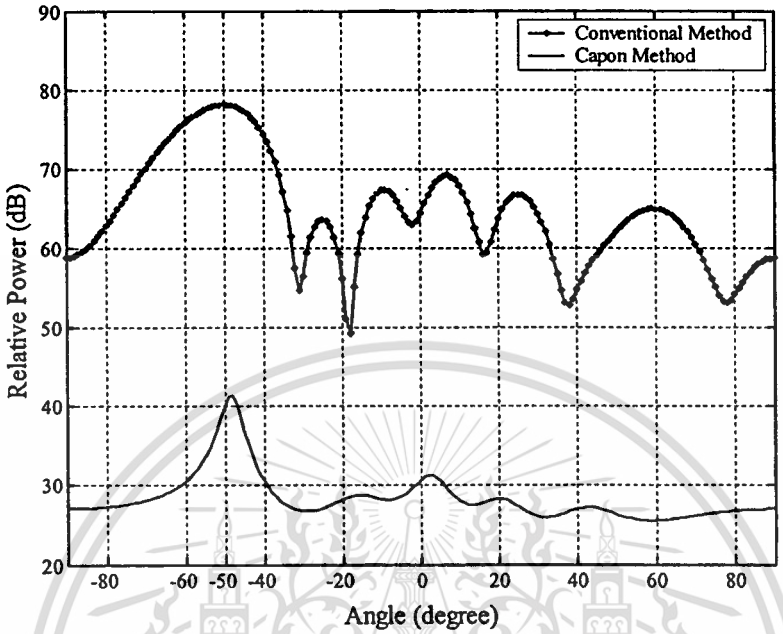


**Fig. 5.9(a)** The experimental results of the DOA estimations using conventional and Capon methods

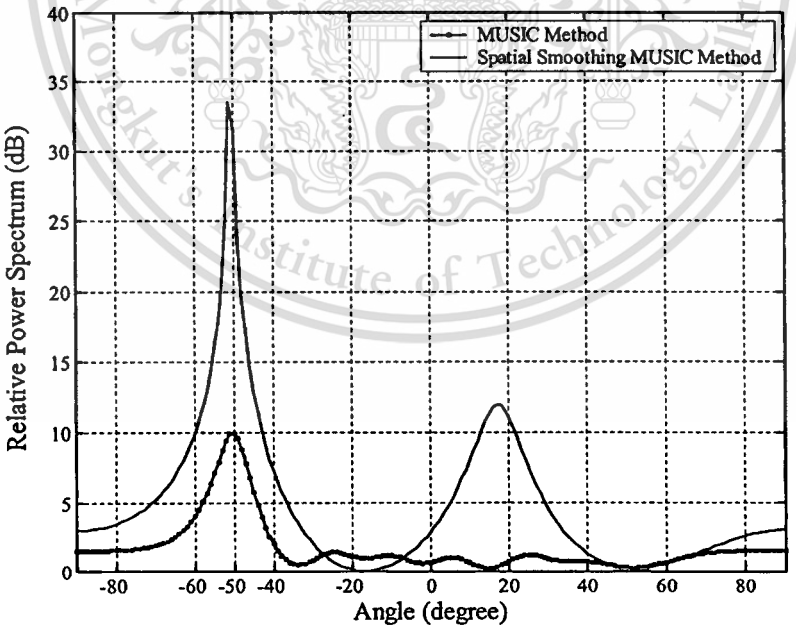


**Fig. 5.9(b)** The experimental results of the DOA estimations using MUSIC and spatial smoothing MUSIC methods

- Beamforming

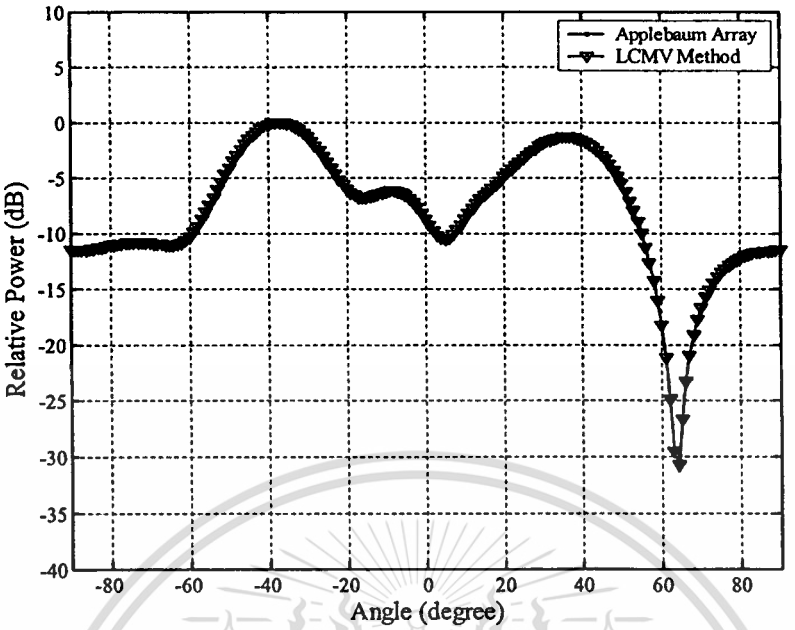


**Fig. 5.10(a)** The simulation results of beamforming

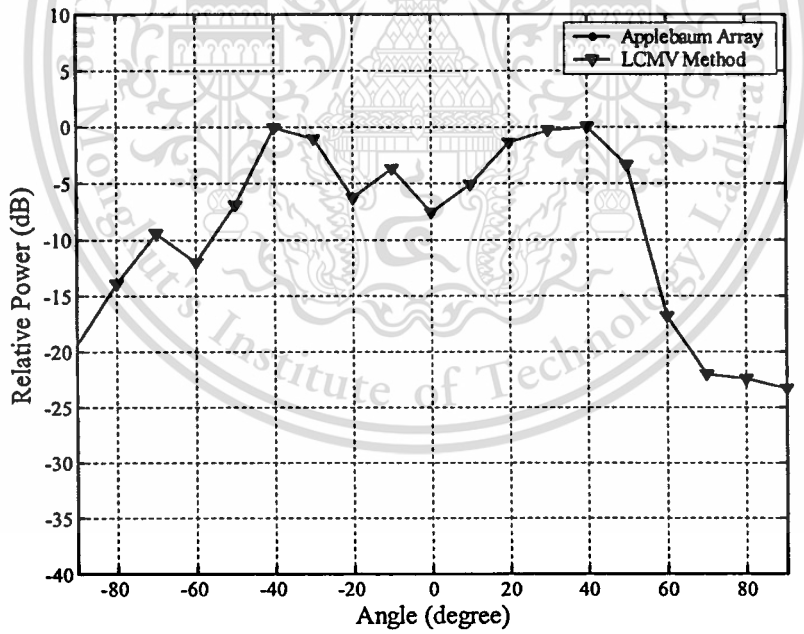


**Fig. 5.10(b)** The experimental results of beamforming

- BER

The BER of this experiment can be provided as Table 5.1.

**Table 5.1** The BER of the experiment 5.5.2.1

| Time of Sampling\BER | Received Signal | Applebaum Array | LCMV Method |
|---|---|---|---|
| 1 | 0.000000 | 0.000000 | 0.000000 |
| 2 | 0.000000 | 0.000000 | 0.000000 |
| 3 | 0.019231 | 0.004808 | 0.004808 |
| 4 | 0.000000 | 0.000000 | 0.000000 |
| 5 | 0.000000 | 0.000000 | 0.000000 |
| 6 | 0.000000 | 0.000000 | 0.000000 |
| 7 | 0.000000 | 0.000000 | 0.000000 |
| 8 | 0.000000 | 0.000000 | 0.000000 |
| 9 | 0.000000 | 0.000000 | 0.000000 |
| 10 | 0.004808 | 0.004808 | 0.004808 |
| 11 | 0.000000 | 0.004808 | 0.004808 |
| 12 | 0.000000 | 0.000000 | 0.000000 |
| 13 | 0.000000 | 0.000000 | 0.000000 |
| 14 | 0.000000 | 0.000000 | 0.000000 |
| 15 | 0.000000 | 0.000000 | 0.000000 |
| Average BER | 0.001603 | 0.000962 | 0.000962 |

The single modulated signal is transmitted to the receiving array antenna that its DOA can be estimated by all methods and the beamforming process can be achieved by the conventional methods shown in Fig. 5.9 and Fig. 5.10, respectively. Since in this case there is only one signal impinging at the receiving array antenna, thus it can operate the adaptive process to form the main beam in the desired signal by conventional methods both Applebaum array and LCMV method. Furthermore, the demonstrated BER in Table 5.1, the capability of the conventional method for enhancing the wireless communication is evident. In addition, at the other DOAs the DOA estimation and the beamforming can still be performed in next section. The simulation and the experiment results give the same trend that clarifies the accuracy of the system used.

5.5.2.2 The DOA is $-20^{\circ}$

- DOA estimation

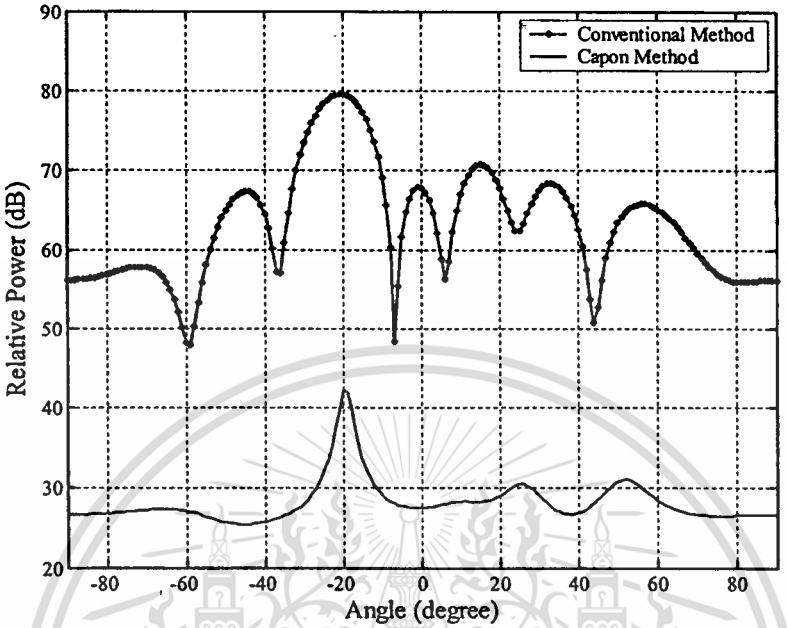


**Fig. 5.11(a)** The experimental results of the DOA estimations using conventional and Capon methods

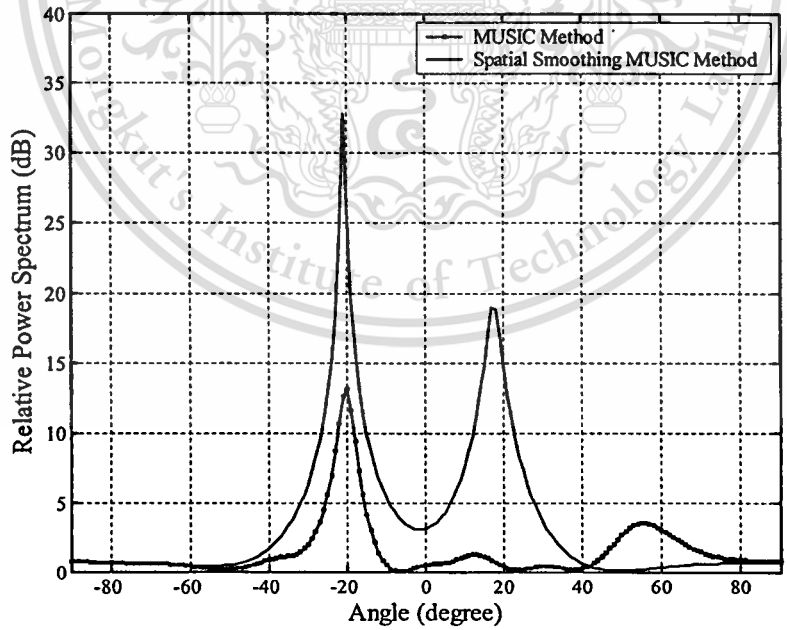


**Fig. 5.11(b)** The experimental results of the DOA estimations using MUSIC and spatial smoothing MUSIC methods

- Beamforming

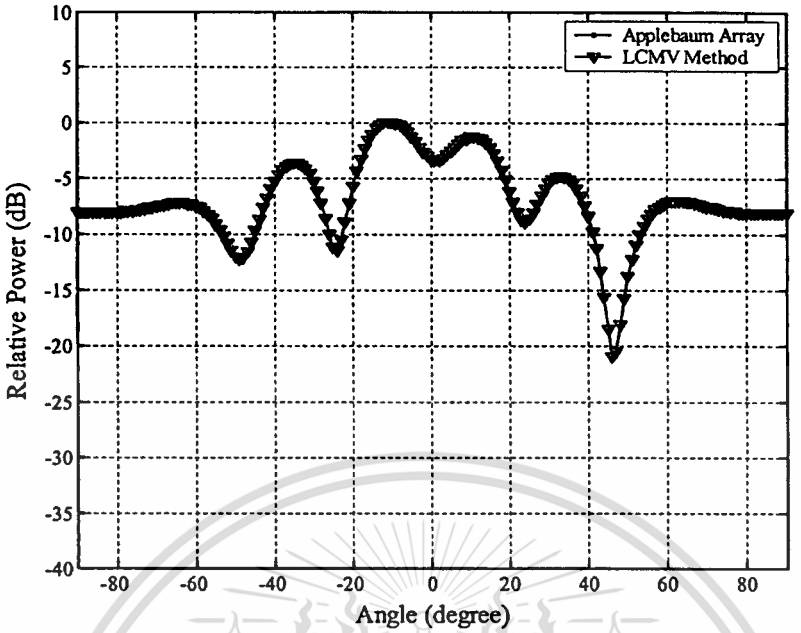


**Fig. 5.12(a)** The simulation results of beamforming

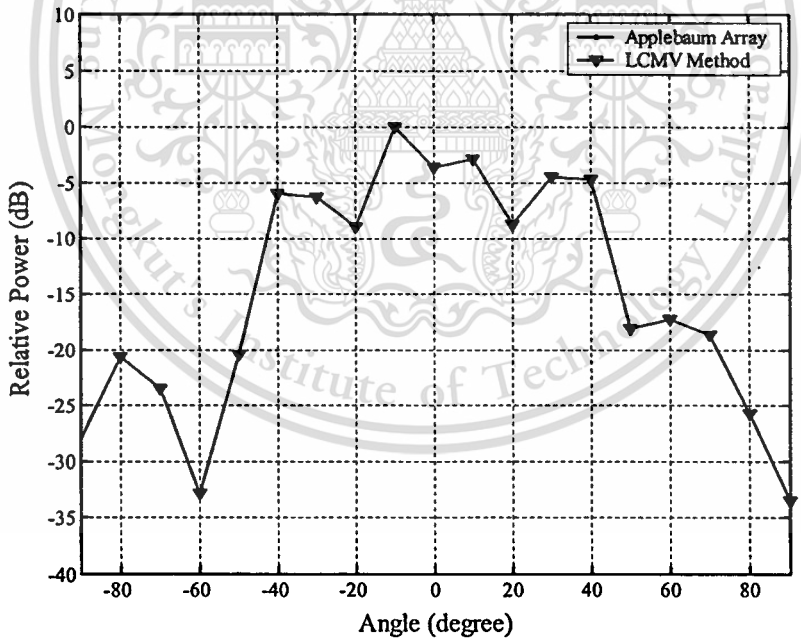


**Fig. 5.12(b)** The experimental results of beamforming

- BER

The BER of this experiment can be provided as Table 5.2.

**Table 5.2** The BER of the experiment 5.5.2.2

| Time of Sampling\BER | Received Signal | Applebaum Array | LCMV Method |
|---|---|---|---|
| 1 | 0.004808 | 0.000000 | 0.000000 |
| 2 | 0.000000 | 0.000000 | 0.000000 |
| 3 | 0.000000 | 0.000000 | 0.000000 |
| 4 | 0.004808 | 0.000000 | 0.000000 |
| 5 | 0.000000 | 0.000000 | 0.000000 |
| 6 | 0.000000 | 0.000000 | 0.000000 |
| 7 | 0.000000 | 0.000000 | 0.000000 |
| 8 | 0.000000 | 0.000000 | 0.000000 |
| 9 | 0.000000 | 0.000000 | 0.000000 |
| 10 | 0.000000 | 0.000000 | 0.000000 |
| 11 | 0.000000 | 0.000000 | 0.000000 |
| 12 | 0.000000 | 0.000000 | 0.000000 |
| 13 | 0.000000 | 0.000000 | 0.000000 |
| 14 | 0.000000 | 0.000000 | 0.000000 |
| 15 | 0.000000 | 0.000000 | 0.000000 |
| Average | 0.000641 | 0.000000 | 0.000000 |

From Fig. 5.11 and Fig. 5.12, the results of DOA estimation and beamforming are demonstrated. All DOA estimations can provide the precise direction of the received signal at $-20^{\circ}$. While the beamforming can achieve both simulation and experimental results which are shown the capability enhancement in the beam pattern of the receiving antenna. In addition, the illustration of BER in Table 5.2 verifies the efficiency of the beamforming process.

5.5.2.3 The DOA is 10°

- DOA estimation

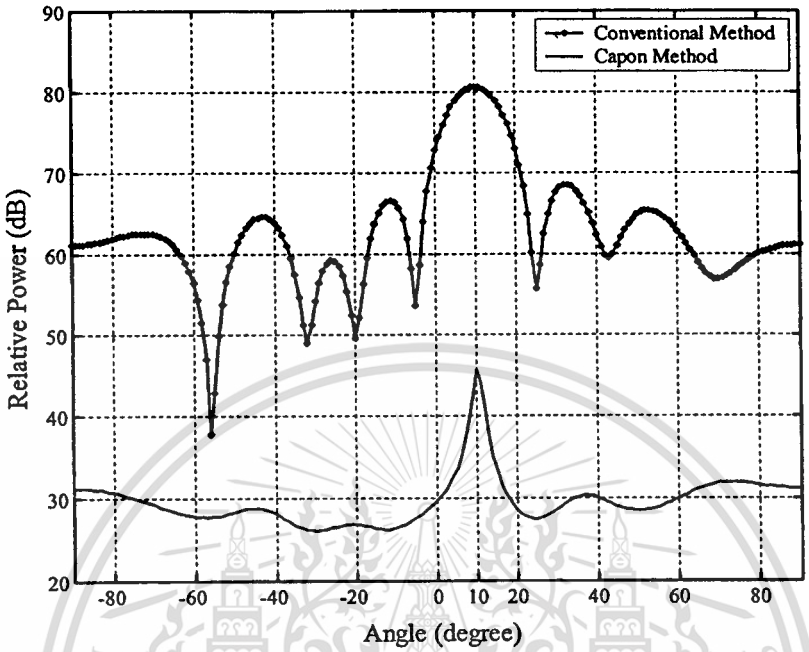


**Fig. 5.13(a)** The experimental results of the DOA estimations using conventional and Capon methods

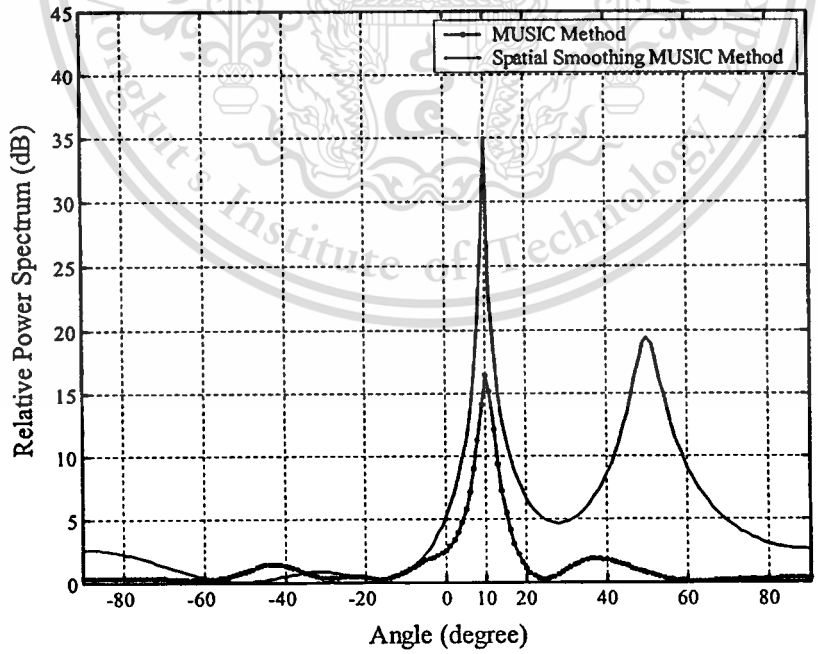


**Fig. 5.13(b)** The experimental results of the DOA estimations using MUSIC and spatial smoothing MUSIC methods

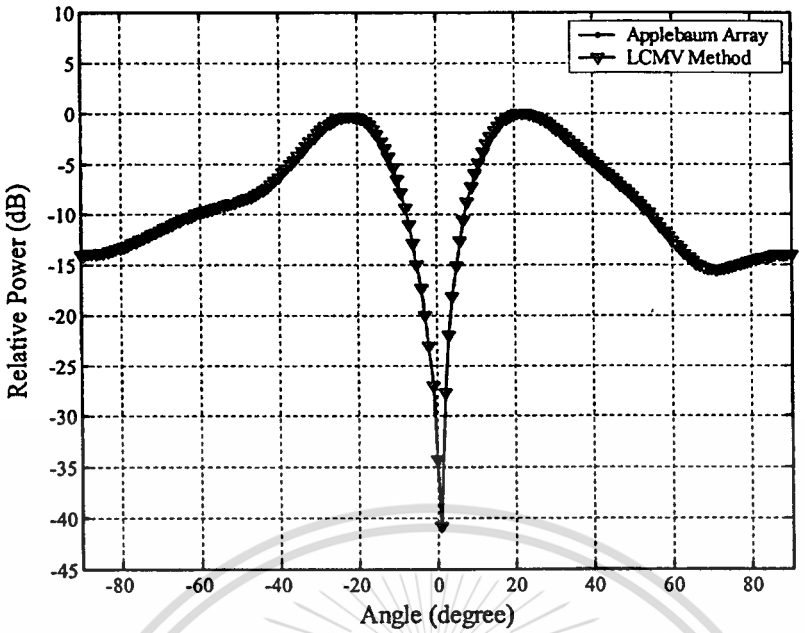


**Fig. 5.14(a)** The simulation results of beamforming

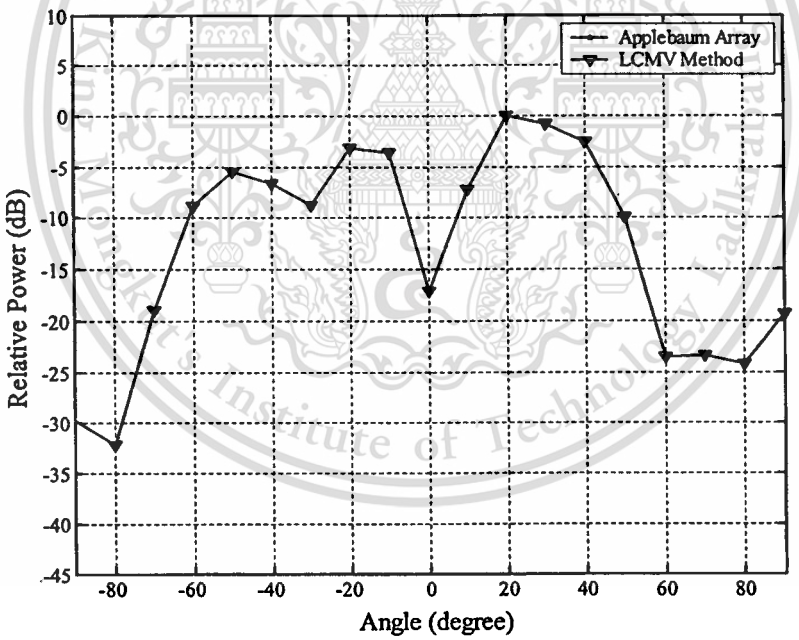


**Fig. 5.14(b)** The experimental results of beamforming

- BER

The BER of this experiment can be provided as Table 5.3.

**Table 5.3** The BER of the experiment 5.5.2.3

| Time of Sampling\BER | Received Signal | Applebaum Array | LCMV Method |
|---|---|---|---|
| 1 | 0.000000 | 0.000000 | 0.000000 |
| 2 | 0.000000 | 0.000000 | 0.000000 |
| 3 | 0.000000 | 0.000000 | 0.000000 |
| 4 | 0.000000 | 0.000000 | 0.000000 |
| 5 | 0.004808 | 0.000000 | 0.000000 |
| 6 | 0.028846 | 0.028846 | 0.028846 |
| 7 | 0.000000 | 0.000000 | 0.000000 |
| 8 | 0.000000 | 0.000000 | 0.000000 |
| 9 | 0.000000 | 0.000000 | 0.000000 |
| 10 | 0.000000 | 0.000000 | 0.000000 |
| 11 | 0.000000 | 0.000000 | 0.000000 |
| 12 | 0.000000 | 0.000000 | 0.000000 |
| 13 | 0.000000 | 0.000000 | 0.000000 |
| 14 | 0.004808 | 0.000000 | 0.000000 |
| 15 | 0.000000 | 0.000000 | 0.000000 |
| Average | 0.002564 | 0.001923 | 0.001923 |

The DOA estimations can be obtained as shown in Fig. 5.13. The estimating direction is exact with the direction of the incoming signal that is $10^{\circ}$. Thus, this can verify the accuracy of the DOA estimation process. Furthermore, Fig. 5.14 and the BER results in Table 5.3, clarify the capability and the BER enhancement of the beamforming process.

To this end, all above experimental results evident that the adaptive array beamforming can provide the effective results in the system. The antenna beam patterns and the BER can clarify their efficiencies.

### 5.5.3 Two non-correlated modulated signals experiment

In this case, the transmitting antennas are fixed in the same position of Fig. 5.2, while the receiving antenna is able to rotate to other directions referring to the position of the desired signal. In the meantime, two non-correlated signals are transmitted from two different signal generators, 0 dB from the output of the 1st signal generator with attenuation of 49 dB for the desired signal and -11 dBm from the output of the 2nd signal generator for the interference signal. The results when the power level of the interference decreases or the output power of the 2nd signal generator is decreased are demonstrated in section 5.5.3.3.

**5.5.3.1** The direction of receiver is $-10^{\circ}$ :

The configuration of this experiment can be shown as Fig. 5.15.

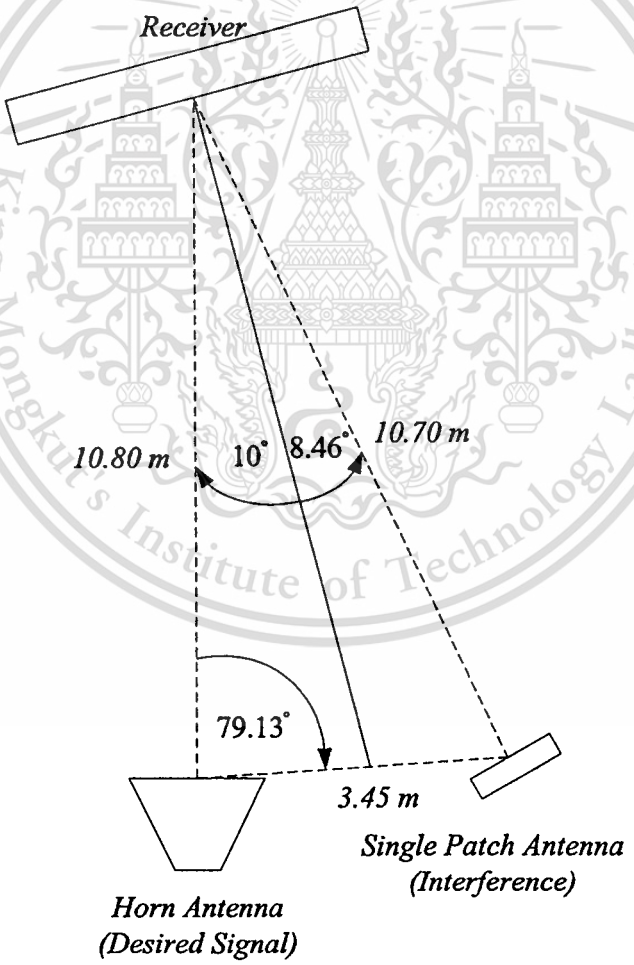


**Fig. 5.15** Configuration of the experiment (not to scale)

- DOA estimation

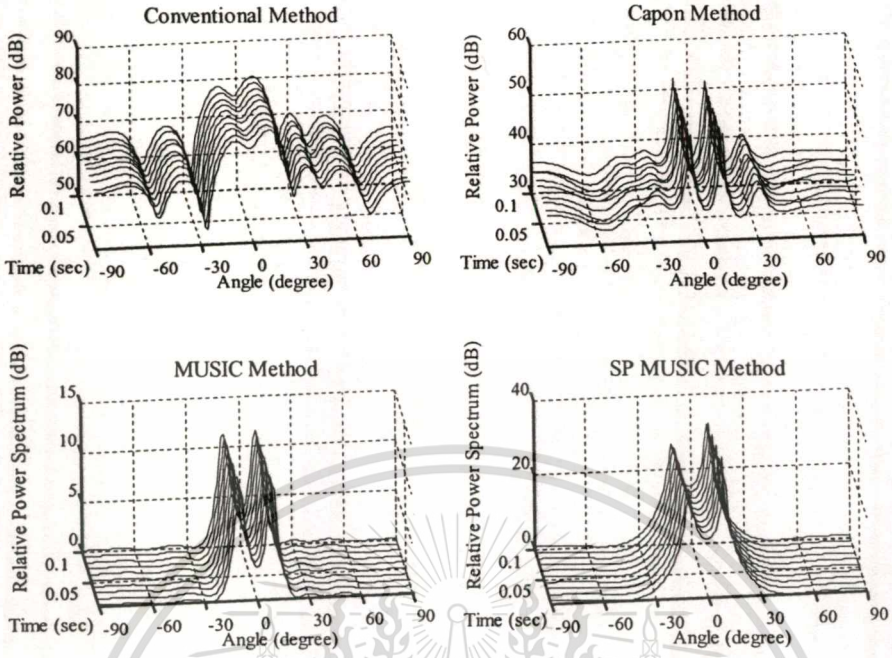


**Fig. 5.16** The experimental results in three dimensions of DOA estimations with 10 time cyclic variations

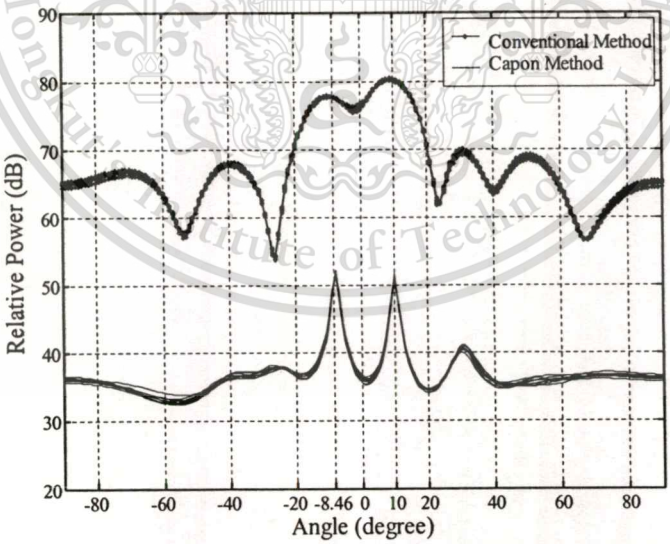


**Fig. 5.17(a)** The experimental results in two dimensions of the DOA estimations using conventional and Capon methods with 10 time cyclic variations

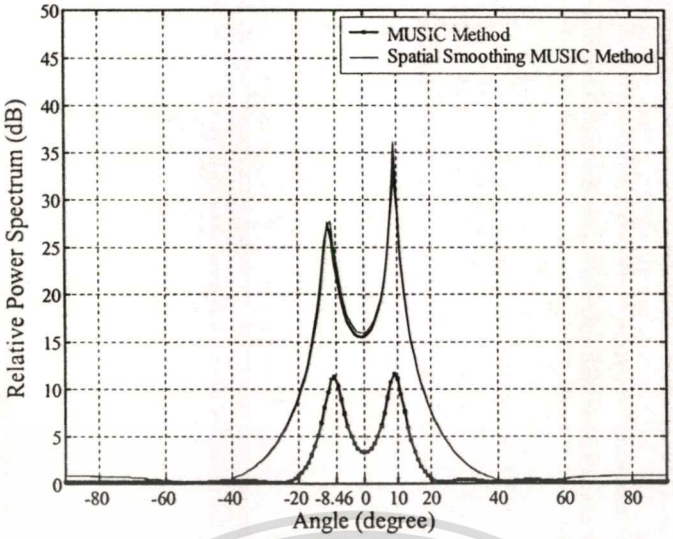


**Fig. 5.17(b)** The experimental results in two dimensions of the DOA estimations using MUSIC and spatial smoothing MUSIC methods with 10 time cyclic variations

- Beamforming

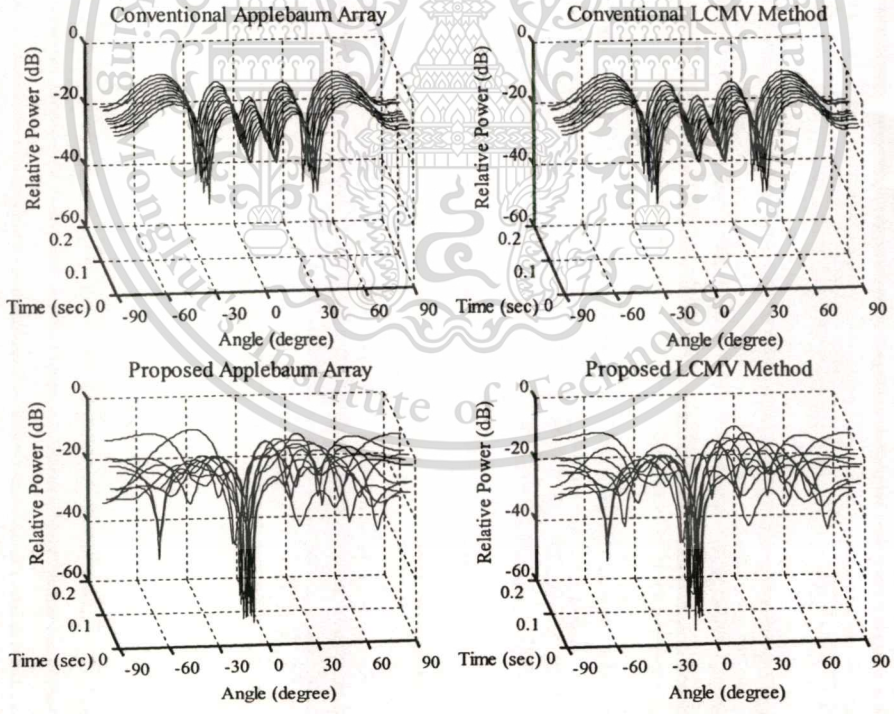


**Fig. 5.18(a)** The simulation results in three dimensions of beamforming with 10 time cyclic variations

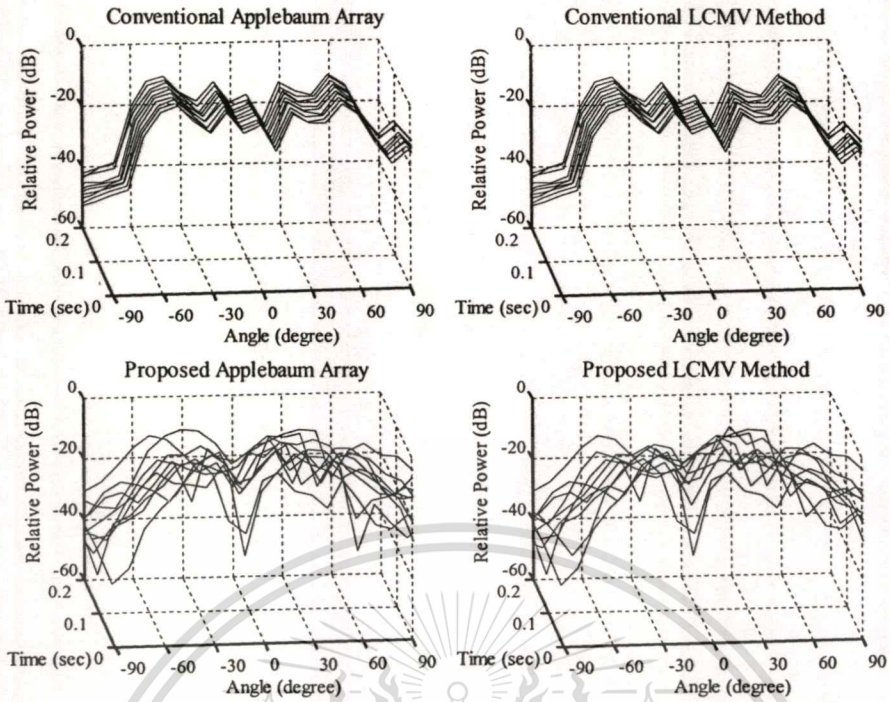


**Fig. 5.18(b)** The experimental results in three dimensions of beamforming with 10 time cyclic variations

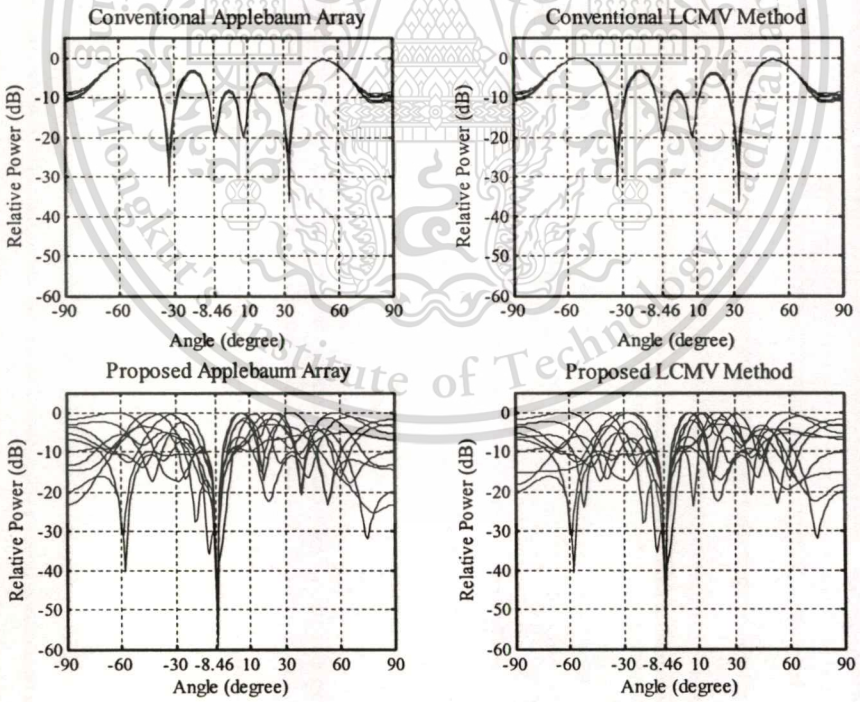


**Fig. 5.19(a)** The simulation results in two dimensions of beamforming with 10 time cyclic variations

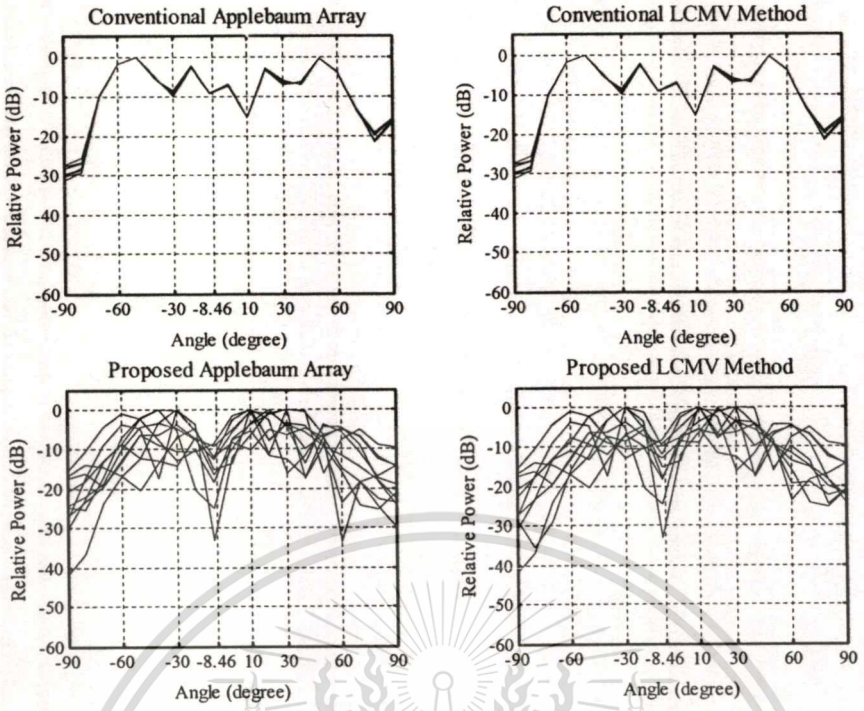


**Fig. 5.19(b)** The experimental results in two dimensions of beamforming with 10 time cyclic variations

- BER

The BER of this experiment is obtained by using 15 time cycles of 1024 samples which can be demonstrated as Table 5.4 and Fig. 5.20.

**Table 5.4** The BER of the experiment 5.5.3.1

| \BER Time of \ Sampling | Received Signal | Applebaum Array | LCMV Method | Proposed Applebaum Array | Proposed LCMV Method |
|---|---|---|---|---|---|
| 1 | 0.201900 | 0.065700 | 0.065700 | 0.011200 | 0.016000 |
| 2 | 0.179467 | 0.044867 | 0.044867 | 0.000000 | 0.000000 |
| 3 | 0.187500 | 0.064133 | 0.064133 | 0.000000 | 0.000000 |
| 4 | 0.169867 | 0.062500 | 0.062500 | 0.001600 | 0.001600 |
| 5 | 0.144233 | 0.057700 | 0.057700 | 0.000000 | 0.000000 |
| 6 | 0.165067 | 0.064100 | 0.064100 | 0.000000 | 0.000000 |
| 7 | 0.187500 | 0.059300 | 0.059300 | 0.000000 | 0.000000 |

**Table 5.4** (continued)

| | | | | | |
|---|---|---|---|---|---|
| 8 | 0.187500 | 0.049700 | 0.049700 | 0.000000 | 0.000000 |
| 9 | 0.241967 | 0.072100 | 0.072100 | 0.000000 | 0.000000 |
| 10 | 0.169867 | 0.059300 | 0.059300 | 0.000000 | 0.000000 |
| 11 | 0.153867 | 0.052900 | 0.052900 | 0.003200 | 0.003200 |
| 12 | 0.174700 | 0.065700 | 0.065700 | 0.000000 | 0.000000 |
| 13 | 0.184300 | 0.076900 | 0.076900 | 0.000000 | 0.000000 |
| 14 | 0.201933 | 0.065700 | 0.065700 | 0.000000 | 0.000000 |
| 15 | 0.200300 | 0.065700 | 0.065700 | 0.000000 | 0.000000 |
| Average | 0.183331 | 0.061753 | 0.061753 | 0.001067 | 0.001387 |

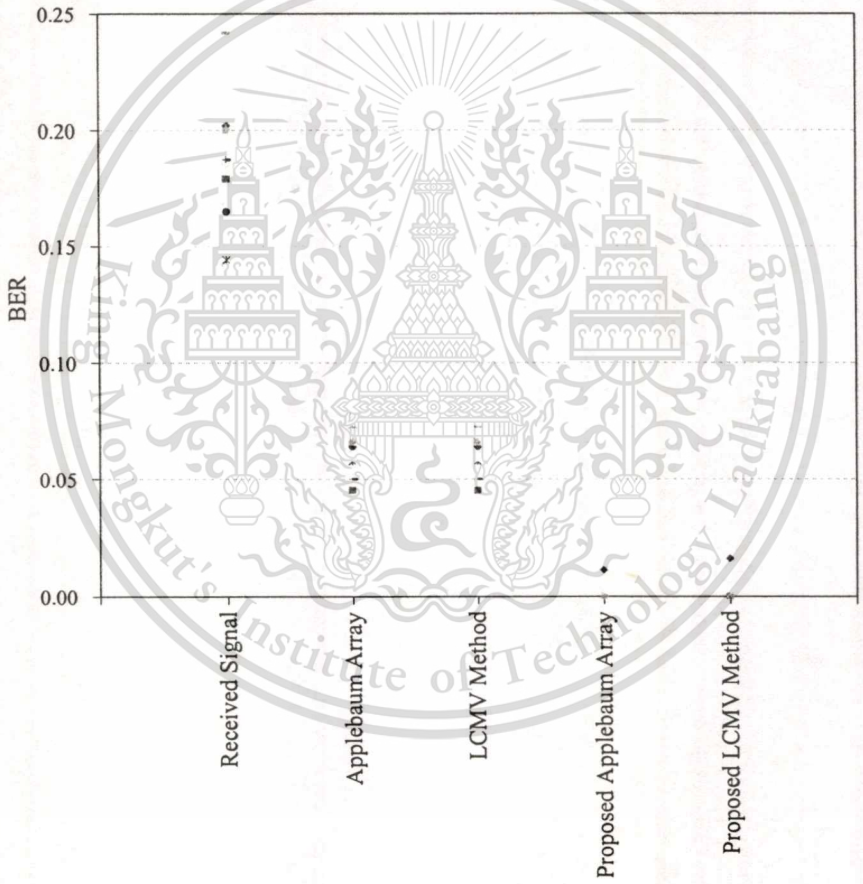


**Fig. 5.20** The BER of the experiment 5.5.3.1

For the two non-correlated modulated signal experiments in this section, the experiment is separated in three sub-sections. In this case the two transmitting signals are transmitted from the different signal generators to simulate the non-correlated signals or the non-coherent signals.

In section 5.5.3.1, the receiving array antenna is pointed to $-10^{\circ}$ while the two transmitting antennas (desired signal and interfering signal) are positioned in the direction $10^{\circ}$ and $-8.46^{\circ}$ of the receiving antenna. The configuration is provided in Fig. 5.15. The illustrations of DOA estimations in Fig. 5.16 to Fig. 5.17 demonstrate that all DOA estimation methods are capable to classify the DOA of the received signal since the number of the interference is less than their degrees of freedom. Thus, the beamforming can use the information from the DOA estimation which their comparative results between the simulation and the experiment are able to perform in Fig. 5.18 and Fig. 5.19 in three dimensions with time variance of 10 time cyclic variations and two dimensions, respectively. From these results, the proposed technique can provide the precise null beam pattern in the interfering direction ($-8.46^{\circ}$) and peak beam pattern in the desired direction ($10^{\circ}$). Also with the BER results in Table 5.4, the proposed technique provides less BER than the conventional methods that their BER results can be clearly compared in Fig. 5.20. For example, the average BER of the proposed Applebaum array is 0.001067 in contrast to the BER of conventional method that is 0.061753.

**5.5.3.2** The direction of receiver is $0^{\circ}$ :

In this case the configuration of the experiment is the same as Fig. 5.2.

- DOA estimation

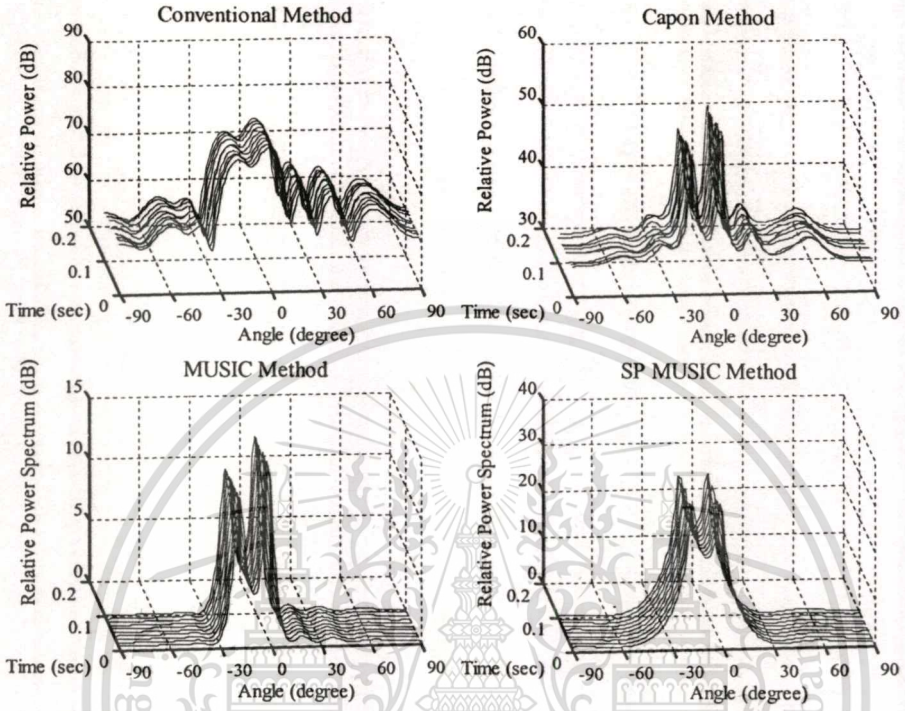


**Fig. 5.21** The experimental results of DOA estimations in three dimensions of 10 time cyclic variations

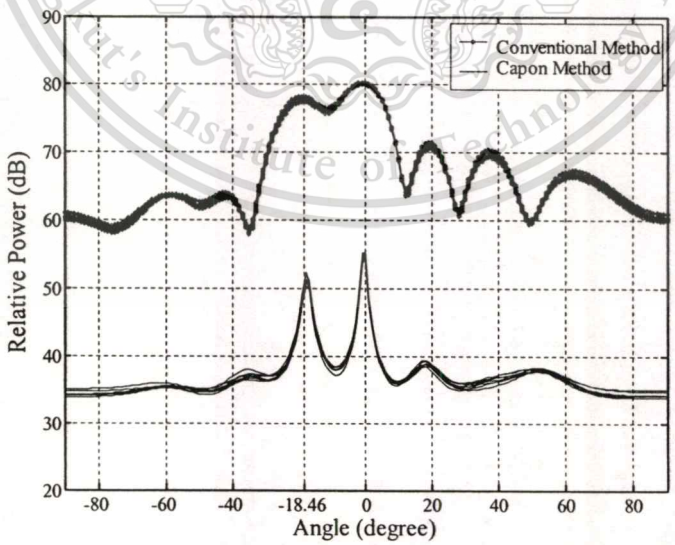


**Fig. 5.22(a)** The experimental results in two dimensions of the DOA estimations using conventional and Capon methods with 10 time cyclic variations

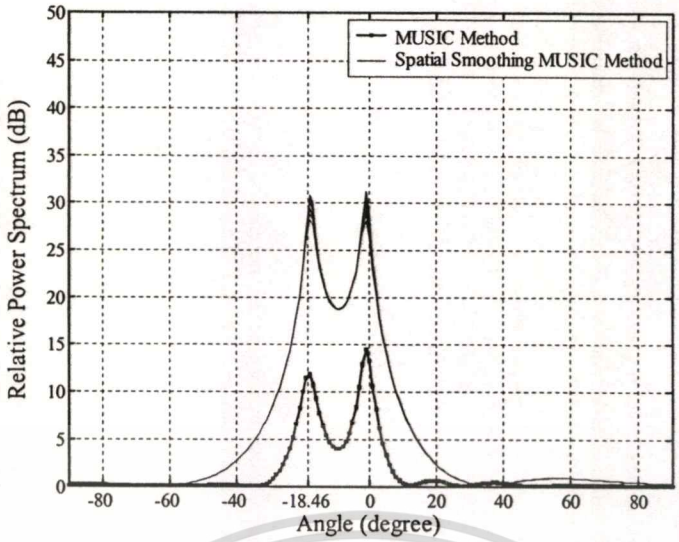


**Fig. 5.22(b)** The experimental results in two dimensions of the DOA estimations using MUSIC and spatial smoothing MUSIC methods with 10 time cyclic variations

- Beamforming

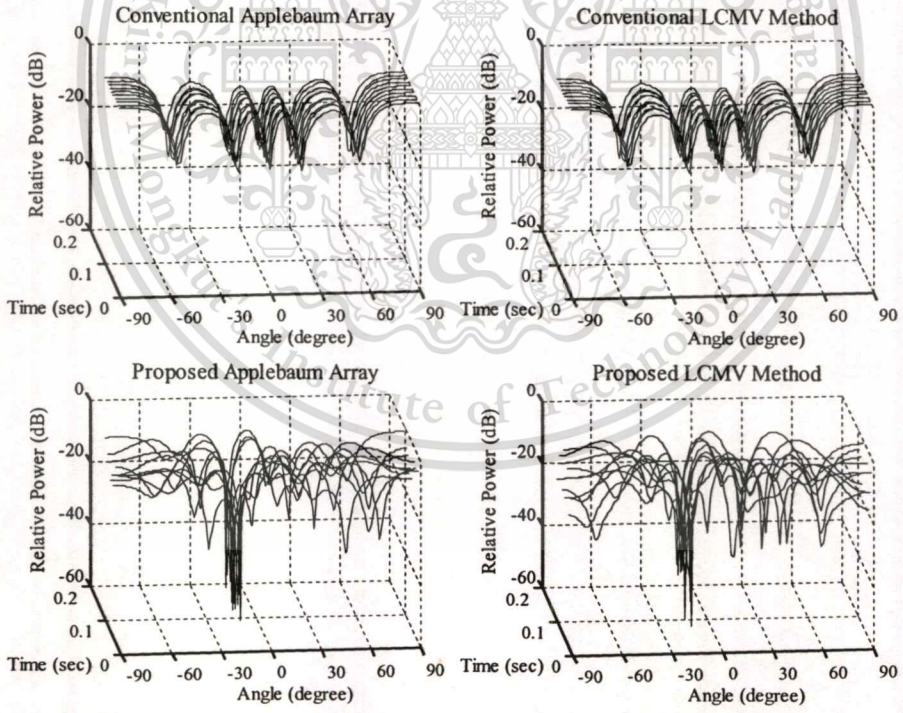


**Fig. 5.23(a)** The simulation results in three dimensions of beamforming with 10 time cyclic variations

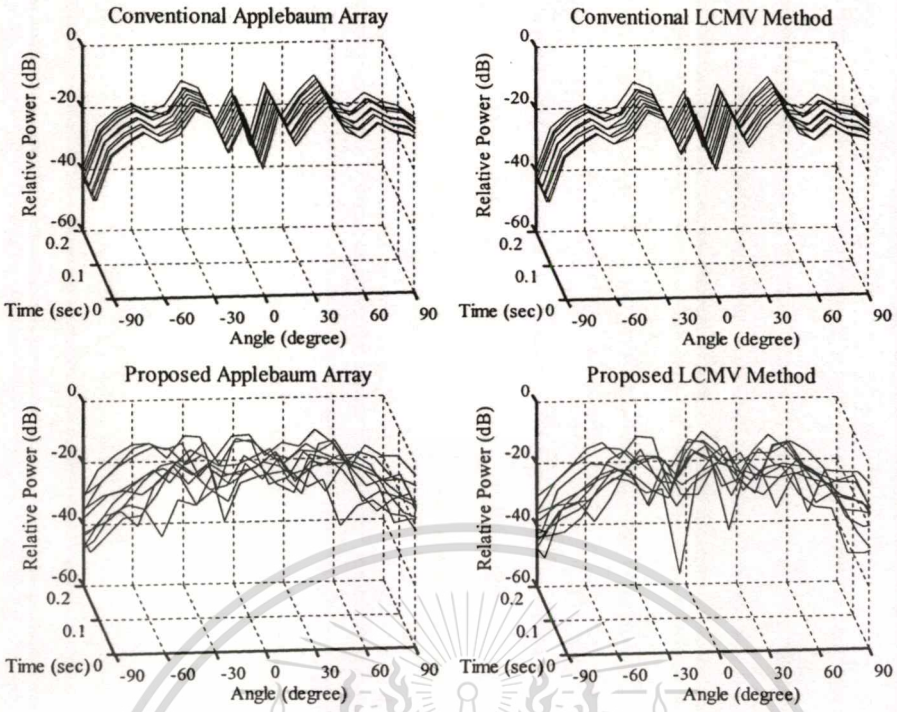


**Fig. 5.23(b)** The experimental results in three dimensions of beamforming with 10 time cyclic variations

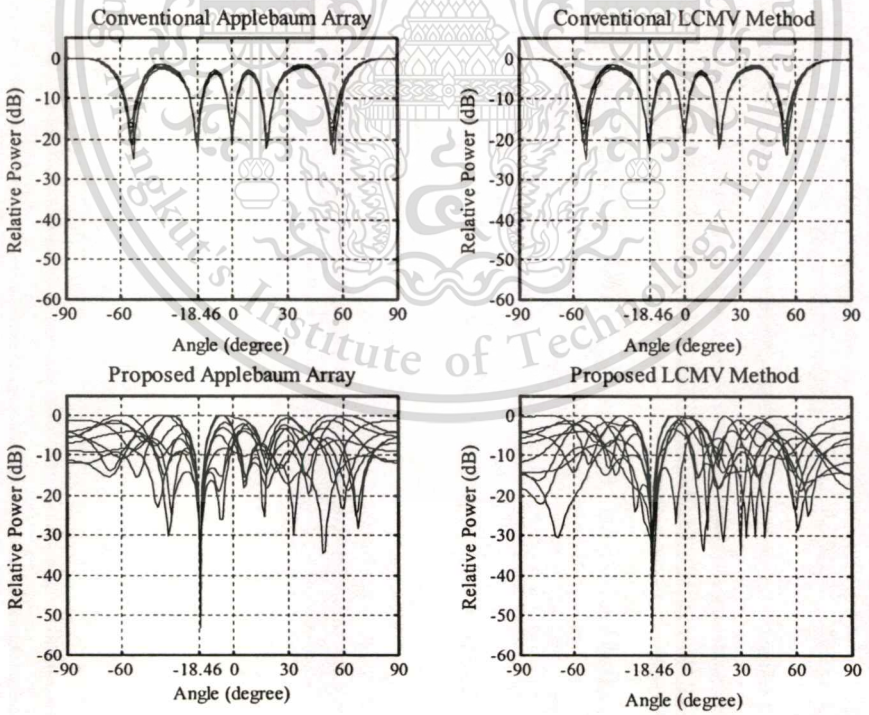


**Fig. 5.24(a)** The simulation results in two dimensions of beamforming with 10 time cyclic variations

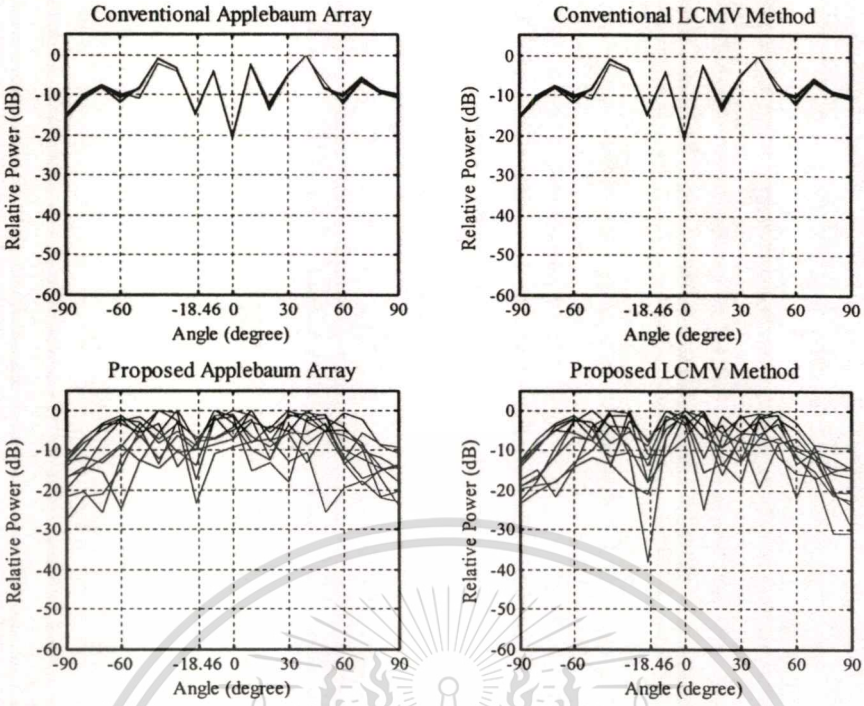


**Fig. 5.24(b)** The experimental results in two dimensions of beamforming with 10 time cyclic variations

- BER

The BER of this experiment is obtained by using 15 time cycles of 1024 samples which can be demonstrated as Table 5.5 and Fig. 5.25.

**Table 5.5** The BER of the experiment 5.5.3.2

| \BER Time of \ Sampling | Received Signal | Applebaum Array | LCMV Method | Proposed Applebaum Array | Proposed LCMV Method |
|---|---|---|---|---|---|
| 1 | 0.012800 | 0.108967 | 0.108967 | 0.003200 | 0.003200 |
| 2 | 0.008000 | 0.113767 | 0.113767 | 0.000000 | 0.000000 |
| 3 | 0.004800 | 0.089767 | 0.089767 | 0.000000 | 0.000000 |
| 4 | 0.008000 | 0.097733 | 0.097733 | 0.000000 | 0.000000 |
| 5 | 0.011200 | 0.115367 | 0.115367 | 0.001600 | 0.001600 |
| 6 | 0.003200 | 0.105800 | 0.105800 | 0.000000 | 0.000000 |
| 7 | 0.011200 | 0.116967 | 0.116967 | 0.000000 | 0.000000 |

**Table 5.5** (continued)

| | | | | | |
|---|---|---|---|---|---|
| 8 | 0.004800 | 0.137800 | 0.137800 | 0.000000 | 0.000000 |
| 9 | 0.011200 | 0.107367 | 0.107367 | 0.000000 | 0.000000 |
| 10 | 0.006400 | 0.104167 | 0.104167 | 0.000000 | 0.000000 |
| 11 | 0.006400 | 0.099400 | 0.099400 | 0.000000 | 0.000000 |
| 12 | 0.016000 | 0.113800 | 0.113800 | 0.003200 | 0.004800 |
| 13 | 0.006400 | 0.086533 | 0.086533 | 0.000000 | 0.000000 |
| 14 | 0.014400 | 0.100967 | 0.100967 | 0.000000 | 0.001600 |
| 15 | 0.000000 | 0.097767 | 0.097767 | 0.000000 | 0.000000 |
| Average | 0.008320 | 0.106411 | 0.106411 | 0.000533 | 0.000747 |

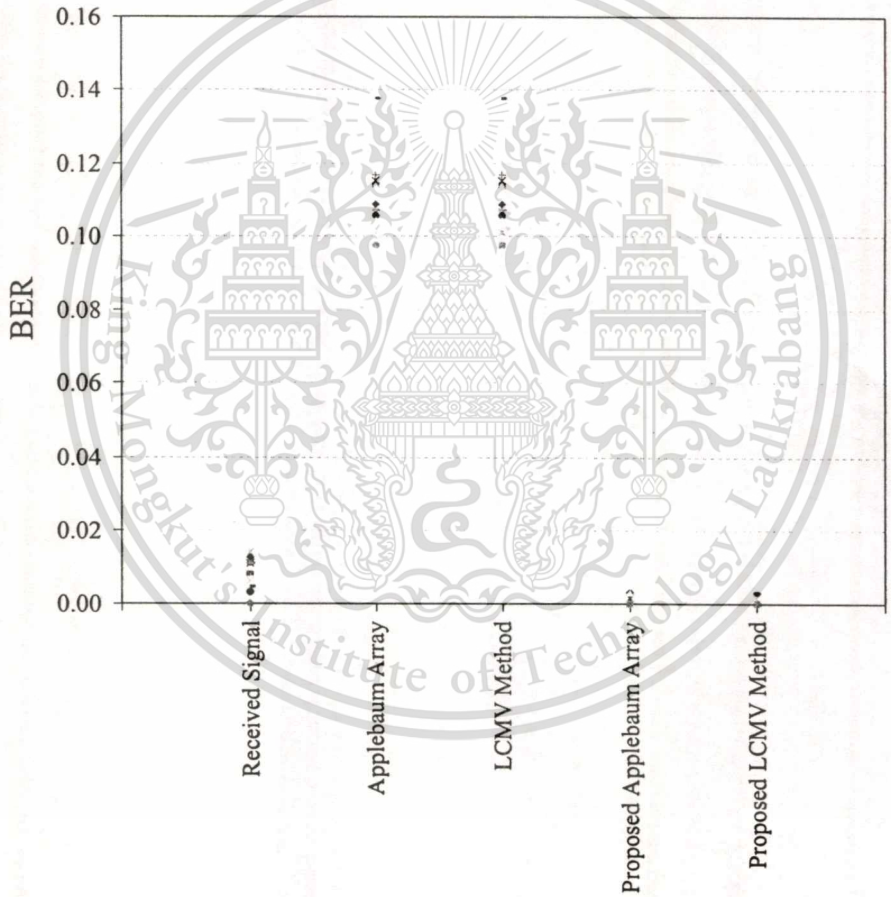


**Fig. 5.25** The BER of the experiment 5.5.3.2

The DOA estimation and beamforming operation can be achieved in Fig. 5.21 to Fig. 5.22 and Fig. 5.23 to Fig. 5.24, respectively. These results clarify the effective of the proposed technique in beamforming. In the mean time, the BER in Table 5.5 and Fig. 5.25 give the conclusive agreement with the advantage of the proposed technique. It can be expected that the conventional beamforming methods can not improve the performance of the receiver of this case both beam pattern and BER, on the contrary the proposed technique can enforce the good beam pattern and BER performance that the average BER of the proposed technique in this case is less than the conventional methods and the received signal without adaptive process.

**5.5.3.3** The direction of receiver is $0^{\circ}$ and the interference power is decreased from -11 dBm to -14 dBm:

The configuration of this experiment is the same as 5.5.3.2.

- DOA estimation

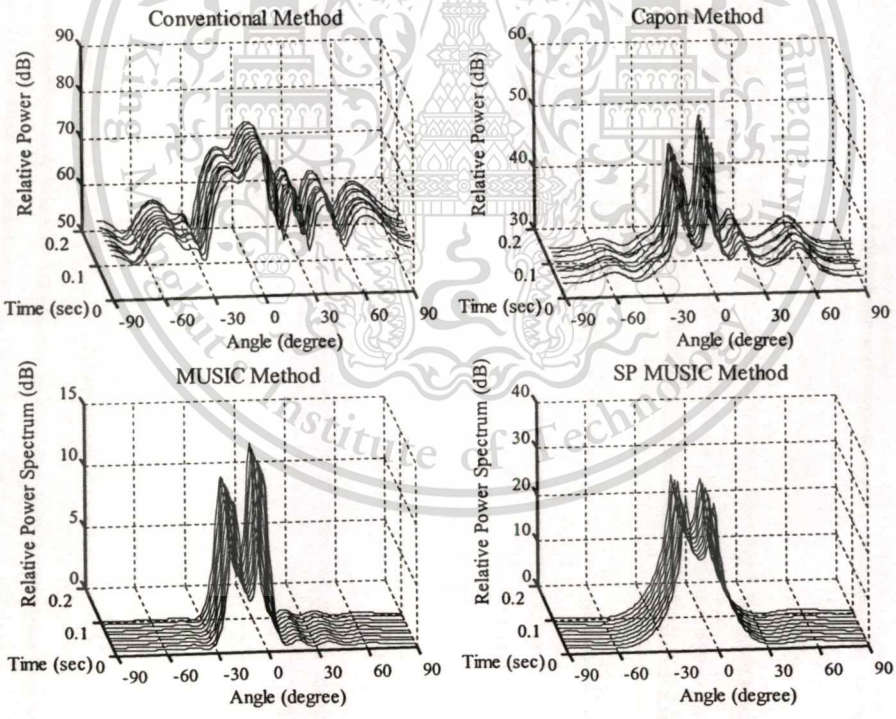


**Fig. 5.26** The experimental results of DOA estimations in three dimensions of 10 time cyclic variations

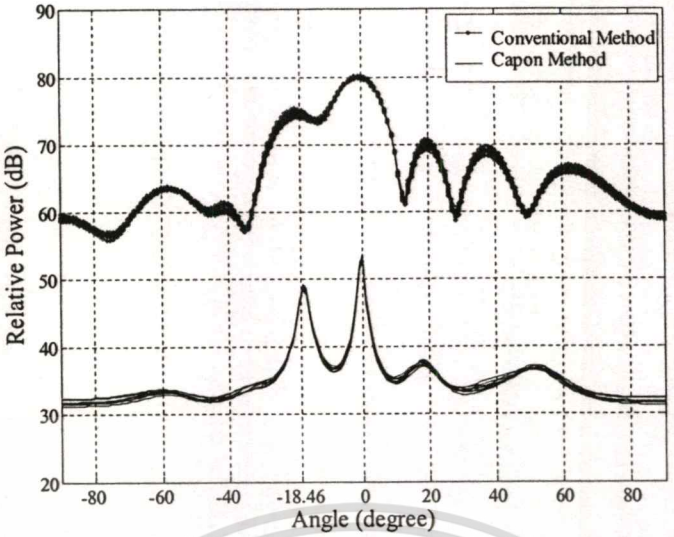


**Fig. 5.27(a)** The experimental results in two dimensions of the DOA estimations using conventional and Capon methods with 10 time cyclic variations

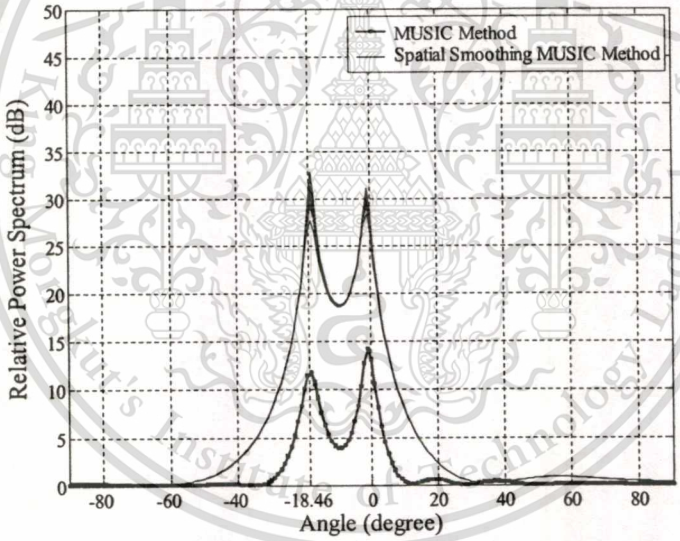


**Fig. 5.27(b)** The experimental results in two dimensions of the DOA estimations using MUSIC and spatial smoothing MUSIC methods with 10 time cyclic variations

- Beamforming

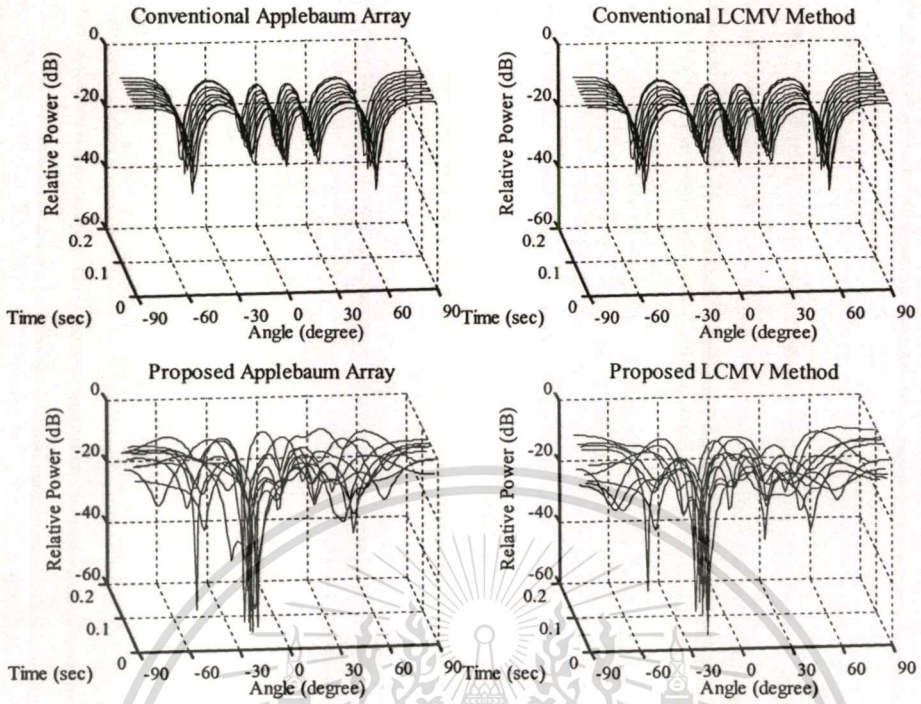


**Fig. 5.28(a)** The simulation results in three dimensions of beamforming with 10 time cyclic variations

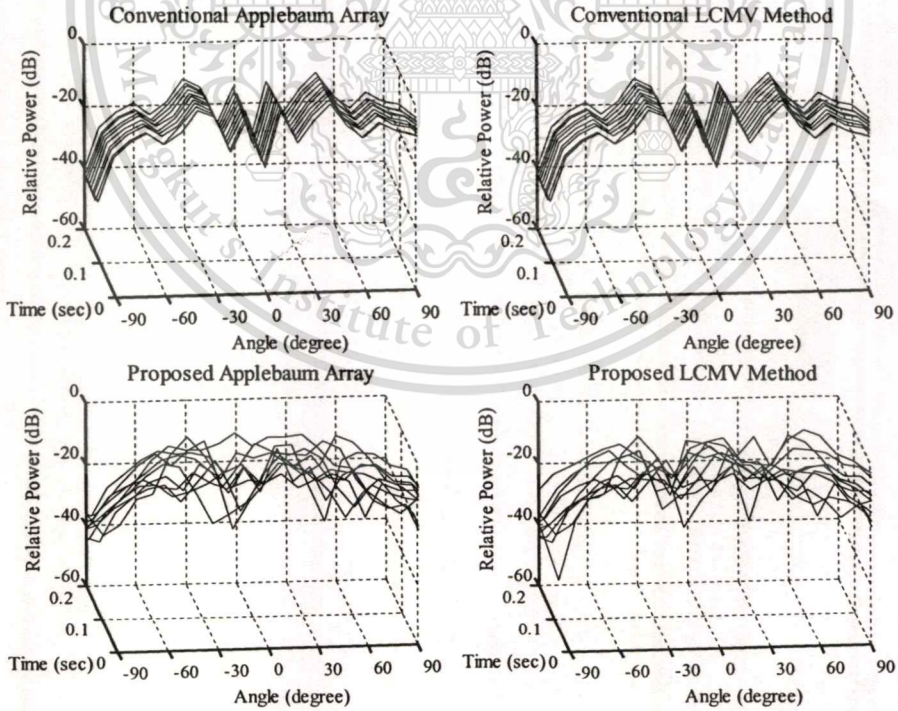


**Fig. 5.28(b)** The experimental results in three dimensions of beamforming with 10 time cyclic variations

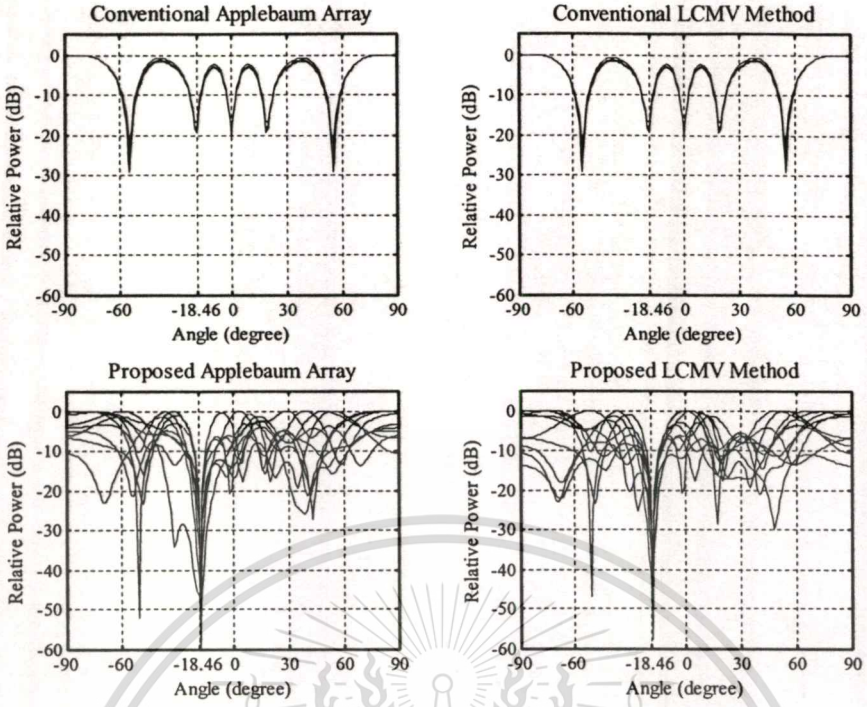


**Fig. 5.29(a)** The simulation results in two dimensions of beamforming with 10 time cyclic variations

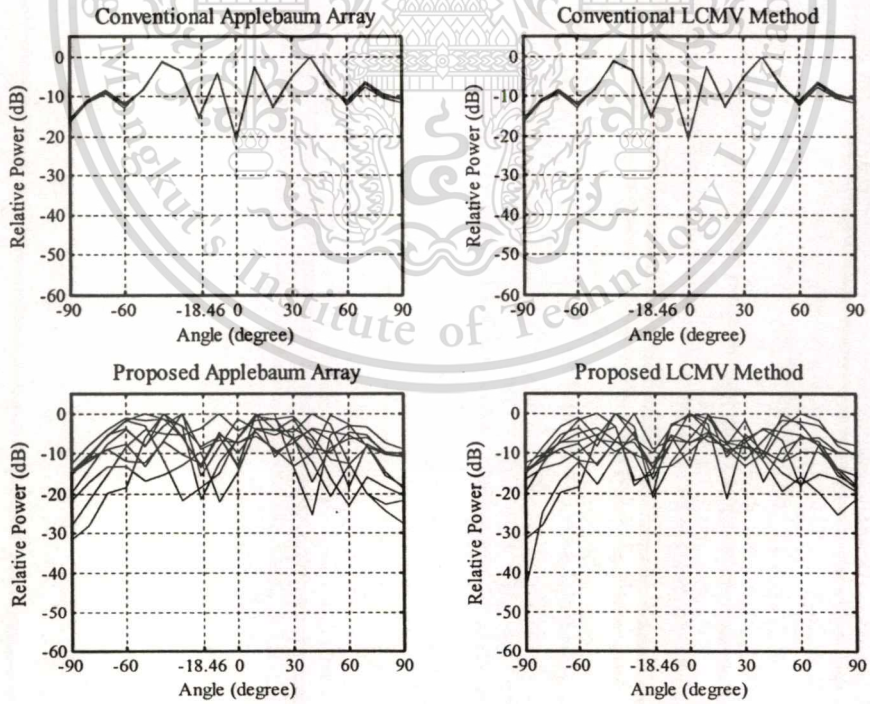


**Fig. 5.29(b)** The experimental results in two dimensions of beamforming with 10 time cyclic variations

- BER

The BER of this experiment is obtained by using 15 time cycles of 1024 samples which can be demonstrated as Table 5.6 and Fig. 5.30.

**Table 5.6** The BER of the experiment 5.5.3.3

| \BER Time of \ Sampling | Received Signal | Applebaum Array | LCMV Method | Proposed Applebaum Array | Proposed LCMV Method |
|---|---|---|---|---|---|
| 1 | 0.012800 | 0.108967 | 0.108967 | 0.003200 | 0.003200 |
| 2 | 0.008000 | 0.113767 | 0.113767 | 0.000000 | 0.000000 |
| 3 | 0.004800 | 0.089767 | 0.089767 | 0.000000 | 0.000000 |
| 4 | 0.008000 | 0.097733 | 0.097733 | 0.000000 | 0.000000 |
| 5 | 0.011200 | 0.115367 | 0.115367 | 0.001600 | 0.001600 |
| 6 | 0.003200 | 0.105800 | 0.105800 | 0.000000 | 0.000000 |
| 7 | 0.011200 | 0.116967 | 0.116967 | 0.000000 | 0.000000 |
| 8 | 0.004800 | 0.137800 | 0.137800 | 0.000000 | 0.000000 |
| 9 | 0.011200 | 0.107367 | 0.107367 | 0.000000 | 0.000000 |
| 10 | 0.006400 | 0.104167 | 0.104167 | 0.000000 | 0.000000 |
| 11 | 0.006400 | 0.099400 | 0.099400 | 0.000000 | 0.000000 |
| 12 | 0.016000 | 0.113800 | 0.113800 | 0.003200 | 0.004800 |
| 13 | 0.006400 | 0.086533 | 0.086533 | 0.000000 | 0.000000 |
| 14 | 0.014400 | 0.100967 | 0.100967 | 0.000000 | 0.001600 |
| 15 | 0.000000 | 0.097767 | 0.097767 | 0.000000 | 0.000000 |
| Average | 0.008320 | 0.106411 | 0.106411 | 0.000533 | 0.000747 |

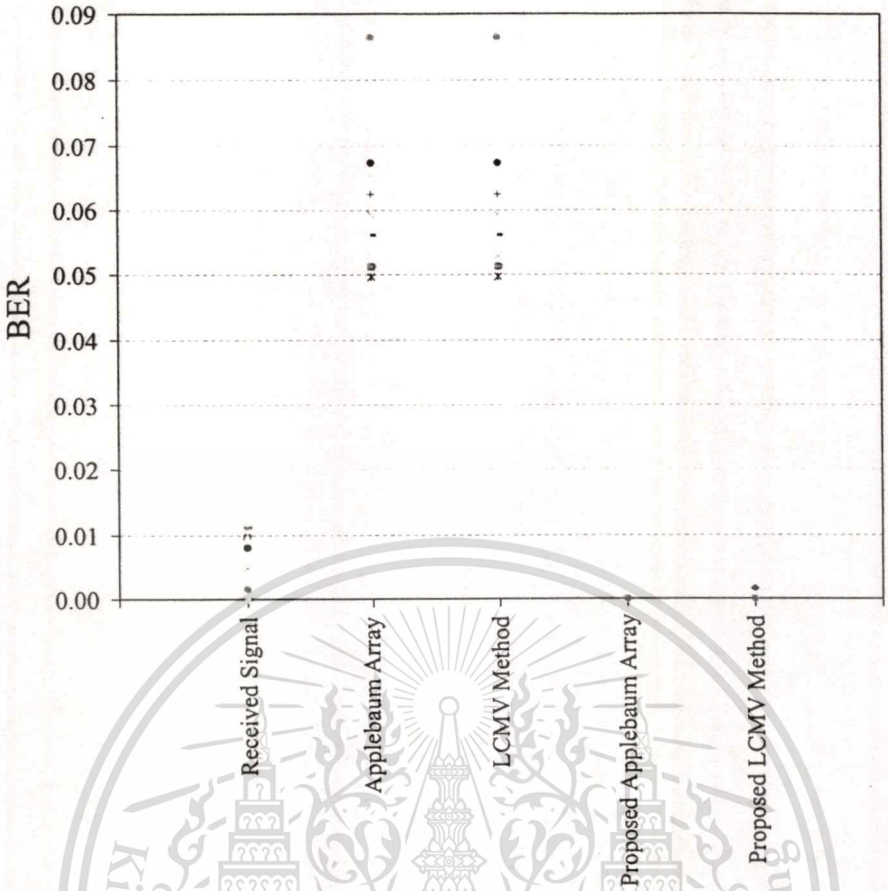


**Fig. 5.30** The BER of the experiment 5.5.3.3

When the power of the interfering signal decreases, the performance of DOA estimation and beamforming in the adaptive array can be performed in this section. In this case the positions of the two transmitters are the same as section 5.5.3.2, which the DOA estimations are provided in Fig. 5.26 to Fig. 5.27. From these results, the DOA of the received signals can be classified. In addition, it was found that, the power level in the interfering direction of the conventional method and Capon method are 3dB less than of the previous section 5.5.3.2, due to the power of the interfering signal is decreased from -11 dBm to -14 dBm. Consider the beamforming results in Fig. 5.28 and Fig. 5.29, the antenna beam patterns of the proposed technique give the more efficient capability of interference rejection than the conventional methods. Conclusively, the BER in Table 5.6 and Fig. 5.30 clarify the enhancement of proposed technique in adaptive array antenna that the BER of the proposed technique is lower than the conventional method and the received signal without adaptive process.

### 5.5.4 Two correlated modulated signals experiment

In this experiment, both two signals are generated from the same signal generator to be the correlated signals. The output of the signal generator is connected with the power divider to separate the signal to two outputs. The signals from these two outputs are attenuated by two attenuators. The attenuation at the attenuator of the desired signal is fixed at 43 dB, while the attenuation of interfering attenuator is varied in various values of 35 dB, 38 dB, 41 dB, 44 dB and 47 dB. The configuration of this experiment is similar to section 5.5.3.

**5.5.4.1** The direction of receiver is $-10^{\circ}$:

The configuration of this experiment is similar to section 5.5.3.1.

- DOA estimation

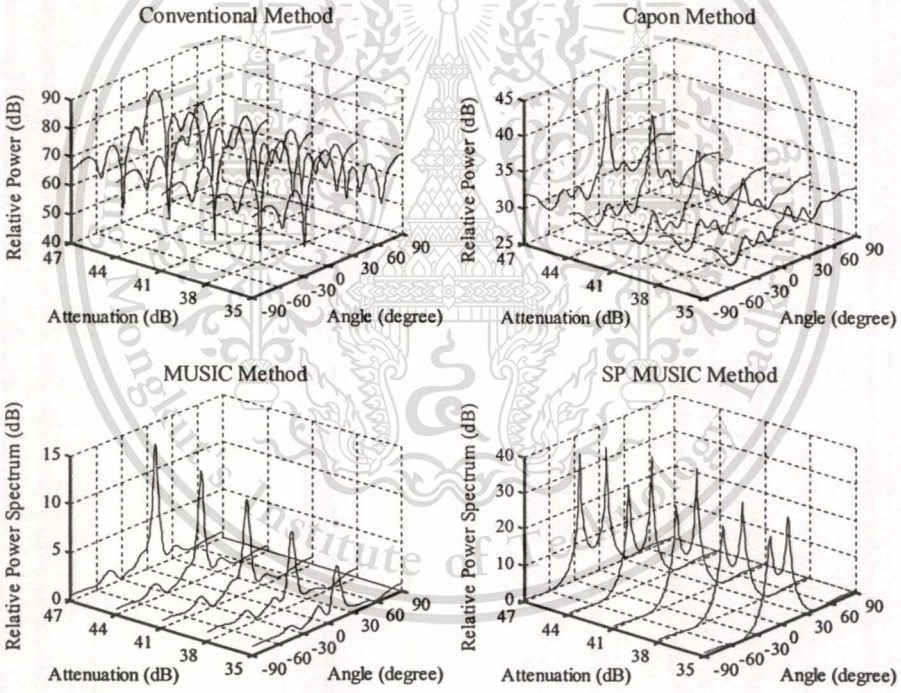


**Fig. 5.31** The comparative experimental results of DOA estimations at various attenuation values of the interfering attenuator

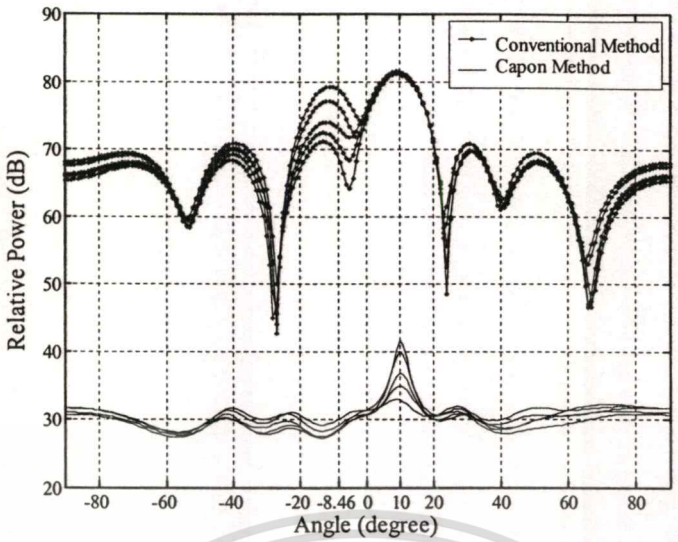


**Fig. 5.32(a)** The experimental results in two dimensions of the DOA estimations using conventional and Capon methods at various attenuation values of the interfering attenuator

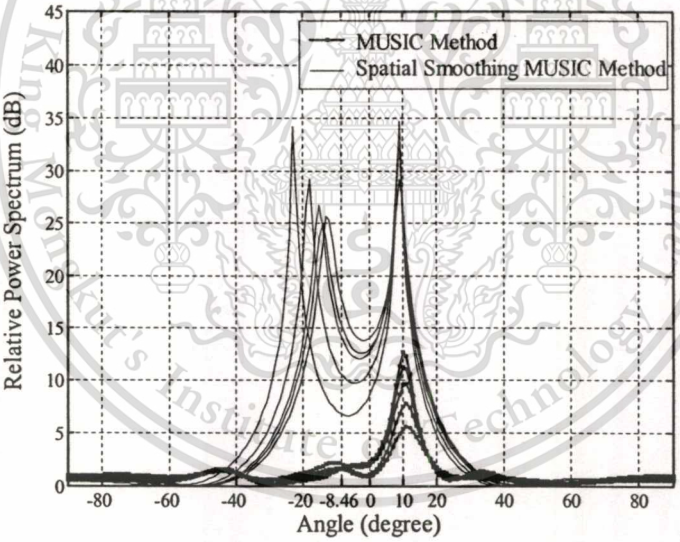


**Fig. 5.32(b)** The experimental results in two dimensions of the DOA estimations using MUSIC and spatial smoothing MUSIC methods at various attenuation values of the interfering attenuator

- Beamforming

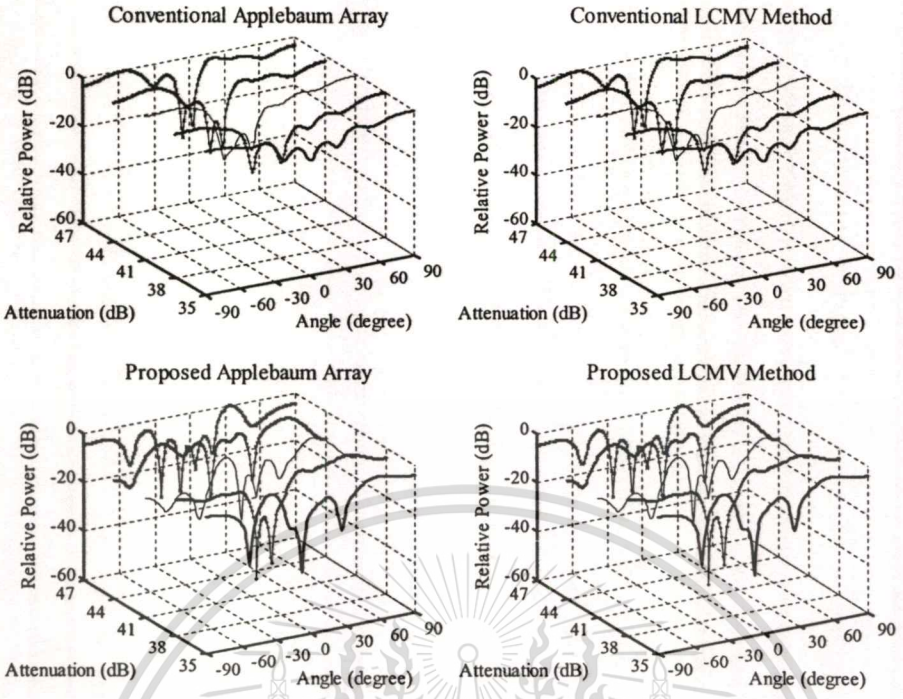


**Fig. 5.33(a)** The simulation results in three dimensions of beamforming at various attenuation values of the interfering attenuator

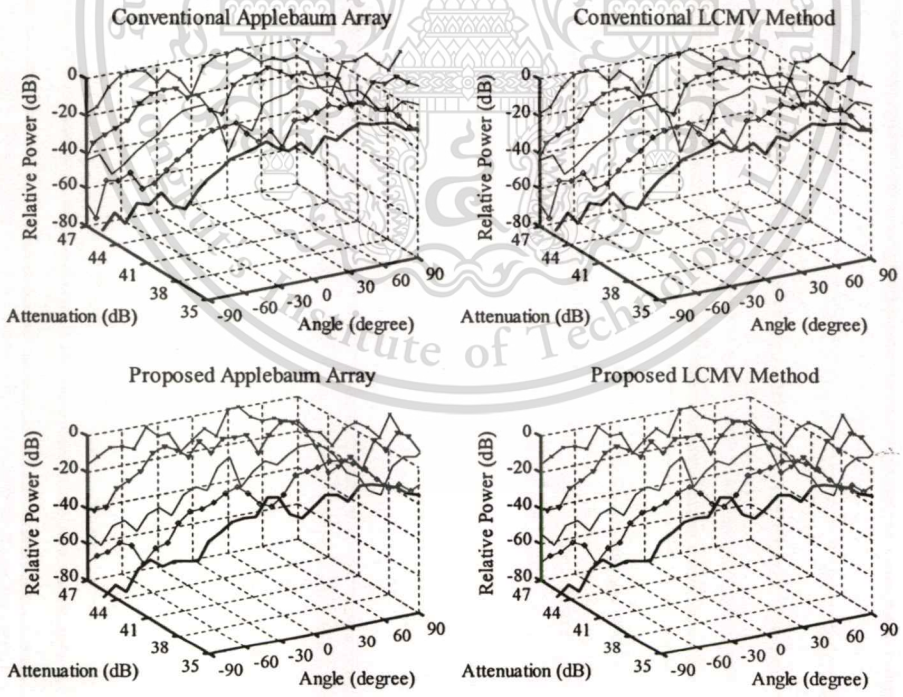


**Fig. 5.33(b)** The experimental results in three dimensions of beamforming at various attenuation values of the interfering attenuator

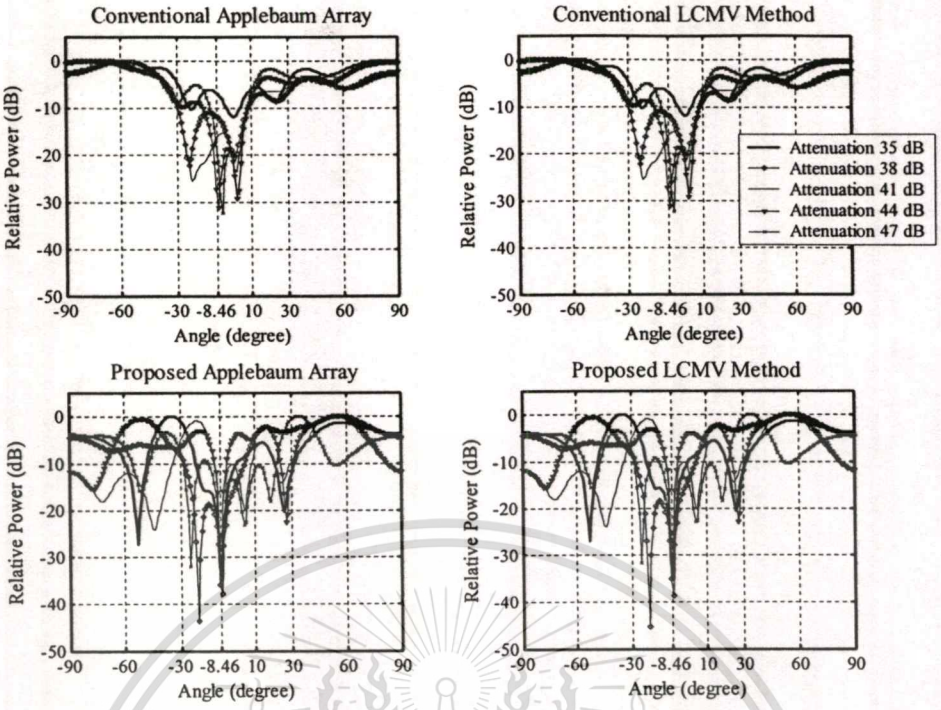


**Fig. 5.34(a)** The simulation results in two dimensions of beamforming at various attenuation values of the interfering attenuator

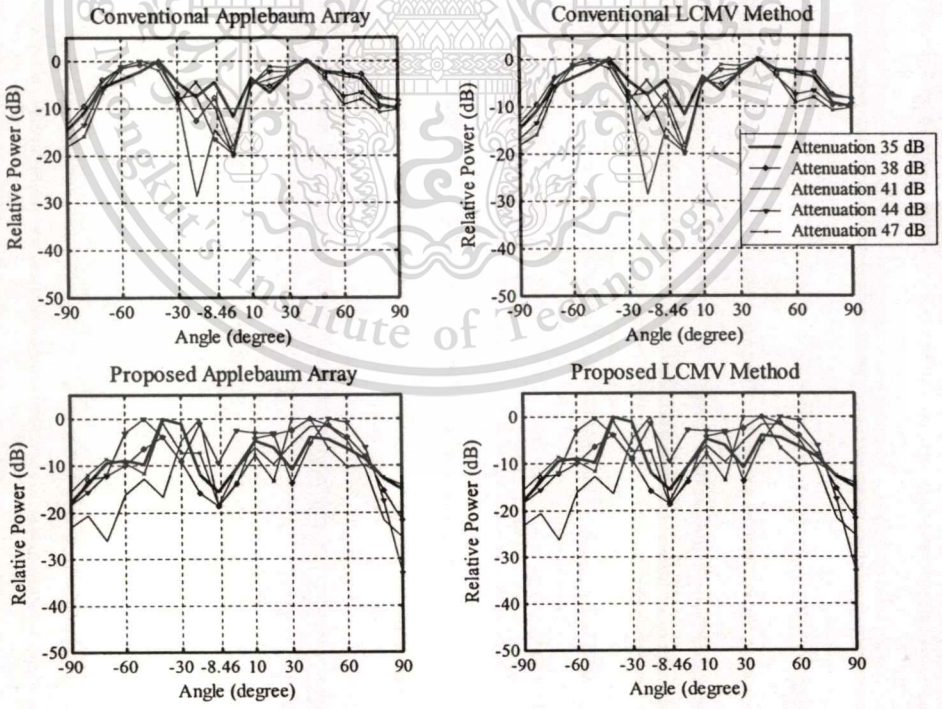


**Fig. 5.34(b)** The experimental results in two dimensions of beamforming at various attenuation values of the interfering attenuator

- BER

The average BER of this experiment is obtained by using 20 time cycles of 1024 samples which can be demonstrated as Table 5.7 and Fig. 5.35.

**Table 5.7** The BER of the experiment 5.5.4.1

| \Average \BER Attenuation\ | Received Signal | Applebaum Array | LCMV Method | Proposed Applebaum Array | Proposed LCMV Method |
|---|---|---|---|---|---|
| 35 | 0.001923 | 0.001923 | 0.001923 | 0.000120 | 0.000120 |
| 38 | 0.001322 | 0.001683 | 0.001683 | 0.000240 | 0.000240 |
| 41 | 0.000721 | 0.000120 | 0.000120 | 0.000000 | 0.000000 |
| 44 | 0.000481 | 0.000481 | 0.000481 | 0.000120 | 0.000120 |
| 47 | 0.000361 | 0.000120 | 0.000120 | 0.000000 | 0.000000 |

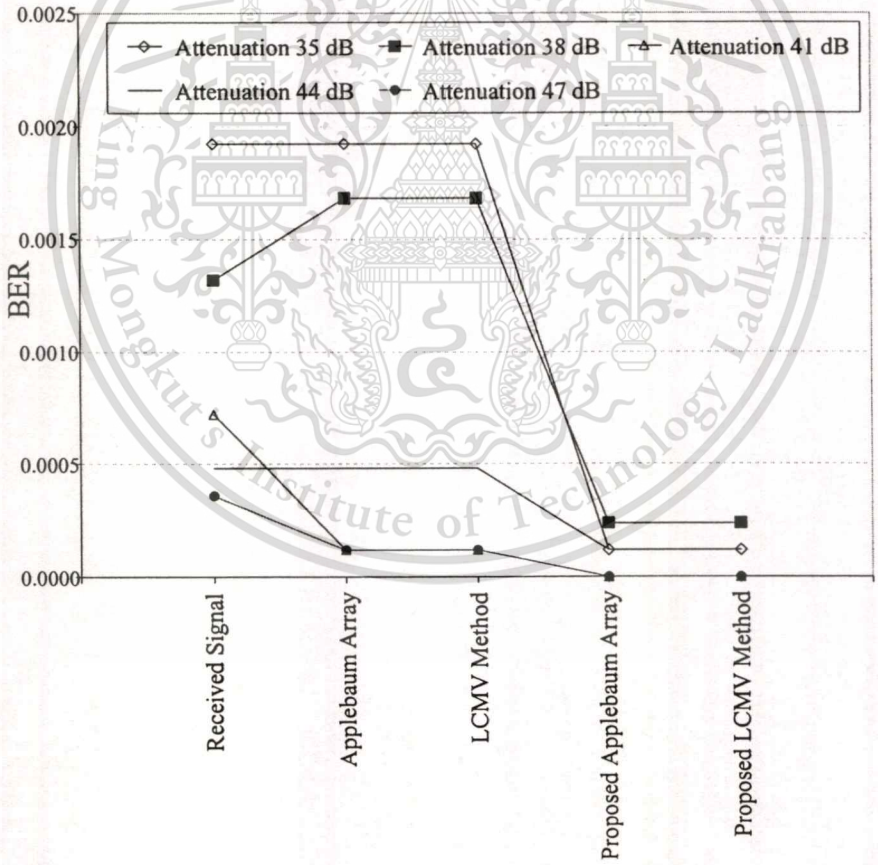


**Fig. 5.35** The average BER of the experiment 5.5.4.1 at various attenuation values

The direction of the received array antenna is $-10^{\circ}$ which the configuration of this experiment is similar to section 5.5.3.1. The DOA estimation of this experiment can not provide the precise direction, which their results are illustrated in Fig. 5.31 to Fig. 5.32. In Fig. 5.31, when the attenuation of the interfering signal is increased or the interfering signal power is decreased, the output power of the DOA estimation is increased. However, the accuracy of the estimation is not increased as the decreasing of the interfering signal power that can be shown in Fig. 5.32. As the power of the interfering signal is decreased, the correlation between the signals is decreased thus the DOA estimation can not achieve the precise direction of the interference. In this case, the spatial smoothing technique is used to improve the performance in DOA estimation but it still can not provide the exact direction of the interfering signal. However, the estimated DOA by spatial smoothing is closed to the actual angle of the impinging signal which their information will be used in the weight computation of the beamforming in adaptive array. In addition, the beam pattern of this experiment can be illustrated in Fig. 5.33 and Fig. 5.34, in three dimensions with attenuation variation and two dimensions, respectively. From Fig. 5.34, it is evident that the proposed technique can set the null beam pattern in the interfering direction that is $-8.46^{\circ}$ more exactly than the conventional methods. Furthermore, the average BER performance is described in Table 5.7 and shown in Fig. 5.35 which clarifies the efficiency of the proposed technique in adaptive array. From Table 5.7, as the attenuation of the interfering signal is increased from 35 dB to 47 dB or the output power is decreased, the BER of the received signal without adaptive process is decreased. The average BER results of the proposed technique is lower than 0.0005 in all case of attenuation value, while the average BER of the conventional method is lower than 0.0005 since the attenuation of the attenuator is higher than 38 dB. Thus, the proposed technique provide more efficient than the conventional technique although the high power of interference impinging at the array.

**5.5.4.2** The direction of receiver is $0^{\circ}$ :

The configuration of this experiment is similar to section 5.5.3.2.

- DOA estimation

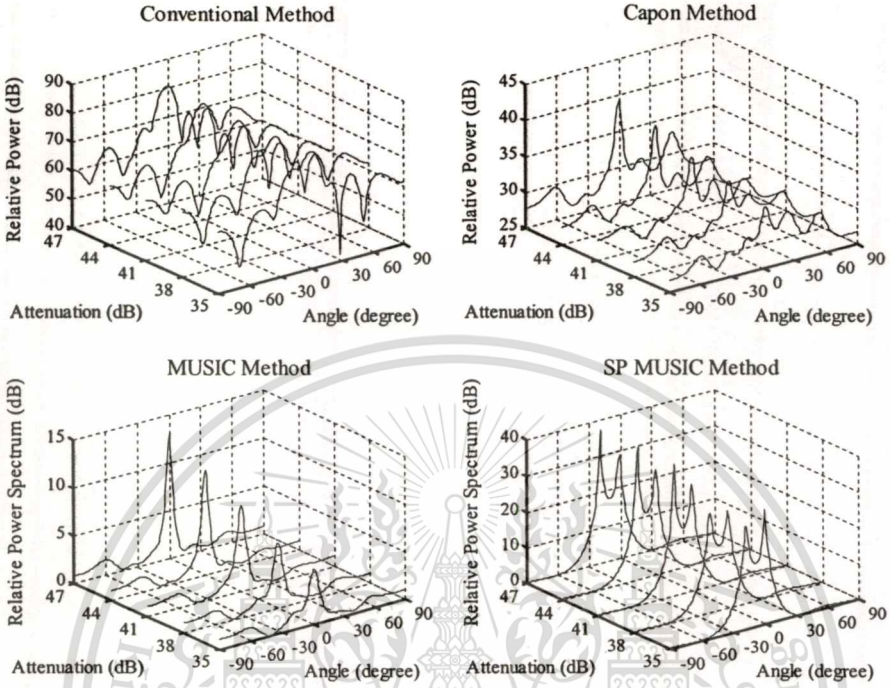


**Fig. 5.36** The comparative experimental results of DOA estimations at various attenuation values of the interfering attenuator

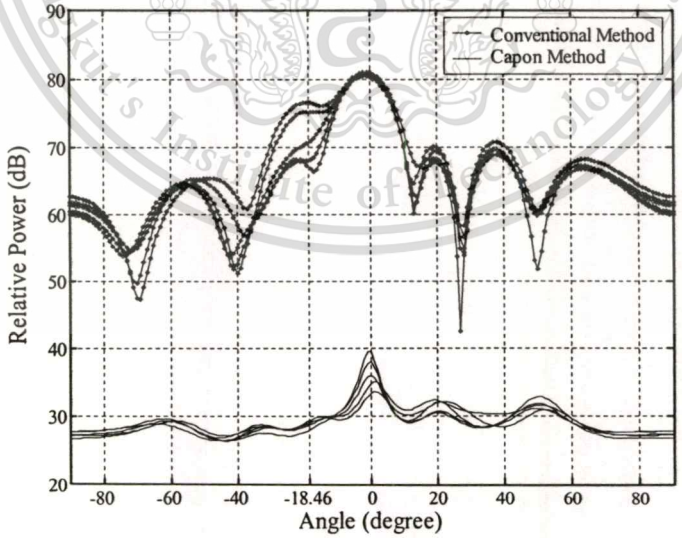


**Fig. 5.37(a)** The experimental results in two dimensions of the DOA estimations using conventional and Capon methods at various attenuation values of the interfering attenuator

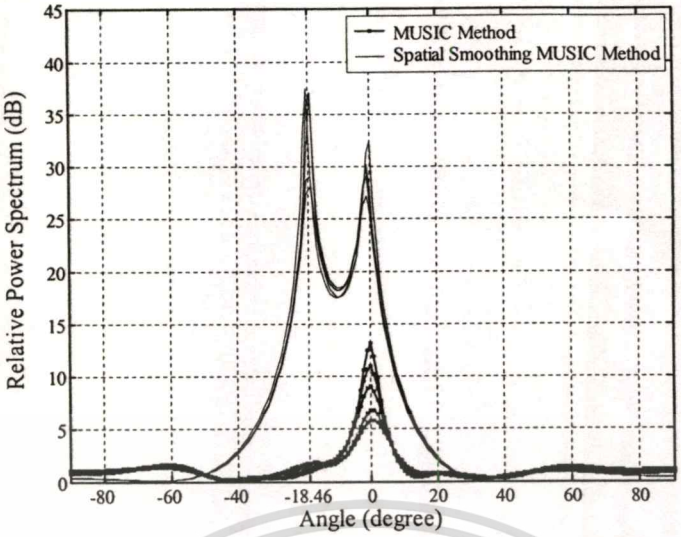


**Fig. 5.37(b)** The experimental results in two dimensions of the DOA estimations using MUSIC and spatial smoothing MUSIC methods at various attenuation values of the interfering attenuator

- Beamforming

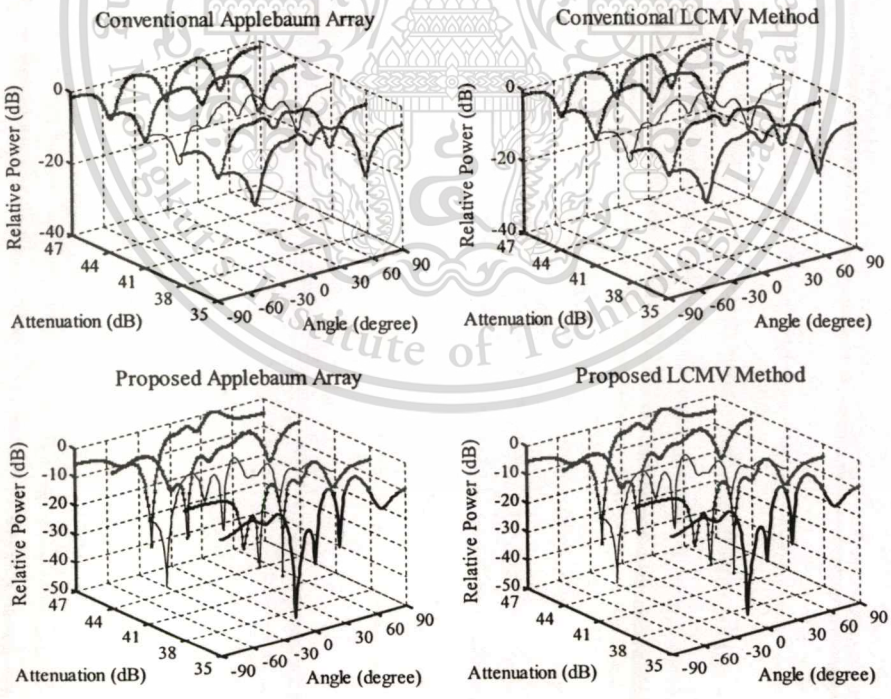


**Fig. 5.38(a)** The simulation results in three dimensions of beamforming at various attenuation values of the interfering attenuator

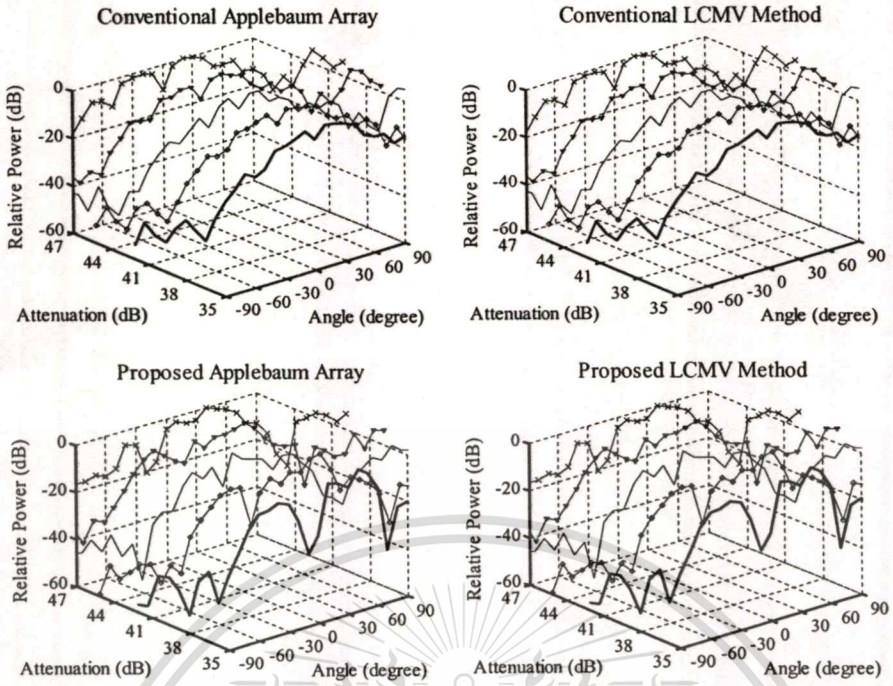


**Fig. 5.38(b)** The experimental results in three dimensions of beamforming at various attenuation values of the interfering attenuator

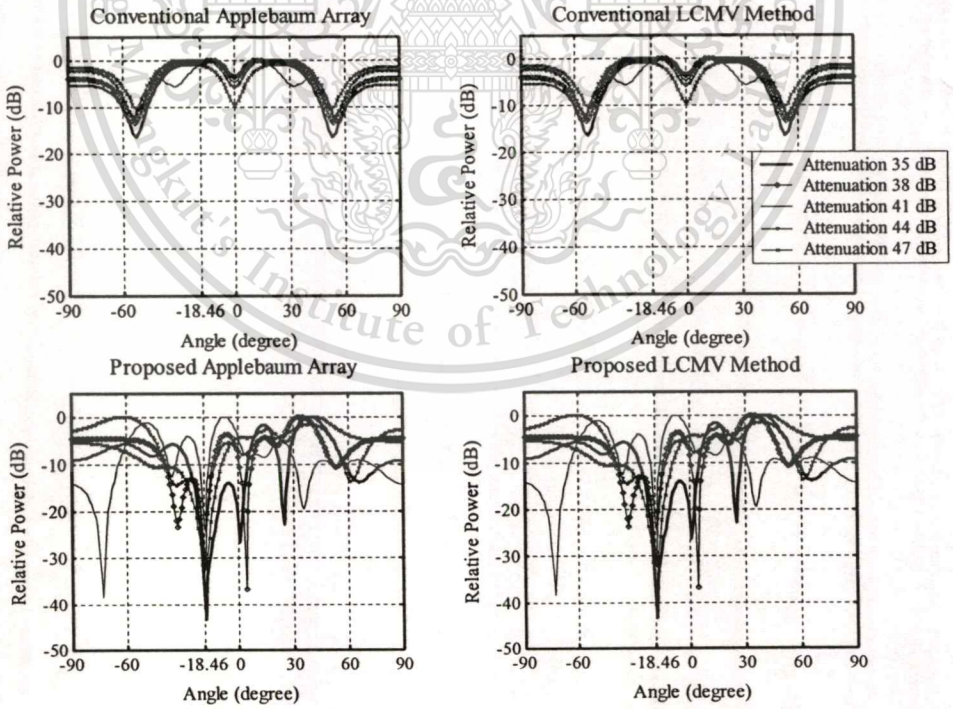


**Fig. 5.39(a)** The simulation results in two dimensions of beamforming at various attenuation values of the interfering attenuator

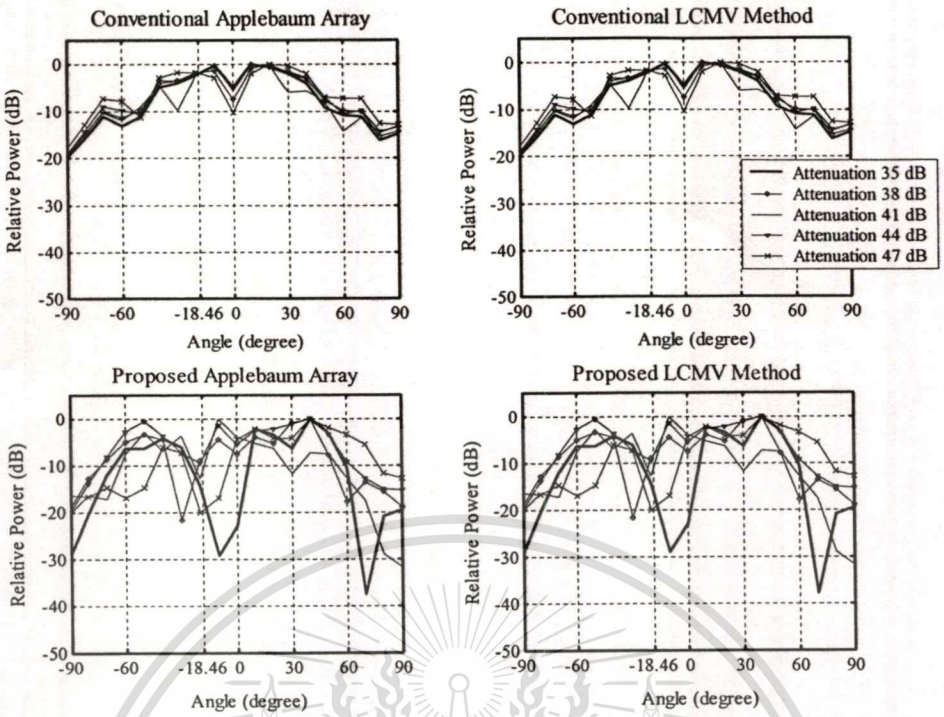


**Fig. 5.39(b)** The experimental results in two dimensions of beamforming at various attenuation values of the interfering attenuator

- BER

The average BER of this experiment is obtained by using 20 time cycles of 1024 samples which can be demonstrated as Table 5.8 and Fig. 5.40.

**Table 5.8** The BER of the experiment 5.5.4.2

| \Average \BER Attenuation\ | Received Signal | Applebaum Array | LCMV Method | Proposed Applebaum Array | Proposed LCMV Method |
|---|---|---|---|---|---|
| 35 | 0.001923 | 0.001082 | 0.001082 | 0.000361 | 0.000361 |
| 38 | 0.000601 | 0.000361 | 0.000361 | 0.000000 | 0.000000 |
| 41 | 0.001322 | 0.000962 | 0.000962 | 0.000481 | 0.000481 |
| 44 | 0.000601 | 0.000000 | 0.000000 | 0.000000 | 0.000000 |
| 47 | 0.001202 | 0.000841 | 0.000841 | 0.000120 | 0.000120 |

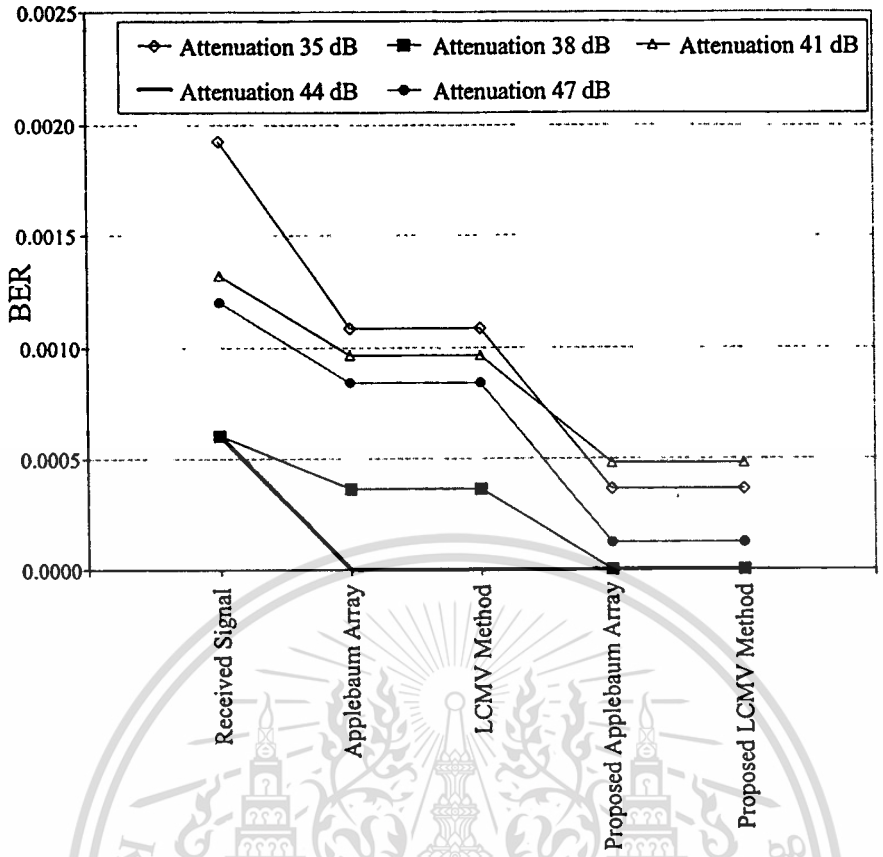


**Fig. 5.40** The average BER of the experiment 5.5.4.2 at various attenuation values

When the direction of the received signal is rotated to $0^{\circ}$, the DOA estimation results in Fig. 5.36 and Fig. 5.37 are similar to the first part that the DOA estimation of the correlated signal is difficult to find the exact angle of arrival. However, spatial smoothing technique can perform the correct DOA in this case ($0^{\circ}$ and $-18.46^{\circ}$) which its DOA spectrum response is high in the angle of arrival. Consider the beamforming in Fig. 5.38 and Fig. 5.39, when the attenuation increases, the null deep of the adaptive array is higher because the interfering signal power decreases. Thus, when the power of the interfering received signal is decreased the beam pattern in that direction is higher. From Table 5.8 and Fig. 5.40, the BER values of the proposed technique are still lower than the conventional method and the received signal without calibration.

## 5.5 Concluding Remarks

This chapter begins with the configuration of the experiment by describing the equipment used. Next part is the calibration process that explains the important and the process of the calibration. In addition, the BER is described and defined. This BER value can be used to clarify the efficiency of the digital system that is used in this experiment. The experiment consists of four main parts. Firstly, the radiation pattern of the array antenna that illustrated the radiation pattern of the receiving antenna. Secondly, the single modulated signal experiment, this section describes the DOA estimation, the conventional beamforming and the BER performance of the single signal. The third part, two non-correlated modulated signals experiment, there are various situations of the experiment in this part which depends on the direction of the receiving array antenna, $-10^{\circ}$ and $0^{\circ}$ with decreasing interfering power. Finally, the two correlated modulated signals experiment. The DOA estimation by using conventional method, Capon Method, MUSIC method and spatial smoothing technique are performed in all cases of the experiment. Moreover, Applebaum array, LCMV method and the proposed technique are obtained in order to clarify the capability enhancement in wireless communication of the proposed technique. The BER is calculated and the efficiency of many kinds of adaptive array beamforming method are shown.

The experimental results can clarify the capability enhancement of the proposed technique in wireless communication that the proposed technique can improve efficiency of the wireless communication system.

# CHAPTER 6
# CONCLUSIONS AND DISCUSSIONS

In this chapter, all the main knowledge achieved in the preceding chapters are summarized. At last, the discussions of future studies are described.

## 6.1 Summary of the Thesis

According to the aforementioned of the purpose and objective of this thesis in chapter 1, the proposed covariance matrix adjustment technique is presented and discussed. In order to achieve this technique, the theory of adaptive array antenna is performed in chapter 2 that consists of the operation and mechanism of the adaptive array antenna, array signal model, adaptive array model, adaptive array vector matrix expression, vector matrix of adaptive array signal calculation and degrees of freedom. In addition, the theory of antenna beam pattern derivation, classical beamforming, linearly constrained minimum-variance (LCMV) method, Applebaum array, an automatic gain controller (AGC) Applebaum array, the estimation of direction of signal arrival, conventional method which contains the Capon's minimum-variance method, multiple signal classification (MUSIC) method and spatial smoothing technique, are already described in chapter 3. These theories are important and indispensable for creating the proposed covariance matrix adjustment technique that is demonstrated in chapter 4. The details of this chapter are composed of the covariance matrix computation, covariance matrix analysis, covariance matrix adjustment technique and simulation results of all descriptive theory, both proposed technique and the conventional theories, which are explained in the previous chapter. To clarify the performance of the proposed technique, the experiments were conducted in the anechoic chamber which their results are presented in chapter 5. The first section of this chapter shows the configuration of the experiment which its calibration process is described afterwards. Since the operation of this experiment is the digital system, thus its results can be performed and evaluated by the bit error rate or BER that is briefly explained in the subsequent section. Finally, the experimentations are obtained and the results are illustrated. The experimental results are composed of the radiation patterns of the receiving array antenna, single modulated signal experiment, two non-correlated modulated signals experiment, two correlated modulated signals

experiment which the DOA estimations, the comparative beam pattern results between the simulation and the experiment of beamforming process and the BER are obtained in each of the experiments. From the results, it is obvious that the beam pattern of the receiving array antenna by the proposed technique enhances more efficient than the conventional beamforming methods. The null level and peak of the beam pattern of the proposed technique are more precise than the conventional methods. Furthermore, the BER values of the proposed technique in all experiments are lower than the conventional methods which the value of occurring BER in each experiment depends on the influence of the interfering signal power level and the position of the interference. For example, in case of the direction of receiver is $-10^{\circ}$ of the two non-correlated modulation signals experiment, the average BER of the proposed technique with Applebaum array and LCMV method are 0.001067 and 0.001387, respectively. On the contrary, the BER of the conventional Applebaum array and LCMV method are 0.061753 and 0.061753, respectively.

## 6.2 Remark for future studies

Although the proposed technique has the more efficient performance than the conventional methods, however there are some points that need to be achieved. Firstly, the accurate DOA estimation has to be used in the adaptive process because the proposed technique has a strong interfering rejection capability. If the DOA estimation can not provide the precise direction of the incoming signals, the beamforming may enforce the incorrect directions of null beam patterns that may be in the direction of desired signal instead. Secondly, the threshold level in the adjusting operation of the adjustable multiplier $B$ and $C$ has to be suitably set dependent on each adaptive array system. Thus, before using this proposed technique, the threshold should be adjusted before the real use. Lastly, error threshold at the final stage should be set to relate the requirement of each system. It should be noted that the limitation of each system is different, thus this error value should be suitable with the system.

# REFERENCES

[1] Chryssomallis M. "Smart Antenna." IEEE Antennas and Propagation Magazine, vol. 42, no. 3, June 2000. pp. 129-136.

[2] Ward C.R., Hargrave P.J. and McWhirter J.G. "A Novel Algorithm and Architecture for Adaptive Digital Beamforming." IEEE Trans. Antennas Propagat., vol. AP-34, no. 3, March 1986. pp. 338-346.

[3] Lee K.M. and Han D.S. "AGC Applebaum Array for Rejection of Eigenvalue Spread Interferences." IEICE Trans. Commun., vol. E84-B, no. 6, June 2001. pp. 1674-16781.

[4] Sukontapong T., Phongcharoenpanich C., Ngamjanyaporn P. and Krairiksh M. "Improvement of Applebaum Array Interference Cancellation in Smart Antenna System by Using Covariance Matrix Adjustment." Proc. ITC-CSCC 2002, Phuket, Thailand, July 2002. pp. 727-730.

[5] Godara L.C. "Application of Antenna Arrays to Mobile Communications, Part II: Beam-Forming and Direction-of-Arrival Considerations." Proc. IEEE, vol. 85, no. 8, Aug. 1997. pp. 1195-1245.

[6] Zhimin Z., Lanfen Q., Ye L. and Ping C. "An Adaptive Array Antenna for Cancellation of Co-Channel Interference." Proc. 2000 2nd International Conference on Millimeter Wave Technology.

[7] Dietrich C.B., Jr, Stutzman W.L., Kim N.K., and Dietze K. "Smart Antennas in Wireless Communications: Base-Station Diversity and Handset Beamforming." IEEE Antennas and Propagation Magazine, vol. 42, no. 5, Oct. 2000. pp. 142-151.

[8] Compton R.T., Jr. **Adaptive Antennas Concepts and Performance.** New Jersey: Prentice-Hall, Inc. 1988.

[9] Krim H. and Viberg M. "Two Decades of Array Signal Processing Research." IEEE Signal Processing Mag., vol. 13, no. 4, July 1996. pp. 67-94.

[10] Ertel R.B. and Cardieri P. "Overview of Spatial Channel Models for Antenna Array Communication Systems." IEEE Personal Communication Magazine, vol. 5, no. 1, Feb. 1998. pp. 20-32.

[11] Balanis C.A. **Antenna Theory: Analysis and Design.** 2nd Ed. New York: John Wiley & Sons, Inc. 1997.

[12] Ogawa Y. and Ohgane T. "Advances in Adaptive Antenna Technologies in Japan." IEICE Trans. Commun., vol. E84-B, no. 7, July 2001. pp. 1704-1712.

[13] Breed B.R. "A Short Proof of the Equivalence of LCMV and GSC Beamforming." IEEE Signal Processing Lett., vol. 9, no. 6, June 2002. pp. 168-169.

[14] Applebaum S.P. "Adaptive Arrays." IEEE Trans. Antennas Propagat., vol. AP-24, no. 5, Sept. 1976. pp. 585-598.

[15] Featherstone W., Strangeways H.J., Zatman M.A. and Mewes H. "A novel method to improve the performance of Capon's minimum variance estimator." Tenth International Conference on Antennas and Propagation, vol. 1, no. 436, April 1997. pp. 322 –325.

[16] Handel P., Stoica P. and Soderstrom T. "Capon Method for DOA Estimation : Accuracy and Robustness." Nonlinear Digital Signal Processing, IEEE Winter Workshop, 1993. pp. P_7.1 -P_7.5.

[17] Schmidt R.O. "Multiple Emitter Location and Signal Parameter Estimation." IEEE Trans. Antennas Propagat., vol. AP-34, no. 3, March 1986. pp. 276-280.

[18] Friedlander B. and Weiss A.J., "Direction Finding Using Spatial Smoothing With Interpolated Arrays." IEEE Trans. Aeros., Electronic Systems., vol. 28, no. 2, Apr. 1992. pp. 574-587.

[19] Van Veen B.D. and Buckley K.M. "Beamforming: A Versatile Approach to Spatial Filtering." ASSP Magazine, vol. 3, no. 2, Apr 1988, pp. 4-24.

[20] Hayes M.H. **Statistical Digital and Signal Processing and Modeling.** New York: John Wiley & Sons, Inc. 1996.

[21] Liberti J.C., Jr. and Rappaport T.S. **Smart Antennas for Wireless Communications: IS-95 and Third Generation CDMA Applications.** New Jersey : Prentice Hall, Inc. 1999.

[22] Griffiths L.J. and Jim C.W. "An Alternative Approach to Linearly Constrained Adaptive Beamforming." IEEE Trans. Antennas Propagat., vol. AP-30, no. 1, Jan. 1982. pp. 27-34.

[23] Hirakawa M., Tsuji H. and Sano A. "Computationally Efficient DOA Estimation Based on Linear Prediction with Capon Method." Proc. ICASSP, vol. 5, 2001. pp. 3009 -3012.

[24] Choi J., Song I., Park S.I. and Yun J.S. "Direction of Arrival Estimation with Unknown Number of Signal Sources." Proc. ICCS/ISITA '92, Singapore, Nov 1992. pp. 30-33.

[25] Jeong J. S., Sakaguchi K., Araki K. and Takada J. "Generalization of MUSIC Using Extended Array Mode Vector for Joint Estimation of Instantaneous DOA and Angular Spread." IEICE Trans. Commun., vol. E84-B, no. 7, July 2001. pp. 1781-1789.

[26] Abraham D.A. and Dey D.K. "The Application of Improved Covariance Estimation to Adaptive Beamforming and Detection." Proc. 1994 Conference Record of the Twenty-Eighth Asilomar Conference on Signals Systems and Computers, 31 Oct-2 Nov 1994. pp. 677-681.

[27] Friedlander B. and Porat B. "Performance Analysis of a Null-Steering Algorithm Based on Direction-of-Arrival Estimation." IEEE Trans. Acous., Speech. Signal processing., vol. 37, no. 4, Apr. 1989. pp. 461-466.

[28] Tsoulos G. V. "Smart Antennas for Mobile Communication Systems: Benefits and Challenges." Electronics & Communication Engineering Journal, vol. 11, no. 2, Apr. 1999. pp. 84-94.

[29] Oodo M. and Miura R. "A Remote Calibration for a Transmitting Array Antenna by Using Synchronous Orthogonal Codes." IEICE Trans. Commun., vol. E84-B, no. 7, July 2001, pp. 1808-1815.

[30] Tsoulos G.V. and Beach M.A. "Calibration and Linearity issues for an Adaptive Antenna System." IEEE 47th Vehicular Technology Conference, vol. 3, May 1997, pp. 1597 -1600.

[31] Dandekar K.R., Hao L. and Guanghan X. "Smart Antenna Array Calibration Procedure Including Amplitude and Phase Mismatch and Mutual Coupling Effects." Proc. IEEE International Personal Wireless Communications, 2000. pp. 293 -297.

[32] Nakagawa Y., Fukagawa T., Kishigami T., Hasegawa M., Kanazawa A. and Tsuji H. "A Study on the Configuration of Adaptive Array Antenna Equipment and the Performance of DOA Estimation and Beam Forming in an Anechoic Chamber." Proc. ISAP2000, Fukuoka, Japan, Aug. 2000. pp. 923-926.

[33] Kanazawa A., Nakagawa Y., Fukagawa T., Tsuji H. and Ogawa H. "An Experiment Study of the DOA Estimation Using the Fast DOA Algorithm in Urban Area." Proc. ISAP2000, Fukuoka, Japan, Aug. 2000. pp. 1649-1652.

# AUTHOR BIOGRAPHY

**Author:** Mr.Thanakorn Sukhonthaphong

**Date of Birth:** March 31, 1980

**Place of Birth:** Nakhonratchasima Province, Thailand

**Bachelor Degree:** Bachelor of Engineering (Telecommunication Engineering)

**Institution:** School of Telecommunication Engineering
Institute of Engineering
Suranaree University of Technology

**Year of Graduation:** 1997

**Interested Researches:** Adaptive Array Antenna, Smart Antenna, Array Antenna DOA estimation, Remote Sensing, Wireless Communication Mobile Communication

**Related Publications:**

- **Sukontapong T.**, Phongcharoenpanich C., Ngamjanyaporn P. and Krairiksh M. "Improvement of Applebaum Array Interference Cancellation in Smart Antenna System by Using Covariance Matrix Adjustment" Proceedings of ITC-CSCC 2002, Phuket, Thailand, vol. 2, July 2002. pp. 727-730.
- **Sukhonthaphong T.**, Ngamjanyaporn P., Phongcharoenpanich C. and Krairiksh M. "Covariance Matrix Adjustment for Interference Cancellation Improvement in Adaptive Beamforming" ECTI Transactions on Electrical Eng./ Electronics and Communications, vol. 1, no. 1, July 2003. pp. 27-37.